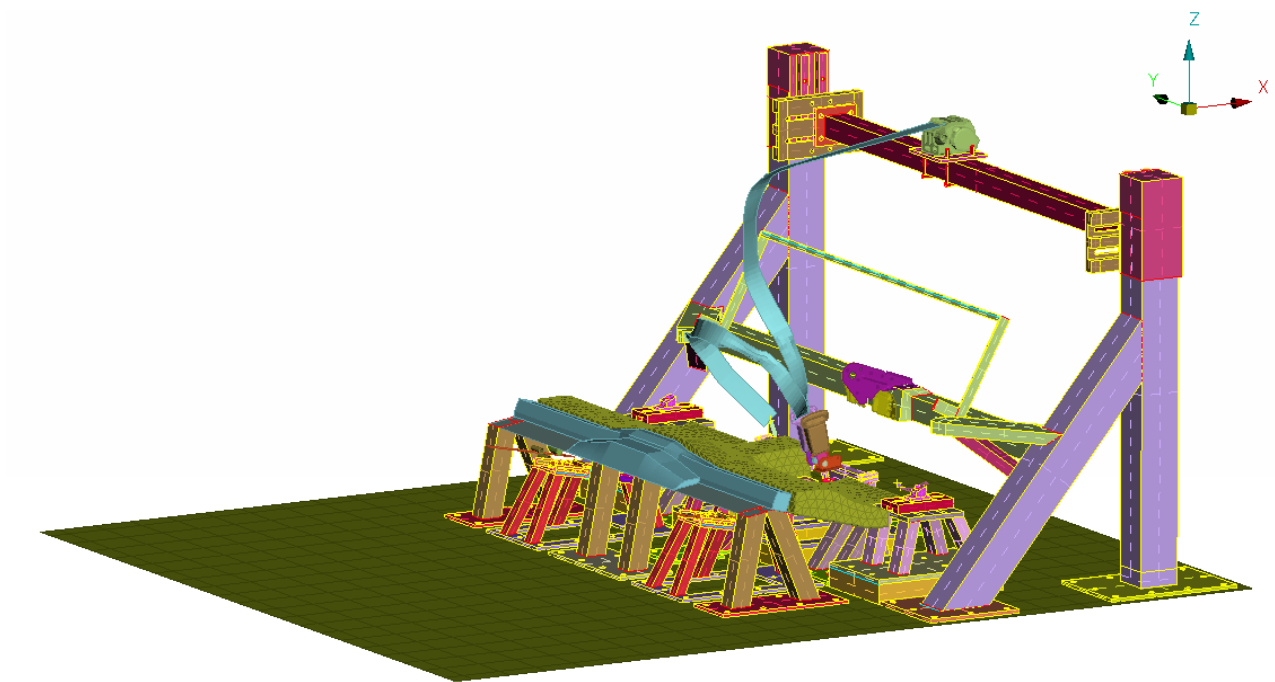




CHALMERS



Prerequisites for a Generic Rear Seat Test Rig

Master's thesis in Applied Mechanics

KARL-JOHAN LARSSON
IDA FRANSÉN

Department of Applied Mechanics
CHALMERS UNIVERSITY OF TECHNOLOGY
Göteborg, Sweden 2015

MASTER'S THESIS IN APPLIED MECHANICS

Prerequisites for a Generic Rear Seat Test Rig

KARL-JOHAN LARSSON
IDA FRANSEN

Department of Applied Mechanics
Division of Material and Computational Mechanics
CHALMERS UNIVERSITY OF TECHNOLOGY

Göteborg, Sweden 2015

Prerequisites for a Generic Rear Seat Test Rig
KARL-JOHAN LARSSON
IDA FRANSÉN

© KARL-JOHAN LARSSON, IDA FRANSÉN, 2015

Master's thesis 2015:37
ISSN 1652-8557
Department of Applied Mechanics
Division of Material and Computational Mechanics
Chalmers University of Technology
SE-412 96 Göteborg
Sweden
Telephone: +46 (0)31-772 1000

Cover:
An overview of the designed generic rear seat test rig concept

Chalmers Reproservice
Göteborg, Sweden 2015

Prerequisites for a Generic Rear Seat Test Rig
Master's thesis in Applied Mechanics
KARL-JOHAN LARSSON
IDA FRANSEN
Department of Applied Mechanics
Division of Material and Computational Mechanics
Chalmers University of Technology

ABSTRACT

In the early stages of a car development project, limited design information is available regarding the safety components and their set-up in the rear seat. If a generic rear seat test rig is developed, which allows for physical testing of different solutions in the early stages of a project, information can be gathered as to how the rear seat environment should be designed to assure a safe environment in the event of a crash. Furthermore, if a virtual analysis model of the same test rig is developed, this virtual model can be used to find preferred solutions before physical testing is performed. In this thesis the frontal crash behaviour of a currently used car platform is studied in two virtual crash tests, in order to determine which components that needs to be represented in a generic rig. Based on the discovered behaviour in these models and investigation of other related parameters, together with given requirements from engineers at the Volvo Cars Safety Center, a concept design for the generic rear seat test rig is produced, along with a simplified virtual crash test model containing the functional parts of the designed concept. In the concept design, the compliance as well as the positioning of different parts are adjustable, and deformations occurring in a real car crash is captured by small replaceable deforming plates. The positioning and size of the deforming elements in the virtual model of the concept rig are tuned using system identification to reproduce the behaviour of the two studied virtual model crash tests. Results show that the virtual model of the concept rig has capability to reproduce the results with good accuracy, especially the crash test with smaller forces present during the crash. In the other case, where larger forces are present, several more components in the real car deform in an interdependent manner, and the results from the simplified rig model deviates slightly. However, the results produced by the rig model in this case follows the existing trends in the reference model and the rig model should be sufficient to evaluate the effects of design changes, in a trend based manner. Furthermore, an existing preprocessing tool for the virtual crash test model seatbelts is implemented, which significantly reduces the preprocessing time required to test different seatbelt configurations. Using this tool, a study on the influence of the seatbelt anchoring points positioning on crash test dummy data is performed and presented.

Keywords: Crash testing, sled testing, test rig, virtual crash testing

SAMMANFATTNING

I ett tidigt skede av ett bilutvecklingsprojekt är mängden tillgänglig information begränsad gällande designen av säkerhetskomponenter i baksätetsmiljön. Om en generisk testtrigg för baksätetsmiljön utvecklas, som möjliggör fysiska tester av olika lösningar i ett tidigt skede av projektet, kan information erhållas gällande hur baksätetsmiljön bör utformas för att säkerställa en säker miljö i händelse av en krock. Dessutom, om en virtuell analysmodell av samma testtrigg utvecklas, kan denna modell användas för att finna fördelaktiga lösningar innan fysiska tester utförs. I det här arbetet studeras frontalkrockbeteende i två olika modeller av en, för närvarande, använd bilplattform, för att avgöra vilka komponenter som behöver vara representerade i en generisk testtrigg. Baserat på studierna av hur dessa modeller beter sig samt utvärderingar av andra relaterade parametrar, tillsammans med givna krav från ingenjörer på Volvo Cars Safety Center, producerades ett koncept för den generiska testtriggen tillsammans med en förenklad virtuell krocktestmodell bestående av de funktionella delarna av framtagna konceptet. I den konceptuella riggen finns det möjlighet att justera styvhet samt positionering av olika komponenter, och deformationer som förekommer i baksätetsmiljön vid en verklig krock fångas av små utbytbara samt deformerbara plattor. Positioneringen och storleken på de deformerbara elementen i den virtuella modellen av den konceptuella riggen ställs in med hjälp av systemidentifiering för att återskapa beteendet för de två virtuella krocktestmodellerna som studerats. Resultaten visar att den virtuella modellen av riggkonceptet har kapacitet att återskapa resultaten med god noggrannhet, särskilt krocktestet med lägre krafter under krocken. I det andra fallet, där högre krafter förekommer, deformeras fler komponenter i den verkliga bilen, beroende av varandra, och resultaten från riggmodellen avviker något. Däremot följer resultaten från riggmodellen i det här fallet de befintliga trenderna i referensmodellen och riggmodellen bör vara tillräcklig för att utvärdera effekter av konstruktionsändringar på ett trendbaserat sätt. Vidare implementerades ett befintligt preprocessorverktyg för säkerhetsbälten i den virtuella krocktestmodellen, vilket reducerar förarbetet avsevärt vid test av olika bälteskonfigurationer. Med hjälp av det här verktyget utfördes en studie av hur olika positionering av bältesinfästningspunkterna påverkar krocktestdockan.

PREFACE

The thesis work has been performed at the Volvo Cars Safety Center (VCSC), rear interior safety group, at Volvo Car Corporation, Torslanda Göteborg. We, the authors, have developed a concept design for a generic rear seat test rig based on results obtained when studying and modifying virtual crash test models developed by the staff at VCSC, as well as given requirements by the staff. Furthermore a virtual model of the concept rig has been implemented, as well as studies of parameters that has been pointed out as interesting by our supervisors. Since the state of the art crash analysis virtual models used at VCSC are immensely complicated, this work could not have been completed without the help of the staff, who readily answered any question we had.

Special thanks goes out to supervisors Mathias Retzlaff and Magnus Björklund, as well as examiner Martin Fagerström, who have shown great support and interest in our work.

CONTENTS

Abstract	i
Sammanfattning	ii
Preface	iii
Contents	v
1 Introduction	1
1.1 Background	1
1.2 Purpose	1
1.3 Goals	1
1.4 Limitations	2
2 Frame of reference	3
2.1 Conventions	3
2.2 Crash test dummies	3
2.2.1 Dummy instrumentation	4
2.3 Seatbelts	7
2.3.1 Three point seatbelts	7
2.3.2 Risks associated with seatbelts	7
2.3.3 Common safety features	8
2.4 Safety rating organisations	8
2.4.1 Crash tests	8
2.5 Sled testing	9
2.6 CAE crash testing	11
2.6.1 Features of a car crash simulation	11
2.6.2 LS-DYNA	13
2.6.3 Ansa	14
3 The generic rig concept	15
3.1 Given requirements and design guide-lines	15
3.2 Finding requirements through model studies	15
3.2.1 Simplified models	16
3.2.2 Rear seat backrest	19
3.2.3 Seat cushion attachment	20
3.3 How to capture necessary behaviour with the rig	20
3.3.1 Foot stop	21
3.3.2 Tilting seat bottom plate	22
3.3.3 Summary of found requirements	23
3.4 The generic rig concept	25
3.4.1 Generic seat bottom structure	25
3.4.2 Seatbelt fixtures	27
3.4.3 Assumptions made for the rig concept	31
3.5 Results from the rig FE model	33
3.5.1 Set-up of rig FE model	33
3.5.2 P4 rig results	36
3.5.3 P5 rig results	39
3.5.4 Rig results for offset deformable barrier crash test	42
3.6 Fulfilment of the requirements	44

4	Implementation of the modelling concepts	45
4.1	Ansa seatbelt module	45
4.1.1	LS-DYNA seatbelt	45
4.1.2	Setting up a dynamic Ansa seatbelt entity	46
4.1.3	Compatibility issues	47
4.1.4	Example model	48
4.2	Automatic parameter configuration using LS-OPT coupled with Ansa and LS-DYNA	48
4.2.1	Ansa and optimisation	48
4.2.2	LS-DYNA input files and optimisation	49
4.2.3	Setting up an LS-OPT optimisation task	49
4.2.4	Example optimisation task	50
5	Parameter study	53
5.1	Seatbelt mounting positions	53
5.2	Dummy friction	60
5.3	Stiffness of seat bottom plate	63
6	Concluding discussion	67
6.1	Fulfilment of goals	67
6.1.1	Describe components and phenomena affecting the rear seat safety	67
6.1.2	Develop a conceptual design for a generic rear seat test rig	67
6.1.3	Develop a CAE model of the rig that can be used to evaluate different safety solutions	68
6.2	Future work	68
6.2.1	Describe components and phenomena affecting the rear seat safety	68
6.2.2	Develop a conceptual design for a generic rear seat test rig	68
6.2.3	Develop a CAE model of the rig that can be used to evaluate different safety solutions	69
	References	69
	Appendix A NCAP crash tests	70
A.1	Euro NCAP	70
A.1.1	Euro NCAP full width frontal impact test	70
A.1.2	Injury criteria	71
A.2	China NCAP	72
A.2.1	China NCAP tests and scoring	72
	Appendix References	73
	Appendix B Simplified model	74
	Appendix C Ansa scripts	76
C.1	Reverse order of slipping sets	76
C.2	Move edgeset script	77
C.3	Update sets of DBCS	78
	Appendix D Auto-recreating seatbelt model	79
D.1	Tutorial: Seatbelt example model	79
D.2	Set up of example model	82
	Appendix E Start LS-DYNA from LS-OPT	85
E.1	LS-DYNA start script	85
E.2	Setting up LS-OPT solver stage	85

1 Introduction

This thesis concerns car crash safety evaluation and is performed at the Volvo Cars Safety Centre (VCSC) at Volvo Car Corporation (VCC). At VCSC, crash safety evaluation is performed both with computer simulated crashes using CAE (Computer Aided Engineering) models, as well as physical crash tests. In the physical tests both full scale crash tests, where a complete car is crashed in a test scenario, and sled tests are used. In the sled tests, a rig representing part of the car that is being investigated is built according to the test case onto a sled that is accelerated in a crash simulator. In the crash simulators, the rig is stationary at the starting point, and accelerated such that the test corresponds to a reversed crash.

The main intention behind the work presented in this thesis is to develop a generic test rig for the rear seat passenger safety evaluation. In this work, three different parts can be identified; the development of a conceptual generic test rig implemented as a simplified CAE model, the implementation of existing software tools that can be used for future work with the generic rig model and, in the third part, a number of parameter studies relevant to rear seat safety evaluation is presented.

1.1 Background

The current designs of the rear seat test rigs used at VCSC are based on prototypes or the final version of the car that is being evaluated, and does not easily allow for changes in the test set-up, such as changing components and their positioning. In early concept phases there is a limited availability of CAD (Computer Aided Design) data to build up representative CAE models since the final interior is still unknown.

This makes it hard to evaluate the influence of a certain component and its position. A generic crash test rig would make it possible to perform crash tests in early design phases, and thus evaluate different design options, and even contribute to design guidelines and requirements for the future car models.

For VCSC, this rig is also interesting in other aspects, especially from a correlation point of view. The current CAE models used consist of several different components, obtained from both internal and external sources such as different design departments, seat and seatbelt manufacturers. In full scale crash test models there are many factors interacting, which make it very difficult to validate that a certain component behaves accurately.

If a CAE generic test rig is developed, that is well correlated to the physical generic crash test rig, it would be possible to design test set-ups to isolate component behaviour and investigate the validity of these models. In that way, the test rig can be used both as a tool for CAE model validation and for decision making in the early design phase.

1.2 Purpose

This thesis work is the first step towards the generic rear seat test rig. Based on phenomena existing in a crash, a virtual generic test rig shall be developed, which shall be realisable as a physical test rig.

1.3 Goals

In order to fulfil the purpose of the thesis work a number of goals have been formulated.

Describe components and phenomena affecting the rear seat safety

A car consists of many components and it is of interest for the development of a generic test rig to investigate which components of these that have a significant impact on the rear seat safety, and also what that impact is, in order to determine which simplifications can be made when constructing a test rig.

Develop a conceptual design for a generic rear seat test rig

Based on components and phenomena affecting the rear seat safety environment, a concept for a generic test rig shall be developed. The design of the concept shall be such that the crash behaviour of the rig is possible to change. It shall be possible to test different components and their relative positioning.

Develop a CAE model of the rig that can be used to evaluate different safety solutions

Along with the designed concept a CAE model that allows for easy evaluation of different test set-ups before performing physical tests shall be produced.

1.4 Limitations

This thesis concerns adult occupant rear seat crash safety and the rig will only be designed with regard to frontal impact crash testing, a limitation set by the thesis supervisors. The crash behaviour of the test rig will be based on the behaviour observed from CAE models of a current Volvo platform carrying adult occupants in frontal impact crash simulations, although care will be taken to ensure that the rig is adjustable to represent other designs. These CAE models will be regarded as accurate and the accuracy of the rig CAE model will be evaluated against these. Furthermore, this thesis focuses on delivering a conceptual design proposal, with focus on the components affecting the rear seat safety, which means that detailed dimensioning and drawings of the surrounding structures is out of scope. Only software available at VCSC will be used, and CAE models will be constructed using existing Finite Element (FE) modelling guidelines regarding element types, mesh densities, material models and contact definitions.

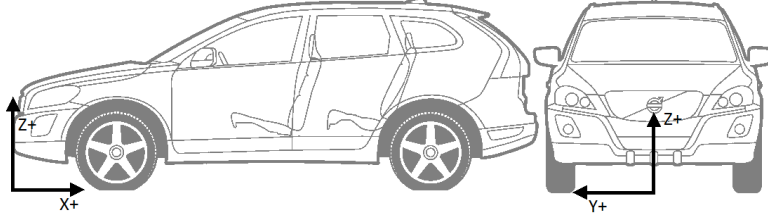


Figure 2.1: The definition of the global coordinate system in the car

2 Frame of reference

The crash safety of Volvo cars is evaluated by both VCC internally and by different safety rating organisations around the world. Since safety is a core value at VCC when designing cars, their internal safety standards and goals are very high. Since a car can crash in many ways and can carry differently sized occupants, there is no general best set-up for the different safety components in a car, such as airbags and seatbelts, and every new car design needs to be carefully investigated. Several physical crash tests, as well as thousands of computer simulated crashes are performed to ensure that every car has a high level of safety in many types of crashes.

Furthermore, the safety rating achieved by different safety rating organisations are very important for the Volvo brand and thus the crash testing cases evaluated here must also be carefully evaluated for each car by VCSC during the design process. In Section 2.4 the different rating organisations and test cases pertinent to this thesis is presented.

Section 2.1 briefly introduces nomenclature used, and in Section 2.2 the crash test dummies used when evaluating occupant safety are described, followed by Section 2.3, where seatbelts and their terminology, safety features as well as associated risks are described.

To evaluate crash safety during the design process at VCC, CAE testing with FE models are utilised, but also physical testing. The physical testing is performed both as full scale testing, where complete cars or prototypes are crashed in different cases and with sled tests, where part of the car environment under investigation is built into a rig that is placed on a sled, which then is accelerated with a pulse corresponding to a reversed crash. The sled testing procedure of interest in this thesis is treated in Section 2.5 and the general features of the CAE virtual crash test models are introduced in Section 2.6.

2.1 Conventions

In order to uniformly refer to positions and directions in the car a global coordinate system is defined, see Figure 2.1, where X-direction is defined from the front of the car to the rear, the Y-direction is from driver left hand side to the right hand side and is zero in the centreline of the car and Z-direction points from the road level and upwards. The directions of the axes is the same between different car models, but the position of the Z,X origin may differ.

Each seat position in the car is associated with a unique number and the numbering convention can be seen in Figure 2.2. This convention is used when referring to which seat position a particular crash test dummy is seated at in a test. In this thesis, position numbers four and five are mainly referred to, using the convention 4th and 5th position respectively.

2.2 Crash test dummies

Crash test dummies are important components in crash safety evaluations. A crash test dummy is an anthropomorphic standardised measuring instrument designed to evaluate risk of human injury in an accident. Since different types of collisions cause risks for different types of injuries, there are dummies specially designed and instrumented for different cases, such as frontal impact, side impact and rear impact. There are dummies representing children of different ages as well as adults. For frontal impact the Hybrid III (HIII) type dummies are used to evaluate risk of injury. Since adult occupants are differently sized the HIII type adult dummy is available in three different sizes, corresponding to the 95th percentile of the adult male population, the 50th percentile of the male adult population and the 5th percentile of the female adult population, see Figure 2.3,

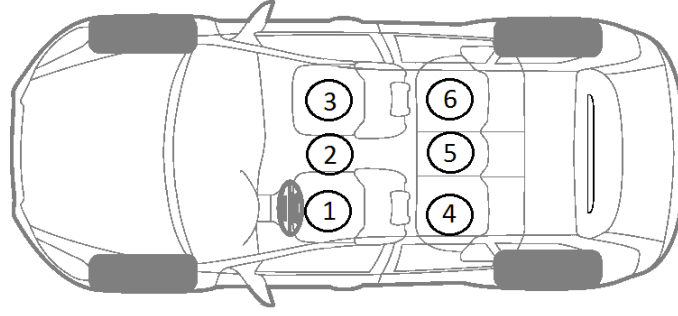


Figure 2.2: The numbering convention for seat positions

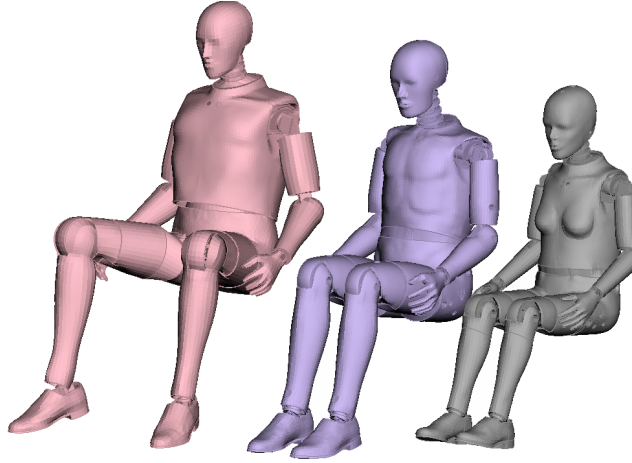


Figure 2.3: Computer models of Hybrid III crash test dummies. From left to right: 95th percentile male, 50th percentile male and 5th percentile female

where computer models of the three dummies are shown. The design and instrumentation of Hybrid III 50th percentile male and 5th percentile female dummies is regulated by U.S Department of Transportation Code of Federal Regulations (CFR) Part 572 Subpart E and O respectively. The 95th percentile male dummy represents the largest segment of the adult population and is not yet incorporated in the Federal Code but is still used in testing and in particular for seatbelt integrity testing [1].

2.2.1 Dummy instrumentation

To measure the risk of injury the HIII dummies are instrumented at several key locations. The measurements recorded from these instruments during a crash are then used to estimate risk of injury according to different injury criteria. Instrumentation include accelerometers in the head, thorax and pelvis, loadcells that measure normal forces and moments in the neck, spine, femur, knee, iliac crests and tibia and also a potentiometer that measures chest compression. Each of these measurement devices are mounted rigidly inside the dummy and will measure normal forces and moments with regard to a coordinate system that moves with the body part it is mounted in, see Figure 2.4, where some local body part coordinate systems are defined. It can be seen that the coordinate systems move with the limb they belong to as displayed with the leg coordinate system as the dummy is seated.

In Figures 2.5 and 2.6, positive force directions are defined for the force transducers. These directions are coincident with the coordinate system directions in the respective dummy body part. Positive accelerometer output corresponds to an acceleration in the respective positive coordinate system axis direction, e.g an impact that would cause the dummy pelvis to accelerate in the pelvis negative z-direction will result in a negative pelvis z-acceleration measurement. When referring to dummy measurement data in this thesis, the direction given will always refer to the local body part coordinate system, i.e chest z-acceleration is the acceleration measured in the z-direction of the chest local coordinate system that moves with the chest, not to be confused with Z, that refers to the global car coordinate system Z-axis.

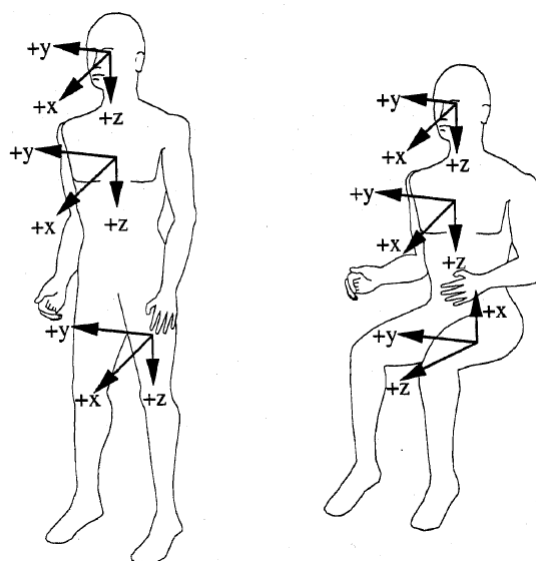


Figure 2.4: Examples of coordinate systems in a dummy that are fixed with regard to a limb, picture from CFR Part 572

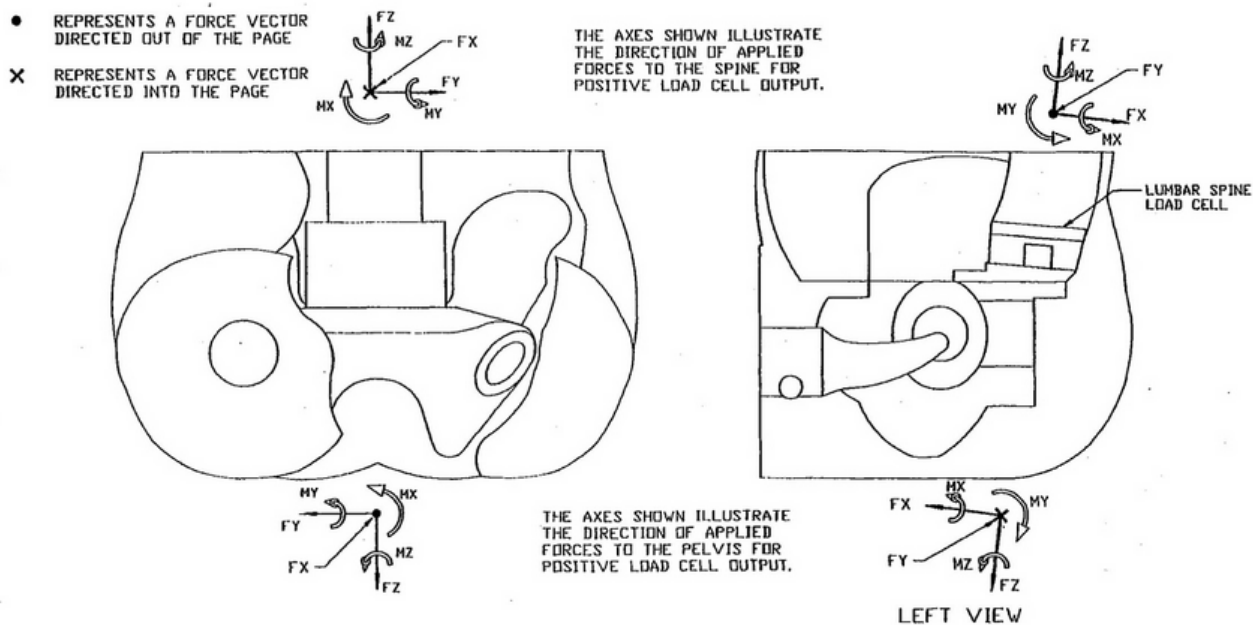


Figure 2.5: Positive forces definition in the dummy lumbar spine. The figure shows the dummy pelvis and the position of the force transducer inside the pelvis, picture from CFR Part 572

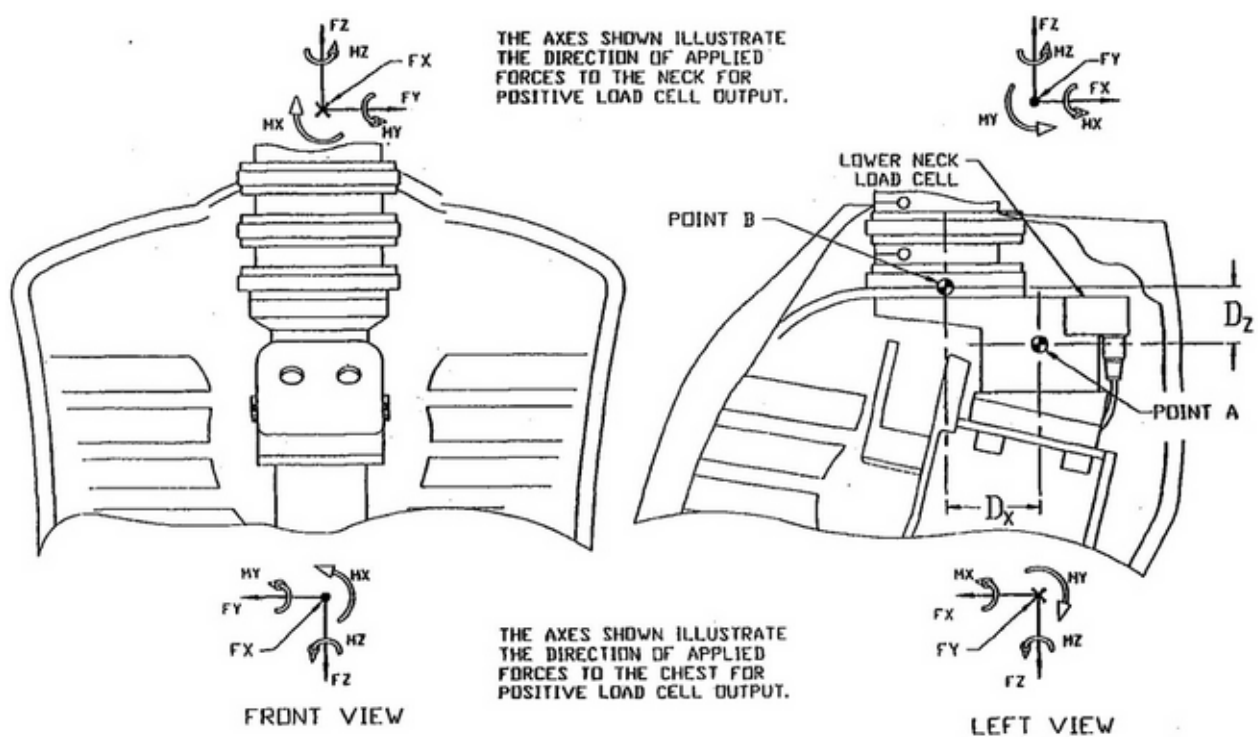


Figure 2.6: Positive forces definition in the dummy lower neck, picture from CFR Part 572

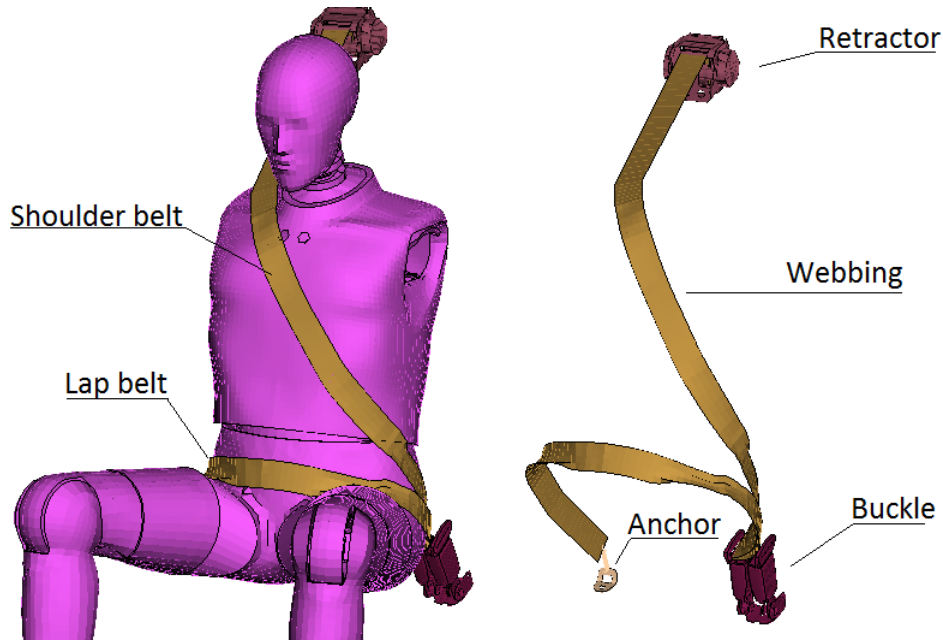


Figure 2.7: The basic parts of a three point seatbelt

2.3 Seatbelts

A component that has a large influence on crash safety is the seatbelt. The main function of the seatbelt is to restrain the occupant to the seat during an accident, and thus reducing the risk of injuries for the occupant by colliding with interior parts or even getting thrown out.

2.3.1 Three point seatbelts

The seatbelts in this thesis are three point seatbelts and are called so because it is attached to the car at three different points: the buckle, anchor and retractor positions, see Figure 2.7. It is also possible to locate the retractor in other positions and re-route the belt using linking points such that the shoulder belt still runs over the shoulder of the occupant. It is not unusual that this linking point is adjustable in height in order to provide comfort and good fit to differently sized occupants. The retractor is responsible for retracting the webbing when the seatbelt is not in use, and also keep a slight tension in the webbing to reduce slack when the occupant is wearing it. The retractor can also lock the feed out of additional webbing when certain criteria are met, such as high accelerations, if the car is tilted to a large degree, or signals from other systems in the car depending on retractor model and car.

2.3.2 Risks associated with seatbelts

Certain safety risks need special attention when designing a seatbelt system for a car, such as submarining, slip-out, maximum forward head displacement and chest compression.

Submarining is the term that describes the phenomena where the occupant slides under the lap belt, causing the lap belt to run over the abdominal area of the occupant. This poses a great risk for severe internal injuries for the occupant in the event of a crash [2].

Slip-out occurs when the occupants shoulder slips out of the shoulder belt and as the torso is no longer constrained by the shoulder belt, this increases the risk of the occupant of hitting the head in the car interior, another occupant or itself, typically in the chest or knee.

The maximum forward head displacement of the occupant is also important to control during a crash when the occupant is belted. It is desirable to use the seatbelt as an energy absorber to minimise the acceleration of the occupant and thus forces exerted by the belt during a crash. If the seatbelt is too compliant the occupant may risk impact of the head with the interior of the car, such as the steering wheel or, in the case of rear seat occupants, the front seat.

The compression of the chest, as well as the velocity of the chest compression, can cause injuries to the ribs, heart, lungs and major vessels in the chest [2, 3].

2.3.3 Common safety features

Common additional safety features in seatbelts are load limiting and pre-tensioning.

Load limiting means that the locking force of the retractor is limited to a certain threshold value. If this value is exceeded the retractor will feed out additional webbing, and thus limit the contact forces exerted on the passenger in the event of a crash. A major advantage of load limiting is that it allows for the seatbelt to decelerate the passenger over some distance and is an effective way to obtain energy absorption in the seatbelt.

Pre-tensioning is a rapid tensioning of the webbing in the event of a crash. This reduces the slack of the seatbelt, often caused by loosely fitted clothing worn by the passenger. This means that the passenger will be firmly restrained early in the crash, and thus the energy absorption provided by the load limiting can work over a larger distance. Pre-tensioning may also help to position the passenger more correctly and can reduce the risks of submarining and slip-out [2]. The pre-tensioning can be incorporated at the buckle, anchor or retractor position, or at several locations simultaneously.

2.4 Safety rating organisations

Around the world there are several organisations that evaluates the safety of cars. The New Car Assessment Programme (NCAP) aims to provide customers with an informed choice regarding the safety of popular cars on the market, as well as stimulate car manufacturers to produce safer cars. A series of standardised tests are used that determines the total safety rating for a car. A safety rating is provided on a five star scale, where five stars is the highest safety rating.

To assure a high rating by these organisations, it is desirable to evaluate the tests performed in a sled test during the design process. The crash test cases considered in this thesis are used by the European NCAP (Euro-NCAP) and China NCAP (C-NCAP) organisations as part of the total safety rating evaluation. In these tests, crashes are performed with dummies in the car, and scores towards the final rating of the car is calculated from measurements obtained from the dummy instruments.

2.4.1 Crash tests

The tests evaluating rear seat occupant safety pertinent for this thesis are the Euro-NCAP full width frontal impact test, the C-NCAP full width frontal impact test and the C-NCAP frontal impact test against deformable barrier with 40% overlap. In both of the full width frontal impact tests, the car is frontally crashed against



Figure 2.8: Offset deformable barrier crash test (picture from Euro-NCAP press room)

a rigid barrier with an initial velocity of 50 km/h. However the dummies used and the scoring procedures differ between the two organisations. For a detailed description of the test setup and scoring procedure, see Appendix A. In the C-NCAP frontal impact test against deformable barrier with 40% overlap the car is crashed

against a deformable barrier that overlaps 40% of the width of the car with an initial velocity of 64 km/h, see Figure 2.8. This test is also used in the Euro-NCAP rating, but only with child dummies as rear seat occupants. A more detailed description of this test is also presented in Appendix A. In the crash test, scores towards the final rating are determined from measurements from the following dummy instruments:

- Head accelerometer, resultant acceleration
- Upper neck load cell, F_x , F_z and bending moment M_y .
- Chest potentiometer, total chest compression and chest compression velocity
- Femur load cell, F_z

Additional factors that affects the final score are applied if submarining occurs, or if any part of the seatbelt fails.

2.5 Sled testing



Figure 2.9: A rig representing the front interior of a car (grey) being prepared for a sled test. The sled (black) can be seen sitting on the rails under the rig

Since full-scale car crash tests are destructive and very expensive, sled testing with crash simulators is often utilised to test subsystems of the car. In a sled test, a rig is built representing the environment investigated, which is then fixed onto a rail-borne sled, see Figure 2.9. A propulsion system then accelerates the sled, and thus the car environment backwards, corresponding to a car crash played in reverse. The propulsion system can deliver a controlled acceleration pulse to the sled derived from either measurements in full-scale physical tests or computer simulated crashes.

VCSC have two sled crash test simulators, where the generic rig may be used for sled testing. KS1, with a power rating of 1.1 million horsepower is the most powerful. It can accelerate a rig from 0 to 90 km/h in 0.1 seconds depending on weight, deliver controlled pulses with a maximum acceleration of 55 g and can also pitch (rotation about the car Y-axis) the rig during the crash simulation using vertical cylinders under the sled rails. The older crash simulator, KS2, has a power rating of 100 000 horsepower, and cannot pitch the rig during the crash simulation.

During e.g, the frontal impact 40% overlap crash tests, the car will often rotate about the Z-axis, due to the non-uniform impact forces over the car-front. The crash simulators cannot simulate this movement, but the rig can however be mounted onto the sled with a fixed rotation about the car Z-axis, see Figure 2.10, and be tested in this configuration, which can approximate the sideways (Y) forces present in such a crash. In Figure 2.11 a test rig previously used for evaluating rear seat safety can be seen. The photo shows that part of the actual rear car body have been built into a stiffening cage structure. The cage structure strengthens the car body such that the rig may be used for several crash simulations.

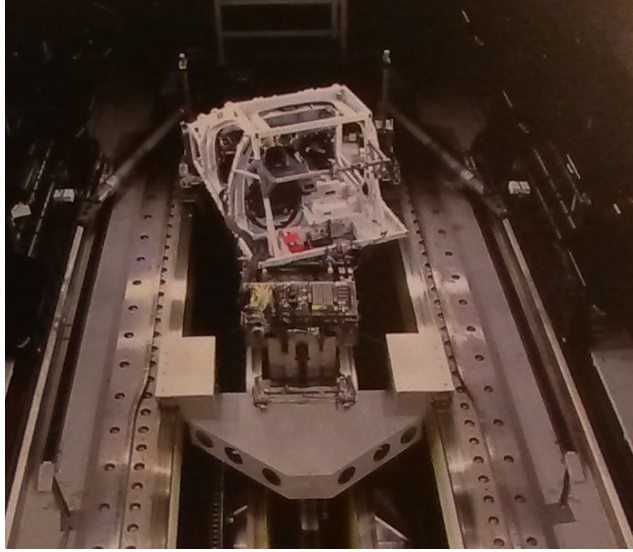


Figure 2.10: A rig in the KS1 sled crash simulator. The rig is mounted with a fixed rotation about the Z-axis onto the sled.



Figure 2.11: A partly dismantled previously used rear seat test rig.

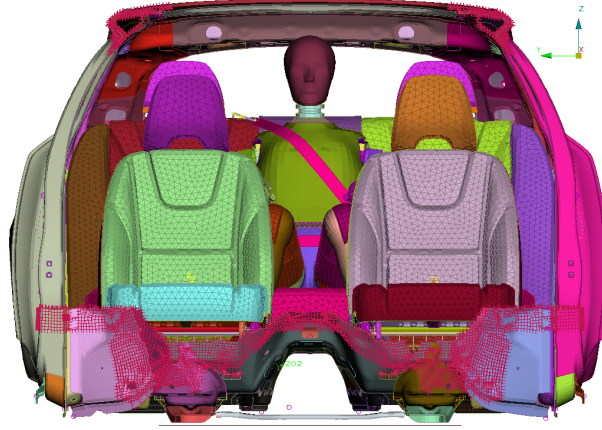


Figure 2.12: Frontal crash rear seat safety evaluation model.

2.6 CAE crash testing

At VCSC computer simulated crashes are an important tool when evaluating the safety of a car model under development. In this section the general features of a car crash simulation is introduced, as well as the preprocessor Ansa, [4], and the FE-solver LS-DYNA, [5], which have been used in this thesis.

2.6.1 Features of a car crash simulation

In a car crash, large forces occur under a relatively short period of time. The large forces are sufficient to cause several non-linear phenomena to occur, such as material yielding and breakage, large deformations causing geometrical non-linearities, contact between different parts or even self-contact of parts, which give rise to sliding friction or penetrations between parts.

At VCSC the aim is to model the car as accurate as possible, while still keeping the computational costs reasonable. Internal guidelines for mesh density, element formulations, material models, connections modelling and contact definitions have been developed to ensure consistent high quality models, and are followed in this thesis.

Simulation model

A modern car is a complex product consisting many different materials, parts and components. Depending on what is investigated, different parts are modelled with varying detail in different sub-models. A typical rear seat frontal crash safety evaluation FE model can be seen in Figure 2.12. Included in this model is part of the car body, the rear and front seats, crash test dummy and seatbelt model. The front most part of the car is evaluated in other models, and the resulting accelerations obtained in these simulations is recorded at reference points in the car body, which can be reapplied as boundary conditions in later models.

To simulate the crash, a rigid plate under the car body gets a prescribed acceleration, see Figure 2.13, and nodes in the front and rear of the car body is constrained to move with this plate. This boundary condition effectively means that the car body will not be compressed in the X-direction during the simulation. Modern Volvo cars have a strong safety cage structure surrounding the passenger compartment. This structure, when crashed frontally together with the doors have been proven to obtain very little compression in the X-direction in a real crash, which justifies this type of boundary condition. This also allows for the doors to be omitted, and thus faster solution times can be obtained.

Even with these sub modelling simplifications, more than 1 million shell elements make up the rear car body in this particular model.

Dummy model

For each HIII dummy type an advanced and verified LS-DYNA FE-model provided by the dummy manufacturer is available. In the dummy model, the dummy parts, materials, joints and instruments are modelled, in order to obtain accurate predictions of the dummy measurements during a physical crash, see Figure 2.14. Each dummy

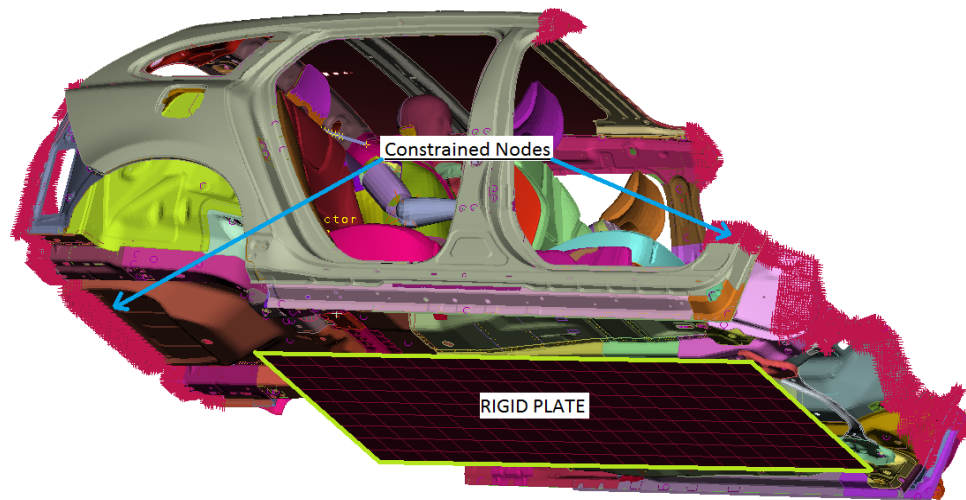


Figure 2.13: The rigid plate that is accelerated, seen under the car body. Nodes constrained to follow the motion of this plate marked in pink at the front and rear of the car body

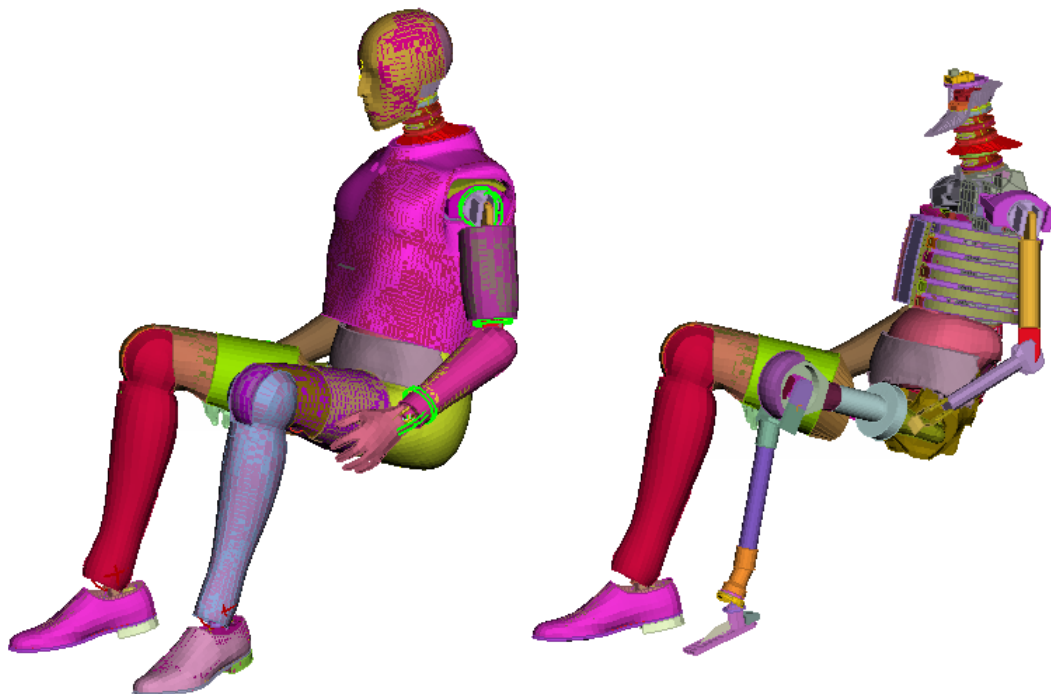


Figure 2.14: (Left) FE-model of HIII 95th percentile male dummy. (Right) Same model with some external parts removed

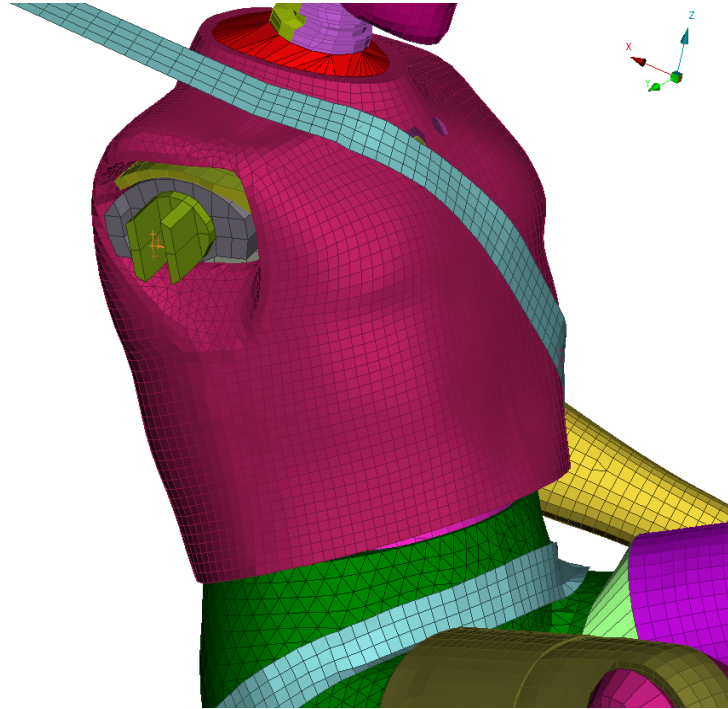


Figure 2.15: The seatbelt webbing mesh seen placed around the dummy

model has a kinematic definition, consisting of all the joints in the dummy. For each new crash simulation case being set-up, the dummy needs to be seated correctly in the car during the preprocessing stage. The kinematic definition in the dummy model can be recognised by different preprocessors, and manipulation of different dummy limbs can be obtained by changing parameters for the defined joints.

As a seated dummy will, in a physical test, depress the seat, this depression has to be obtained in the simulation model once the dummy has been seated, and is obtained by a small simulation just focusing on dummy seat depression. The simulation will result in the seat being deformed, and the stresses in the seat due to this deformation can be saved and prescribed as initial stresses in a simulation, however they are often neglected. Once this operation is performed, the seated dummy and the depressed seat configuration can be saved, to be used in later crash simulations. This means that the dummy positioning and the seat depression only needs to be performed once for every dummy-seat-position combination.

Seatbelt model

The seatbelt model consists of retractor, webbing, buckle and anchor. The functionalities of the retractor, such as locking, load limiting, and webbing feed-out is obtained by a retractor model, often provided by the retractor manufacturer. That is, the components of the retractor is not modelled in full detail, but the functionalities are represented by special model entities designed to provide the same behaviour as the physical retractor. Since this is the case, it is desirable to be able to verify the retractor model with physical testing.

The seatbelt webbing model consists of shell elements, with the webbing material properties. In a preprocessing stage, the webbing elements must be carefully placed around the dummy, see Figure 2.15. The webbing mesh cannot be placed too loosely around the dummy since this would introduce extra slack in the seatbelt, and care must also be taken that the webbing mesh does not intersect other meshes, such as the dummy or seat mesh, since elements may become locked together due to the contact modelling between different parts. Since the webbing mesh is so tightly positioned around components, this means that if any component that the webbing wraps is moved, the webbing needs to be re-positioned in the preprocessing stage.

2.6.2 LS-DYNA

LS-DYNA is an FE solver with capabilities to solve highly non-linear transient dynamic FE problems, which makes it suitable for crash analysis. Special entities are available to model common car safety features, such as

airbags and their inflation, seatbelts with retractors and pre-tensioners [5]. LS-DYNA has no graphical user interface and is entirely command line driven, and all input to the solver must be performed with **ASCII** text files. These text files are most often generated by a preprocessor capable of producing LS-DYNA formatted files. Version 971 release 6.85274 of LS-DYNA is used in this thesis.

2.6.3 Ansa

Ansa, version 15.2.3, is the preprocessor used to write the LS-DYNA input files used in this thesis. In Ansa, all LS-DYNA required input can be defined. Ansa also has several tools implemented to aid in the preprocessing of a car crash analysis, such as tools to define airbags and seatbelts, and an integrated rigid body kinematics solver, which can be used to position CAE models of dummies or other entities,[4]. Furthermore, Ansa has a Morphing tool that can be used to change the geometry of an FE-mesh, which can be used to quickly generate a number of alternative designs. It is possible to couple Ansa with optimisation software, such that Ansa can perform design changes to the structure being evaluated to find an optimum configuration. Ansa also allows the user to define scripts that can be used to perform operations that is not implemented.

3 The generic rig concept

This section contains a description of the final rig concept and the development process towards this. It includes the requirements on the rig, both those given by VCSC at the starting point of this work and also those found during the process of studying and simplifying existing CAE models. During the process, different sub-concepts were evaluated and these will also be presented in the following section. Some of these resulted in new requirements while others were further developed.

3.1 Given requirements and design guide-lines

The following requirements and requests are based on the initial problem description together with consultations, with experienced engineers and technicians at VCSC, about different phenomena and concerns that is of interest in a rig environment. Some of these are quantifiable and can be measured, others are not and the fulfilments of these will be discussed in Section 3.6.

Since the field of car safety is under constant development there shall be possibilities to test new components in the rig. This implies that the rig shall be easily modified to test different components and set-ups, including different dummies. The rig shall be generic in terms of e.g. car model, seat geometry and seatbelt positioning. This means that seats from different car models can be used in the same rig. Also, the seatbelt attachments shall be adjustable, preferably continuously. To reduce the costs as many parts as possible shall be reusable. The components that needs to be changed or moved between tests shall be easy to remove and attach. They shall also be easily produced at the workshop at VCSC at a reasonable cost.

The rig shall also be possible to use for correlation with CAE models of the rig and the components included. Phenomena which are typically hard to measure in real life, and thus hard to model accurately in a CAE environment, such as contacts and friction between sliding parts, need to be kept to a minimum.

Since the test rig will be a simplification of a full scale car, it is not expected that all data gathered from a rig test will be fully comparable to a real car crash test. However, some crash test dummy data is considered more important to capture correctly to estimate occupant safety and the following list is given by the supervisors:

- Pelvis resultant acceleration
- Chest resultant acceleration
- Upper neck F_x and F_z
- Chest deflection

These should not differ significantly from the behaviour in a corresponding full-scale crash test.

Another stated requirement is that the compliance of the seatbelt fixtures shall be possible to adjust, since different car models have dissimilar rigidity of the parts responsible of carrying this load, and there is a need to evaluate the effect of this from a safety point of view.

3.2 Finding requirements through model studies

In order to investigate further requirements for the rig, several questions needed to be answered. How much of the actual crash physics must be captured by the rig in order to gather sufficient data to make design decisions? Which parts deform and how much do they deform? Does this deformation have a significant impact on the passenger safety? To answer these questions it was necessary to gather information about important dynamics in the crash regarding the rear seat safety and a first step was therefore to study already performed full scale rear seat model tests, from now on referred to as full models. From this point, mainly two reference models were studied. One with a 5th percentile female dummy at the 4th position in 50 km/h and one with a 95th percentile male dummy at the 5th position in 64 km/h, both subjected to crashes with a full frontal rigid barrier. The first case will be referred to as the P4 model and the later to the P5 model.



Figure 3.1: Set-up for the simplified P4 model, a model with a HIII 5th female dummy at the 4th position

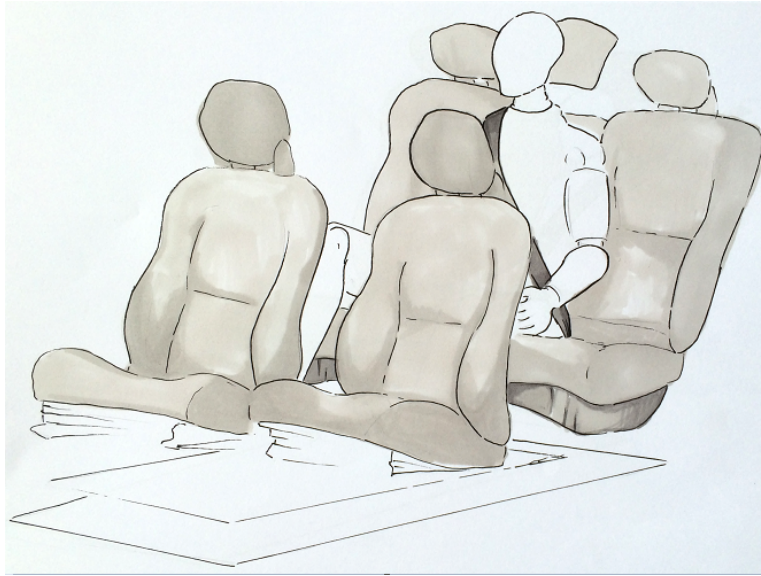


Figure 3.2: Set-up for the simplified P5 model, a model with a HIII 95th male dummy at the 5th position

3.2.1 Simplified models

Starting from the dummy, some components are obvious to have significant impact on the safety, e.g. the seatbelt and the rear seat. These are mounted on other parts of the car which in turn are mounted on other parts and so on, each one with certain behaviour and purpose which may differ between different existing and future car models. Thus, there was a need to decide which components should be represented in the rig, and how.

Seat bottom plate

The previous full scale simulations suggested that there should be possible to neglect components at a certain distance from the passenger, thanks to the stiff cage environment surrounding the passenger compartment. Simplified models were set up where only the components immediately surrounding the respective crash test dummy were extracted from the reference models and fixed relative to the rigid sled plate, see Figure 3.1 and Figure 3.2. The following components were included:

- A rigid sled plate used to accelerate the rig

- The crash test dummy
- The seatbelt system including webbing, retractor model, buckle and anchor. The seatbelt components are attached by the same fixture elements as in the full models, and these fixture elements are constrained to follow the rigid sled plate, resulting in rigid belt fixture points
- The rear seat with the seat bottom plate that the bottom rests on and necessary fixtures for holding the backrest in position. The seat bottom plate is modelled as rigid and the fixtures are constrained to follow the sled
- The front seat at the 1st position for the P4 model and the front seats at the 1st and the 3rd position for the P5 model
- A rigid plate replacing the original floor

The results from an analysis with these simplified models showed that modelling the seat bottom plate as rigid had significant impact on the data obtained from the dummy. When hitting the bottom plate the dummy was subjected to a much higher impact force as measured by the pelvis and chest accelerometers ($Force = mass \times acceleration$). This is due to the fact that a rigid bottom plate offers no energy absorption by deflection. The result from the P4 model can be seen in Figure 3.3 where the curves labelled "Simplified –

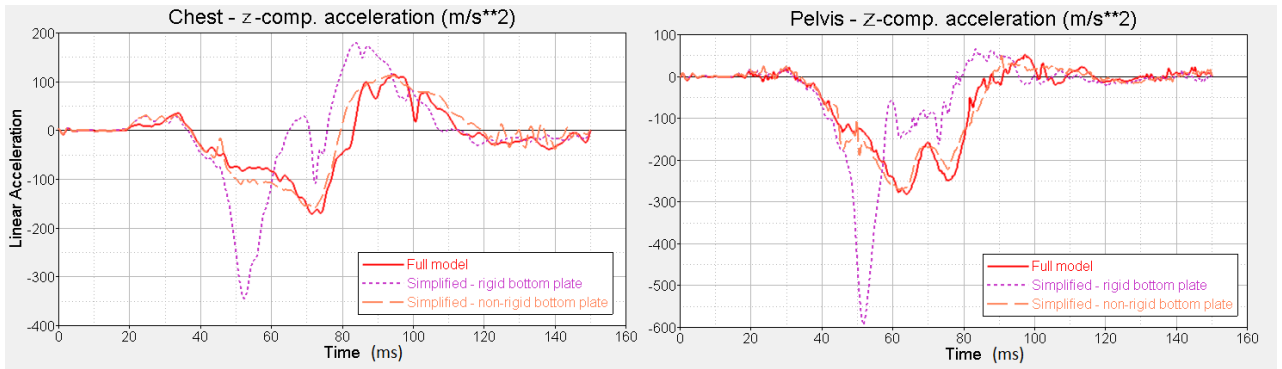


Figure 3.3: Chest and pelvis acceleration in the z-direction for the dummy in the P4 model. The graphs show the full model and two simplified models, one with rigid and the other with non-rigid seat bottom plate

rigid bottom plate" shows the chest and pelvis acceleration in the z-direction, for this simulation. The chest and pelvis accelerations in the z-direction for the P5 model are shown in Figure 3.4. The peak value for the accelerations at 50 ms represents the bouncing into the seat bottom plate and it affects all subsequent data which makes it hard to ignore this effect. The same behaviour can be observed for other dummy data as well and the reason is assumed to be the shock from the impact with the rigid bottom plate that goes through the whole body. For more dummy data from these runs see Appendix B.

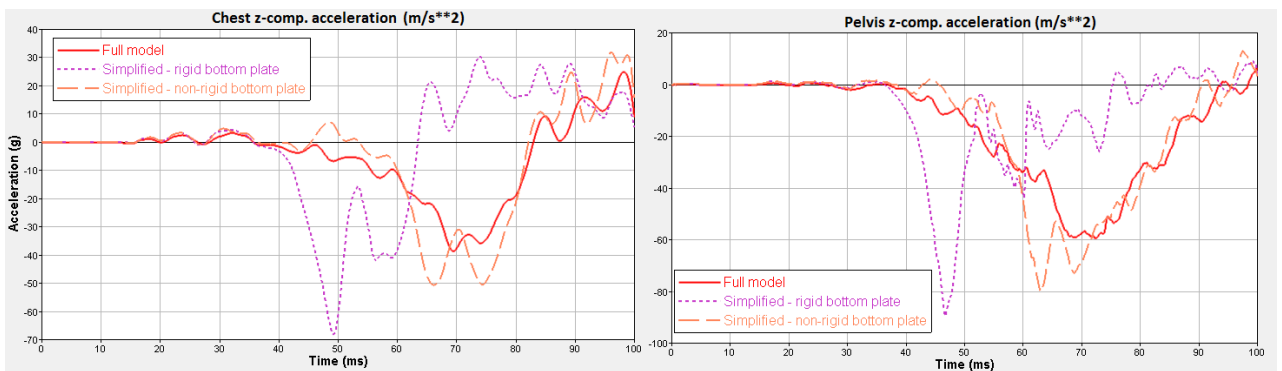


Figure 3.4: Chest and pelvis acceleration in the z-direction for the dummy in the P5 model. The graphs show the full model and two simplified models, one with rigid and the other with non-rigid seat bottom plate

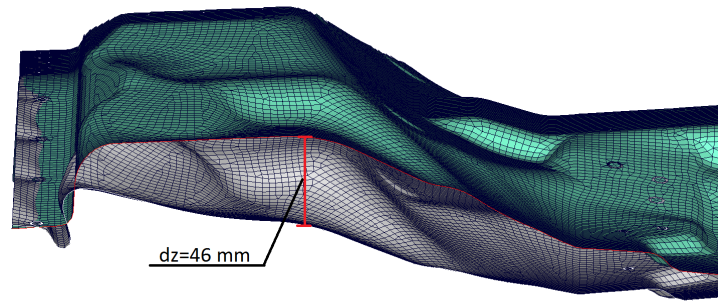


Figure 3.5: Deformed and undeformed seat bottom plate, showing the difference between a rigid seat bottom plate and a non-rigid for the P4 model. The z-deflection at an arbitrary point is highlighted in the figure

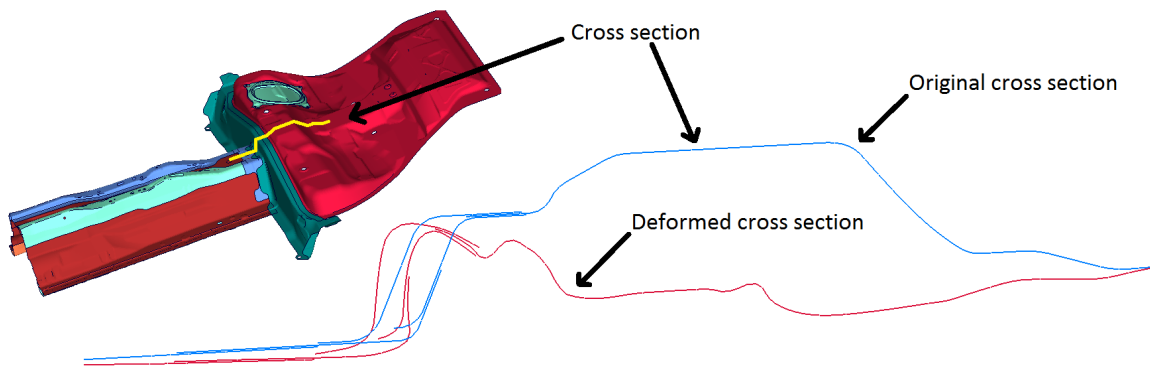


Figure 3.6: The components contributing to the total response from the seat bottom plate at the 5th position, and a cross sectional cut through the 5th position showing the deformation profile in the P5 reference model

Figure 3.5 shows the significant difference between the deformed non-rigid seat bottom plate compared to the rigid undeformed plate. According to experienced analysts at VCSC this specific seat bottom plate is unusually compliant, and in order to investigate how the compliance of the seat bottom plate affects the results obtained from the dummy, the stiffness of the bottom was varied in a parameter study presented in Section 5.3.

New runs were performed with the same set-ups except for the bottom plate which now was assigned with the original material properties and fixed rigidly to the sled by the existing weld points. The results for the P4 model confirmed the assumption made for the seat bottom plate. The peak values observed in the previous run were now gone and the results can be seen in Figure 3.3, curves labelled “Simplified – non-rigid bottom plate”. For more results see Appendix B.

The conclusion drawn from this was that the structure underneath the rear seat need to be somehow deformable, otherwise certain data will be significantly affected. When studying the P5 model it can be seen that the new simplified model with the non-rigid seat bottom plate did not give as good result as the P4 model, see Figure 3.4, curves labelled “Simplified - non-rigid bottom plate”.

The impact forces from the larger dummy cause deflection to occur in several more components underneath the seat bottom plate. Thus, more components under the seat bottom would need to be included in order to get as close as the P4 model. In Figure 3.6 the components involved in the total response at the seat bottom plate in the reference P5 model are displayed, together with the deformation profile of a cross section in the seat bottom.

Seatbelt mounting

In the two simplified models, the seatbelt mounting points are attached rigidly to the sled, hence they allow for no deformation. This deformation might be significant for the results and could partly explain why the results for the simplified P5 model were more off than for the P4 model. The 95th dummy caused more deformation in the buckle and anchor attachments than the 5th dummy, due to its weight. Therefore, the P5 model was run again in full scale but this time the seatbelt was mounted in the same way as in the simplified model. The

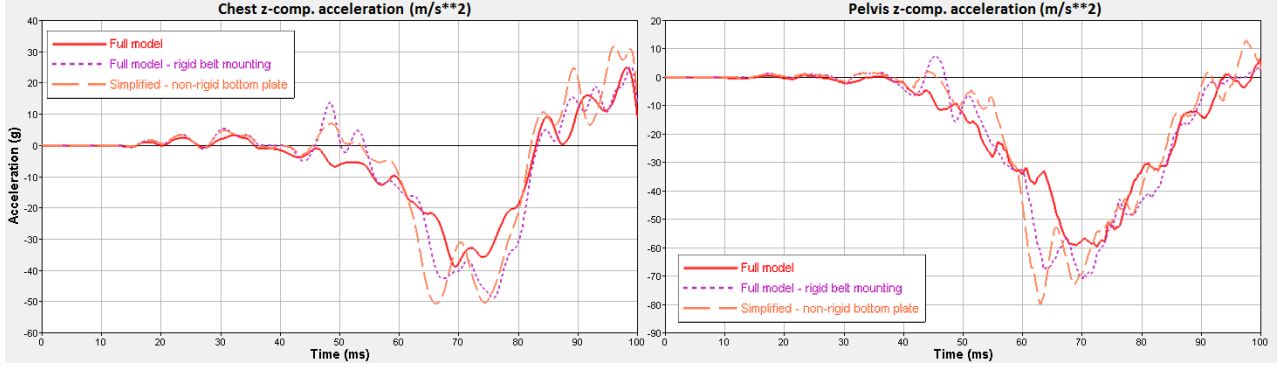


Figure 3.7: Chest and pelvis acceleration in the z-direction for three variants of the P5 model.

result can be seen in Figure 3.7.

The curves in Figure 3.7 indicates that the deformation in the seatbelt attachment points are significant for the 95th dummy at the 5th position. For the reference model in this case the deformation in the Z-direction for the buckle attachment point is more than twice as large as for the anchor attachment point. Thus, the compliance of the buckle fixture point is deemed as significant.

When it comes to the retractor, the difference in attachment is that for the simplified model the retractor is allowed to bend down when the belt is loaded. In the original model it is prevented from doing this because of a supporting basis, compared to the simplified model where the rear part of the retractor is fixed to the sled by a small beam element. To see how much this rotation affects the results another simulation was performed where the whole retractor was rigidly constrained to the sled. The results from this shows that this difference does not affect the dummy data significantly, thanks to the compensation from the load limiting in the seatbelt. Some results can be seen in Figure 3.8 which show the upper neck forces, F_x and F_z . To summarise, for this car platform, the buckle attachment point should be deformable but the anchor as well as the retractor may be rigidly attached to the sled. This confirms the importance of the given requirement that the compliance of the seatbelt attachments shall be adjustable, at least for the buckle.

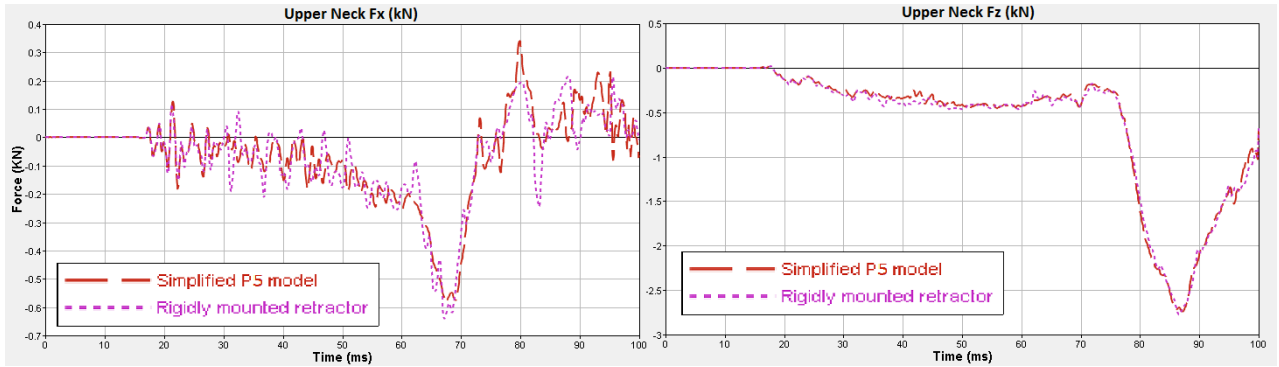


Figure 3.8: Upper neck forces, F_x and F_z , for the simplified P5 model when the retractor is rigidly constrained compared to when it is allowed to tilt

3.2.2 Rear seat backrest

In the initial position, the dummy rests against the backrest. Simulations from front crashes show that immediately after the crash the dummy leaves the backrest, see Figure 3.9. Thus, in a frontal crash testing point of view, the main function of the backrest is to give the initial position to the dummy. Depending on how the seatbelt is positioned it may affect the belt force and the dummy due to friction and the fact that the shoulder belt passes the backrest and may come into contact. Therefore it may be possible to replace the original backrest with a simplified component in a frontal crash test rig.

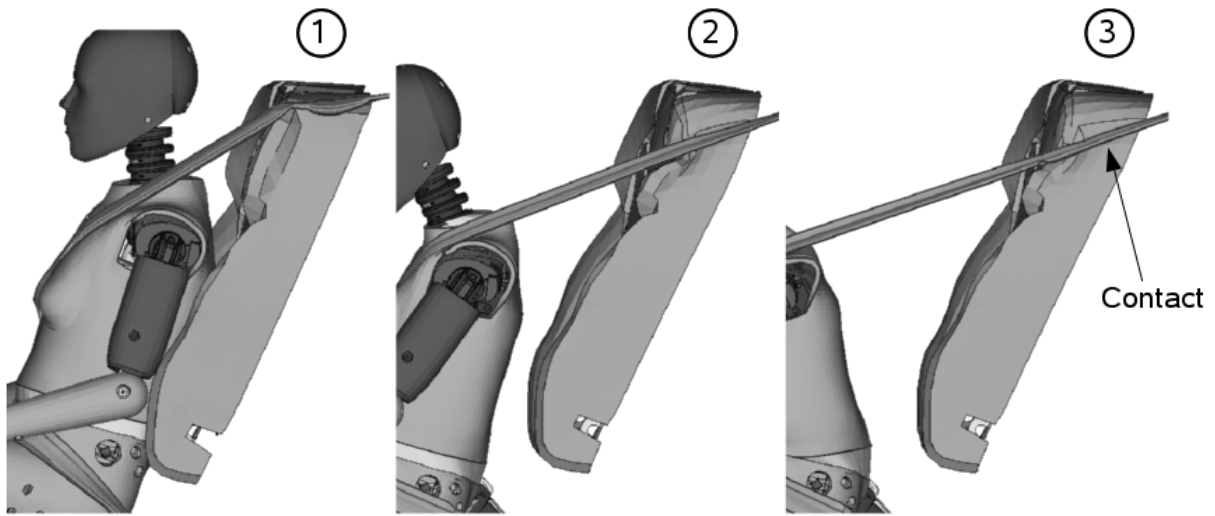


Figure 3.9: Interaction between dummy and rear seat backrest for the P4 model. 1. Initial position 2. After 40 ms 3. After 80 ms

3.2.3 Seat cushion attachment

In the original seat bottom model the seat cushion is only fastened to the seat bottom plate in three points in the front end of the seat. This allows a large area of the seat cushion to slide against the seat bottom plate during the crash. To find out if this affects the results significantly a simulation was performed where the cushions were modelled as glued to the bottom plate, by not allowing any relative movement between the lower seat cushion surface nodes and the seat bottom plate. The simplified models with non-rigid seat bottom plates were used. Figure 3.10 show the chest deflection and the pelvis acceleration in the z-direction for the P4 model. It can be seen that the two set-ups give similar results. This could also be seen for the rest of the dummy data. The pelvis acceleration for the P5 model can be seen in Figure 3.11 and this shows the same result. The conclusion drawn from this is that the mounting of the seat cushion to the seat bottom has less significance.

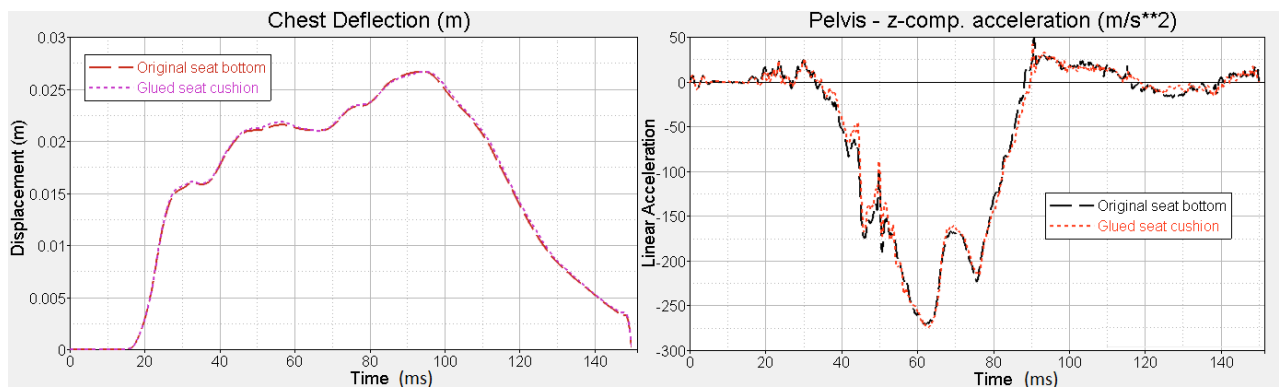


Figure 3.10: Chest deflection and pelvis acceleration in the z-direction for the simplified P4 model with non-rigid seat bottom plate, using the original seat cushion mounting compared to gluing the seat cushion to the bottom plate

3.3 How to capture necessary behaviour with the rig

In the previous section the focus was to find what characteristics are most important for the rig to have. This section will instead focus on how to capture these characteristics and still fulfil the given requirements described in Section 3.1. The approach was to replace components with solutions having a similar behaviour and which

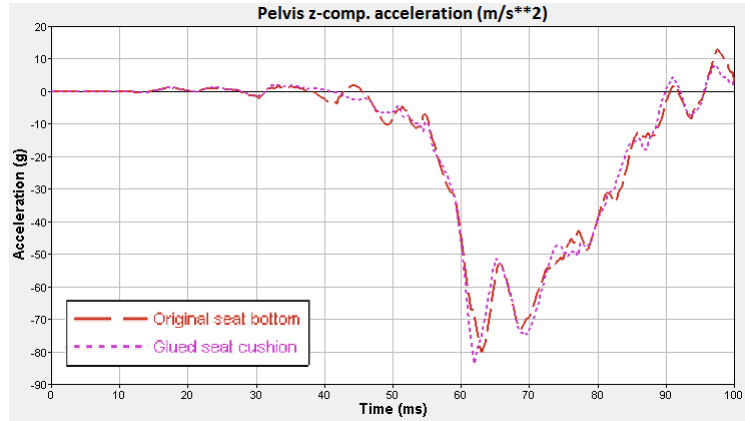


Figure 3.11: Pelvis acceleration in the z-direction for the simplified P5 model with non-rigid seat bottom plate, using the original seat cushion mounting compared to gluing the seat cushion to the bottom plate

can be part wise correlated. The reason was to avoid special-case solutions, i.e. combinations of many solutions happens to give a good result for one case but while, in general, it is hard to adjust for an arbitrary case.

3.3.1 Foot stop

In certain rig tests the front seats are not included, and in such cases something is needed to restrain the dummy's legs realistically, otherwise they will not behave as in a crash and will thus affect the obtained results, see Figure 3.12. Some different kinds of foot stops were tested at different distances and the best result was obtained using a rigid bar, see Figure 3.13. Using this kind of foot stop bar had large impact on the legs and thus it can not be used if leg related data are of interest.

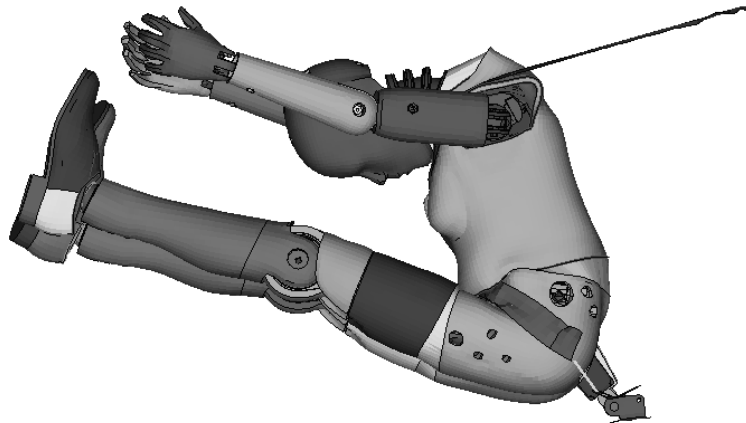


Figure 3.12: Simulation without front seat or anything else to stop the dummy's legs

Mainly two phenomena was observed when studying the results using the foot stop. The first has to do with the initial impact from the bar and it appears as distinct spikes in e.g. the pelvis acceleration. Figure 3.14 shows the pelvis acceleration in the x-direction, where the spikes mentioned can be seen between 40 and 50 ms. The second phenomenon observed was that the feet may get stuck in an unnatural way, especially if the bar is placed at an inappropriate position, see Figure 3.15. This foot stop concept was not further evaluated but future results will be studied with these results in mind.



Figure 3.13: This figure shows the bar used as foot stop at the 4th position when the front seat was not included

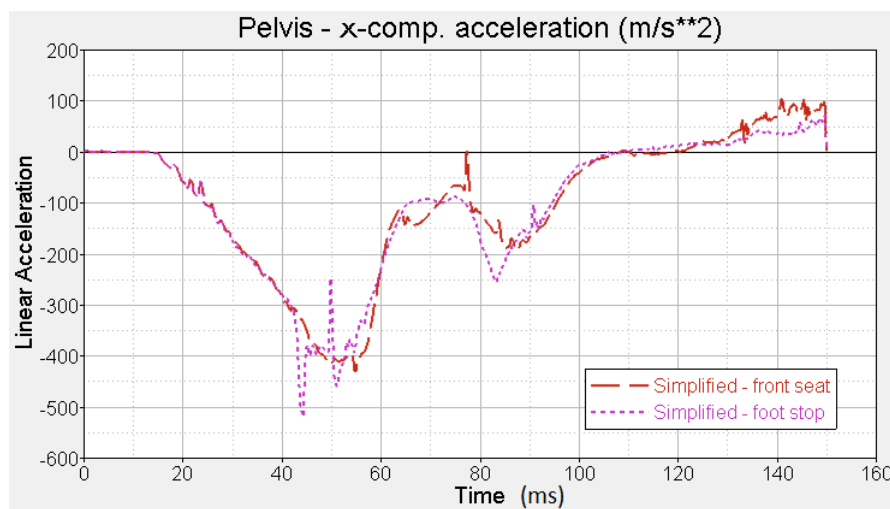


Figure 3.14: Pelvis acceleration in the x-direction for the P4 model when using front seats compared to a foot stop bar

3.3.2 Tilting seat bottom plate

Simulations of the deformable seat bottom plate were studied in order to see if it would be possible to use a rigid seat bottom plate and still catch the right behaviour by letting it tilt or move in a predefined path. In Figure 3.16 two lines are drawn, for the P4 model, to clarify the main deformation shape of the seat bottom plate and how it is related to its initial shape. The arrow points out where the dummy pelvis acts upon this rear part. These lines gave the idea of a tilting rigid bottom plate employing some kind of deformable element which can be exchanged for each run.

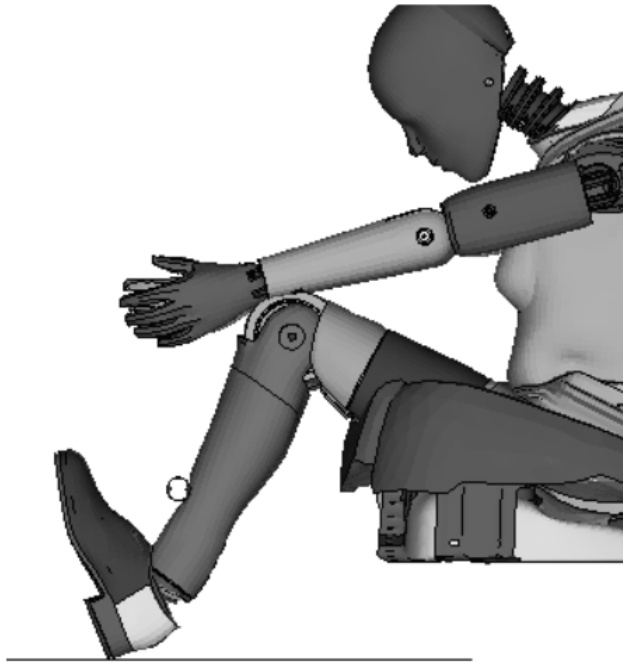


Figure 3.15: Foot stop bar is placed too close to the dummy, causing the legs to get stuck, hindering the pelvis and femur to move forwardly as they would have otherwise

Springs

To investigate this idea of a tilting seat bottom plate, a first step was to replace the welds, attaching the seat bottom plate, with a hinge in the rear part and two linear elastic springs in the front part, see Figure 3.17. As reference model in this case, the simplified model, with non-rigid seat bottom plate, was used. The reason was that this model has the same set-up except for the seat bottom plate and thereby this difference could be evaluated separately.

Different spring stiffness were tested through rough estimations and some of the results can be seen in Figure 3.18. The chest acceleration shows a similar negative peak value, but the elastic springs causes significantly more throwback and overshoots the reference model results, which has plastic deformation in the seat bottom. Between 80 and 100 ms higher values can be observed for both the acceleration and the moment. This has to do with the elasticity of the springs and the shape of the seat bottom plate. After maximum displacement of the seat, the springs pushed the dummy back which was not the case for the plastically deformed original seat bottom plate. Figure 3.19 shows the difference in motion, of the dummy's hip and thighs, between the reference model and two different spring models. The two images are taken just before and after the peak values shown in the graphs just described. For both spring models the pelvis location was rather close to the reference but the thighs had tilted down too much at maximum displacement. However, after 30 ms the thighs had been pushed up to a similar position as for the reference model. In this case the original shape was used for the rigid bottom plate in order to keep the model clean and free from special-case solutions. The shape makes the plate more stiff in the front part, hence a pure tilting solution could not capture the right behaviour. The conclusion from this investigation is that some kind of permanent deformation in the seat bottom plate is desirable and the the seat bottom shall appear somehow more stiff in the front.

3.3.3 Summary of found requirements

Except for the given requirements described in Section 3.1, the simplified models and the sub-concepts described in previous and current sections contributed to additional requirements. A summary of these are listed below.

- The seat bottom need to be deformable with the possibility of permanent deformation
- The buckle mounting shall be deformable to some extent

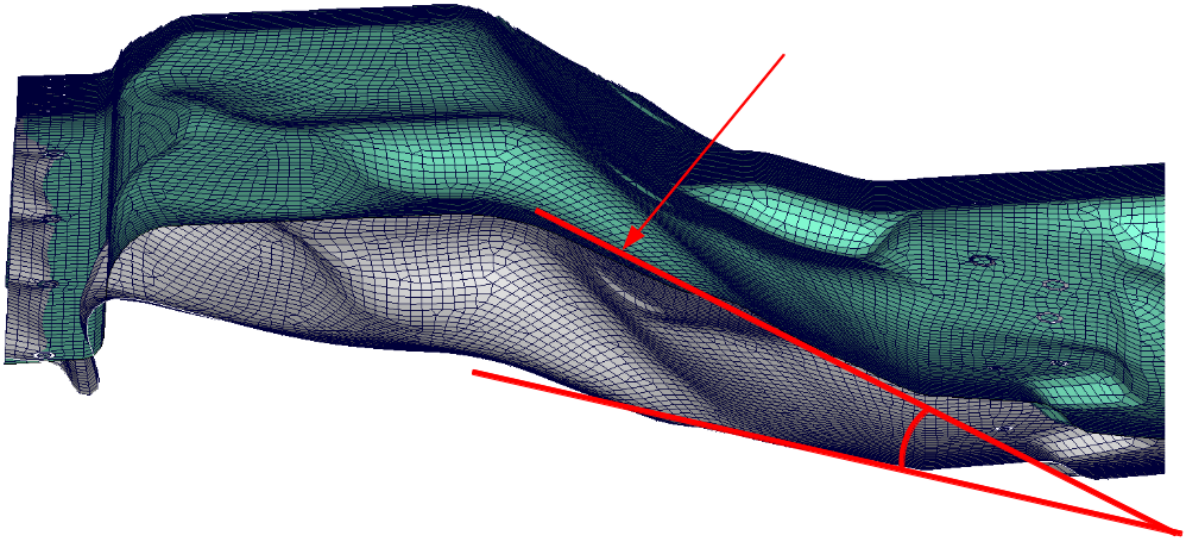


Figure 3.16: Main deformation shape of the seat bottom plate for the P4 model. The arrow points out where dummy pelvis acts upon this rear part

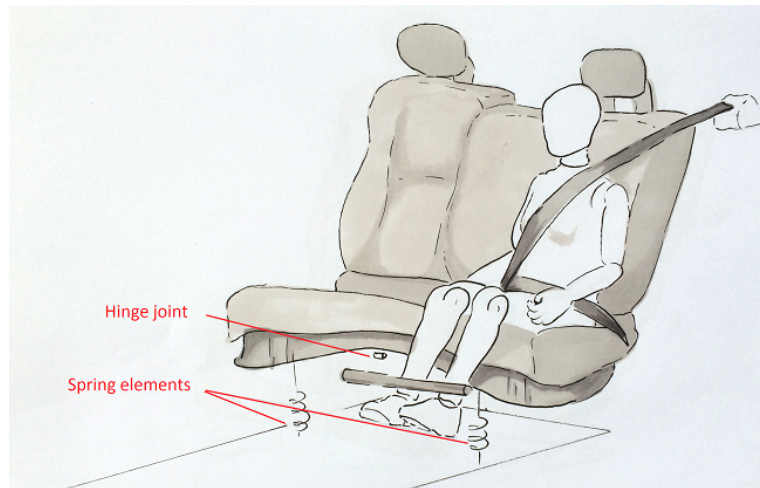


Figure 3.17: Set-up for the simplified model with rigid seat bottom plate mounted with two springs in the front and a hinge joint at the rear part of the plate

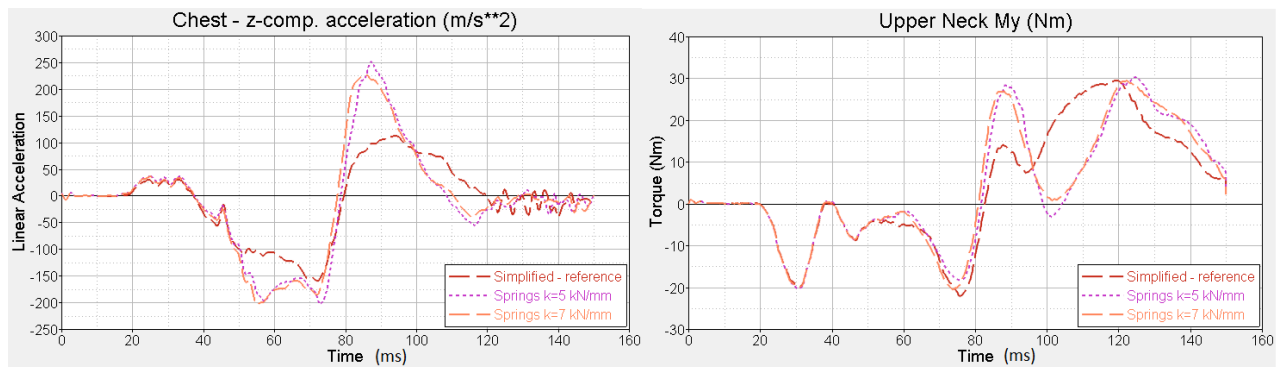


Figure 3.18: Chest acceleration in the z-direction and the upper neck bending moment, M_y , for the P4 model when using linear elastic springs compared to the simplified model with non-rigid seat bottom plate

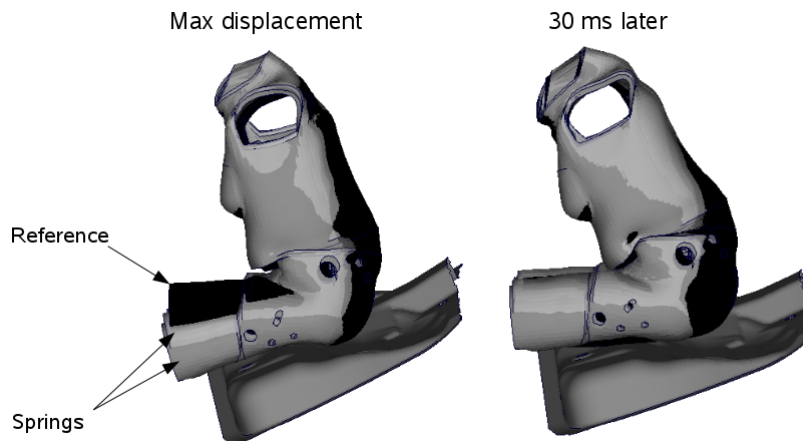


Figure 3.19: Difference in motion of the dummy's hip and thighs at two different moments. The two gray shapes are from spring models and the black shape is the reference

- The front seats may be replaced with some kind of foot stop, depending on what is studied. In that case, care must be taken when placing it, since the dummy's legs might get stuck, which can affect other data
- Rear seat cushion mounting has minor importance for the results

3.4 The generic rig concept

The rig concept displayed in Figure 3.20 is designed to be generic and allow for easy changes in the test set-up, while capturing the effects present in a real car environment during a crash. The rig concept is based on an available sled test plate, with screw holes spaced 100 mm apart in X and Y-direction, see Figure 3.21. As every component is screwed to this plate, changing a component is easily obtained, which allows for easy updating of the test rig. The rig concept has two main functions, emulate the car structure under the rear seat (seat bottom plate), and provide adjustable fixing points for the seatbelts.

3.4.1 Generic seat bottom structure

The rig seat bottom consists of three main parts:

A rigid bottom plate

Forms the base of the whole seat bottom structure and serves to obtain the main deformation path identified in Section 3.3.2. The plate is divided into two parts; a front part rigidly attached to the hole plate and a rear part mounted on the hole plate with hinge joints, see Figure 3.22.

A seat bottom foam

Expanded PolyPropylene (EPP) foam is attached to the bottom plate. The upper side of the foam is shaped like the seat bottom plate in the full scale reference models, to keep the initial condition for the dummy, see Figure 3.23. Different foam density can be used in the front and rear part respectively to adjust the stiffness. In the current concept, a lower density softer foam is used in the rear part and a higher density stiffer foam is used in the front part. The EPP foam material allows for easy creation of different seat bottom geometries, since it can be easily cut into different shapes that can be glued together.

Exchangeable plates

Small plates, referred to as bendplates, supporting the rear part of the seat bottom plate. Spikes attached to the rigid bottom plate rests on the plates, see Figure 3.24. When the bottom plate is loaded, the bendplates deform resulting in a tilting motion of the rigid rear seat bottom plate. The geometry, in terms of length, width and thickness of the bendplates can be customised to capture the right behaviour. The plates have supporting rollers which can be moved along the plates to change the point of bending relative to the spikes. The fixture point of the plates can also be adjusted relative to the spikes.

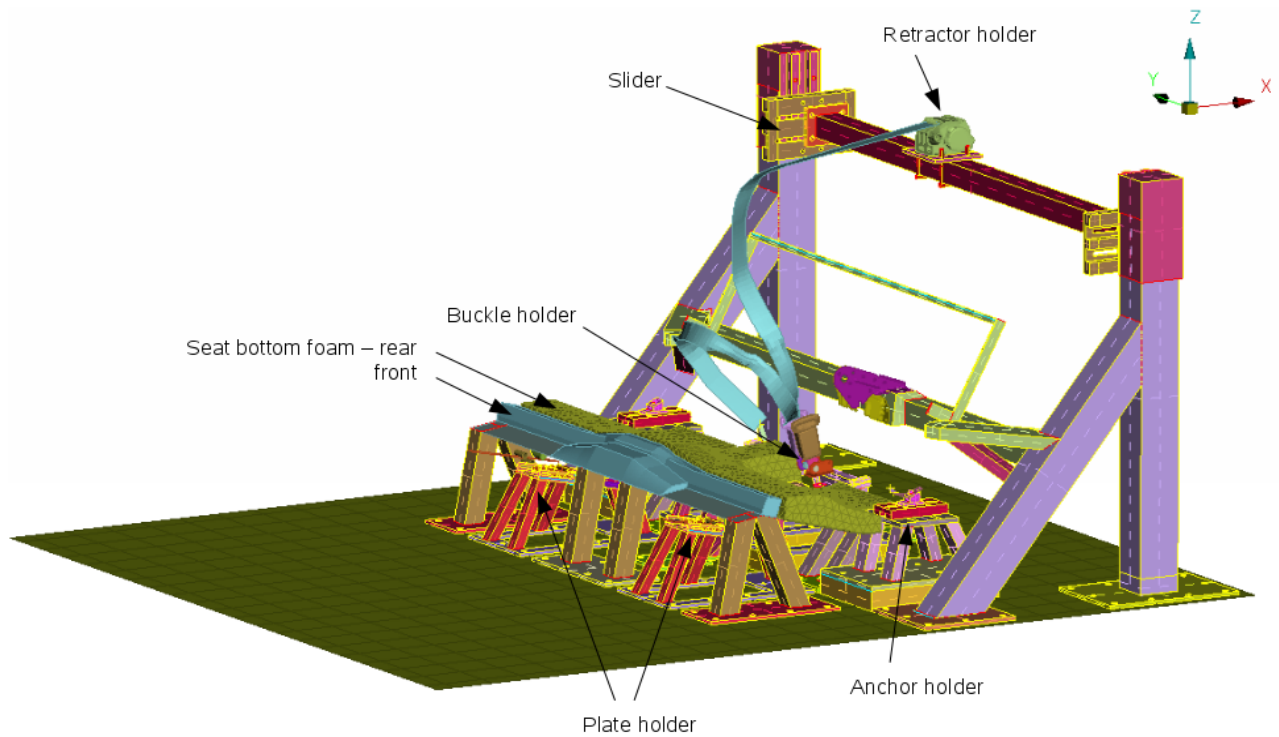


Figure 3.20: The designed generic rig concept



Figure 3.21: A plate with screw holes used today for sled testing

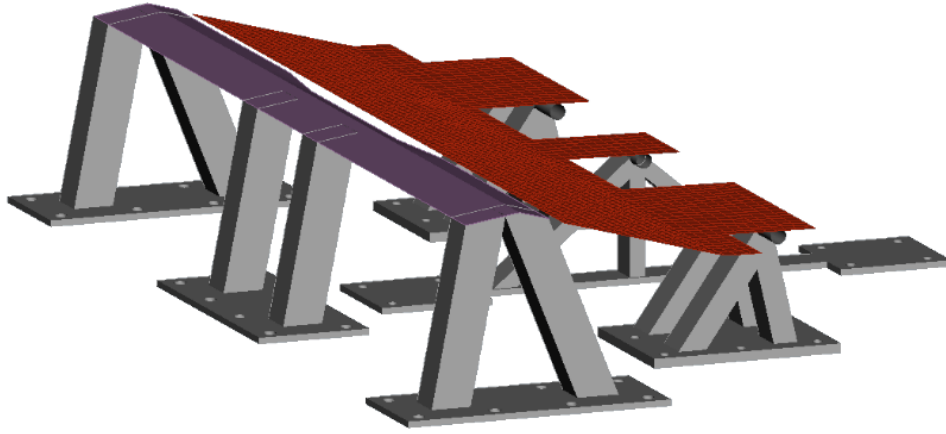


Figure 3.22: Rigid bottom plate

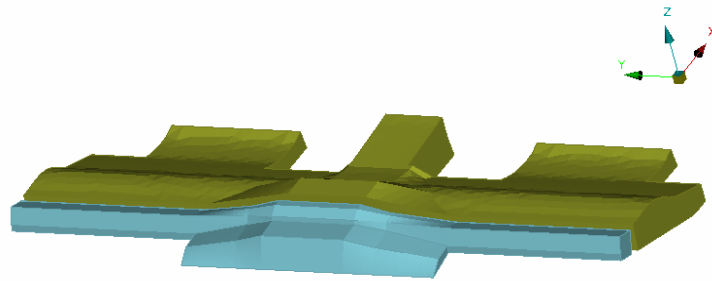


Figure 3.23: Seat bottom foam made out of EPP foam

The seat bottom is shaped to allow for a variation in seatbelt positioning, see Figure 3.25. If there is a need to perform a test with a rigid seat bottom, the spikes and the bendplates can be replaced with a rigid structure under the seat bottom, thus locking the tilting motion.

3.4.2 Seatbelt fixtures

In order to adjust the seatbelt attachment points three different concepts will be presented; for the retractor, the buckle and the anchor respectively. All of them allow for movements in the X, Y and Z-direction.

Retractor

Figure 3.26 shows the overall concept for the retractor attachment. Two towers with an interconnecting beam form the backbone. On top of each tower there is a hat resting on a screw in the tower. It can be extended 50 mm in the Z-direction by adjusting the height of the screw. The beam is attached to the hat via a slider device, which allows for the bar to be moved ± 50 mm in the X-direction, see Figure 3.26. The slider can be fixed to the hat at two different levels in the Z-direction 50 mm apart, giving a total flexibility of 100 mm. The slider can be seen in detail in Figure 3.27 and Figure 3.28. Since the main load will act in the sliding direction there is also a concept of stop screws to avoid unwanted sliding in the X-direction, see Figure 3.29. The retractor is then mounted on the beam according to Figure 3.26. It can therefore be placed at an arbitrary position with respect to the Y-direction.

Anchor

The anchor holder is based on two sliders similar to the one described for the retractor. They allow moving in the X and Y-direction, ± 50 mm in each direction. For the Z-direction the position can be varied ± 50 mm using shims to obtain the desired height. An overview of the anchor holder can be seen in Figure 3.30.

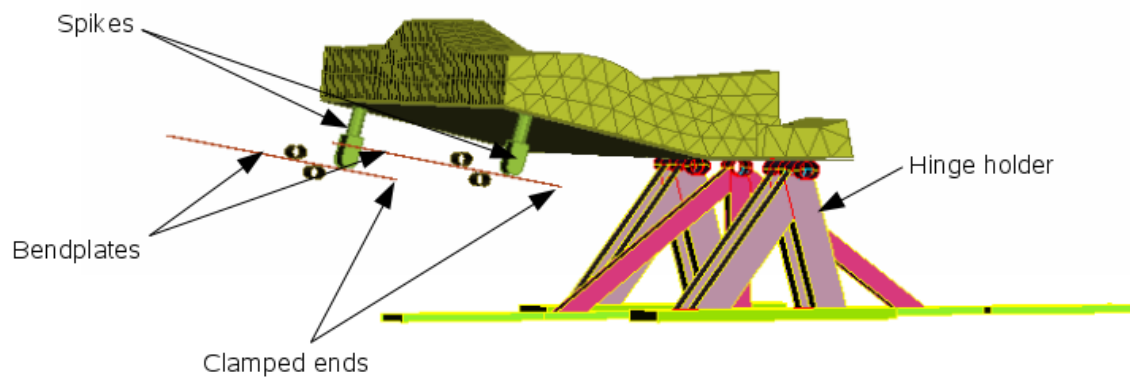


Figure 3.24: Deformable plates under a tilting seat bottom plate

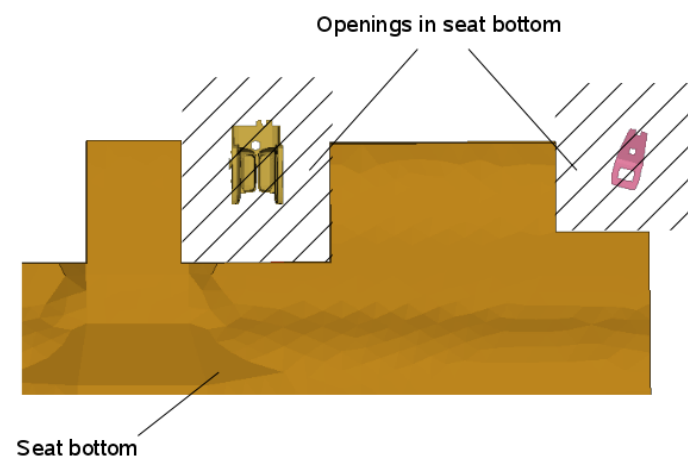


Figure 3.25: Seat bottom from above

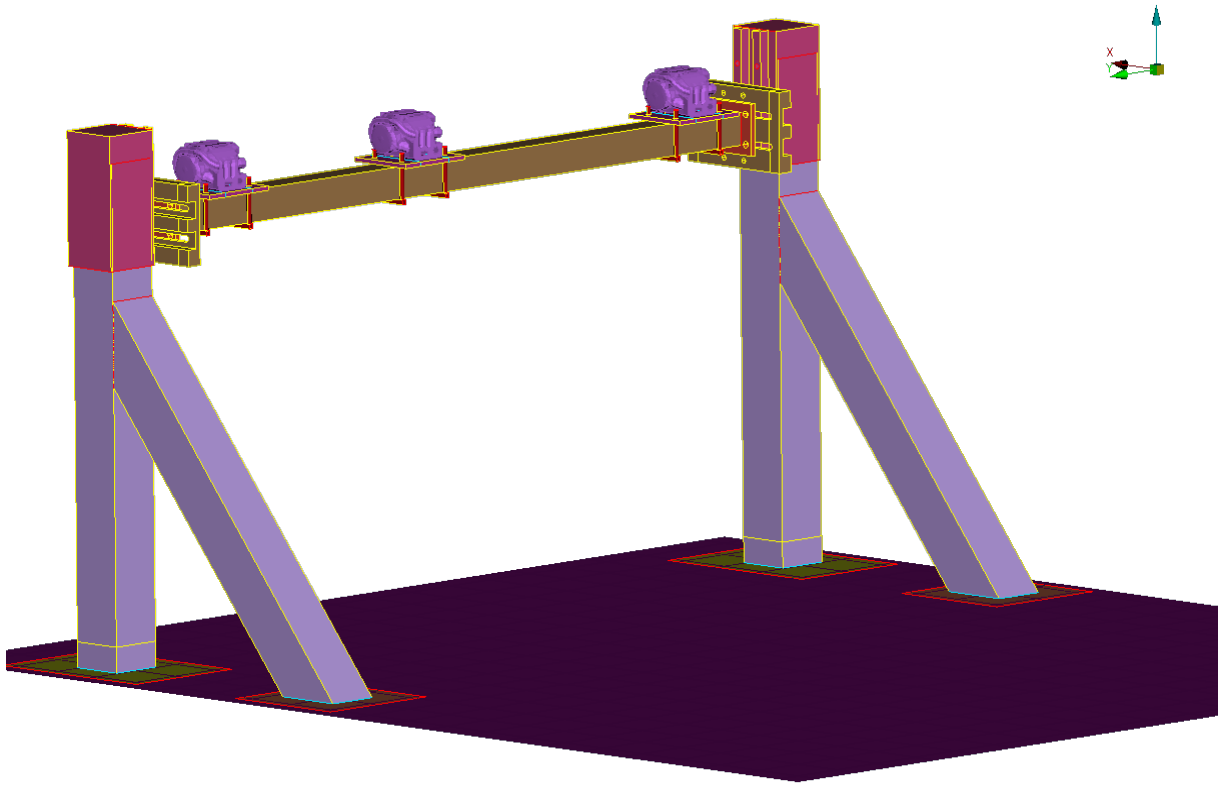


Figure 3.26: Towers for retractor attachment

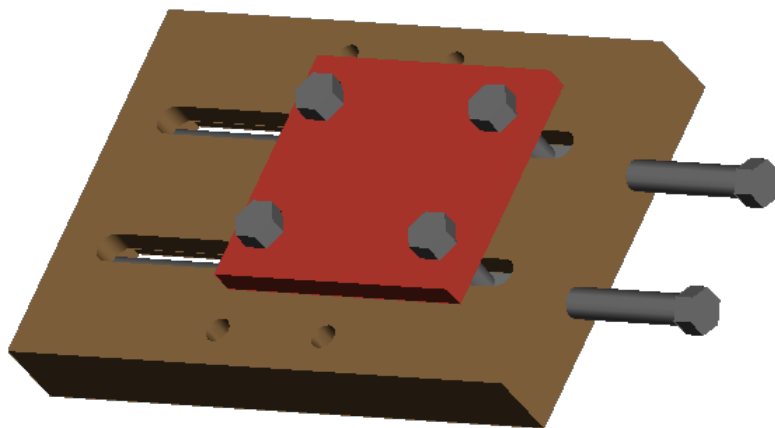


Figure 3.27: Detail of a slider attachment

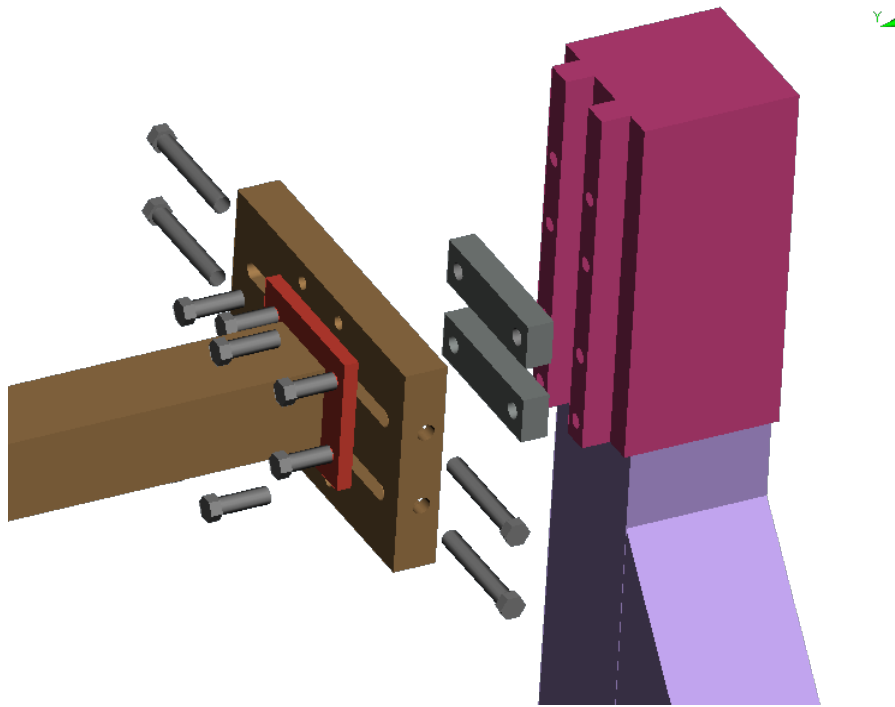


Figure 3.28: Exploded view of the slider mounting of the beam between the two towers

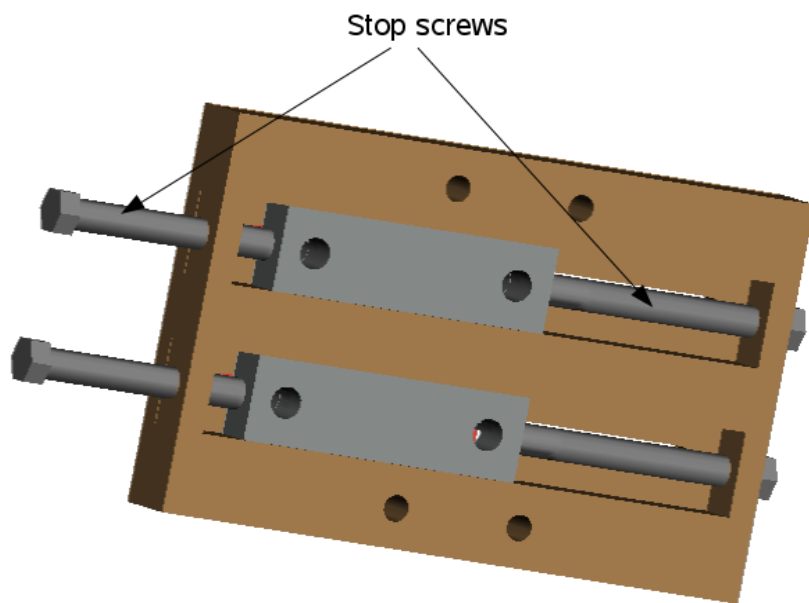


Figure 3.29: Concept of a slider attachment with extra screws to prevent it from slide when tightened

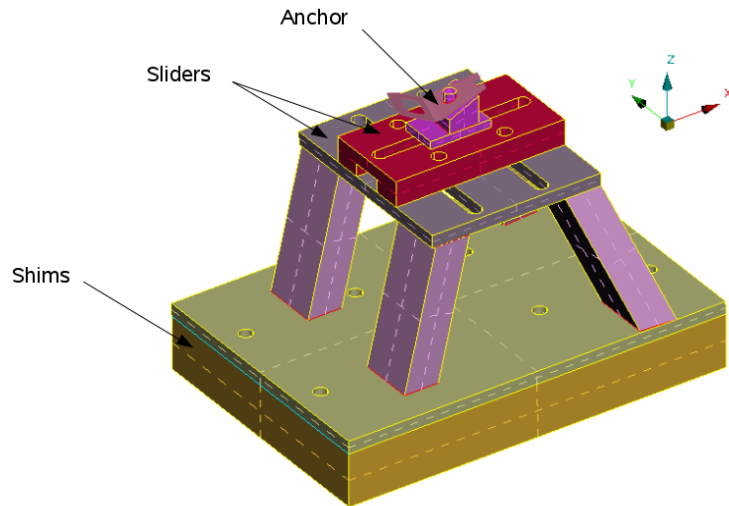


Figure 3.30: Anchor holder

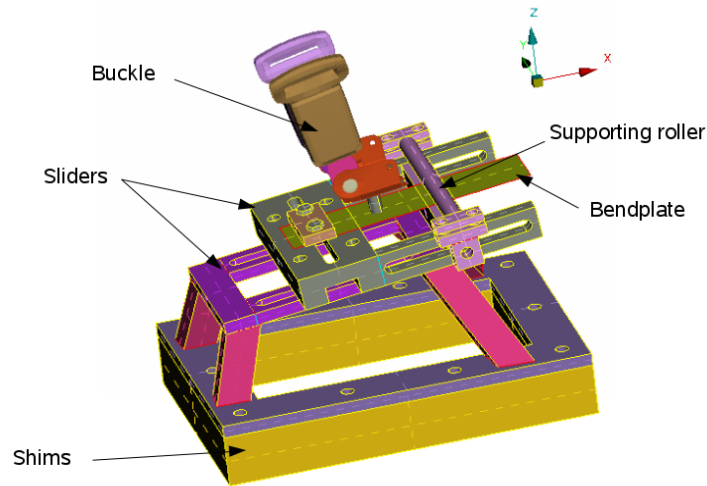


Figure 3.31: Buckle holder

Buckle

The concept for the buckle holder is similar to that described for the anchor. There are two sliders for positioning in the X and the Y-direction respectively and shims are used to adjust the height. The main difference is that the deformation in the buckle attachment point was found in Section 3.2.1 to be significant. To capture this behaviour, a concept with a deformable plate, similar as for the seat bottom plate, is applied here. The buckle is attached to a bendplate which in turn is mounted on the top slider. When the buckle is loaded, the plate will deform and the buckle is pulled up, see Figure 3.31. This deformation can be adjusted by changing the position of the supporting rollers relative to the buckle fixing point as well as the thickness and the width of the deformation plates.

An overview of the anchor, buckle, plate and hinge holders can be seen in Figure 3.32 and Figure 3.33 shows how the different components can be attached to the hole plate. Please note that it is possible to add front seats to the rig if there is a need for that and there is also room for measurement equipment behind the seat.

3.4.3 Assumptions made for the rig concept

There are some uncertainties regarding the rig concept and a few assumptions were made:

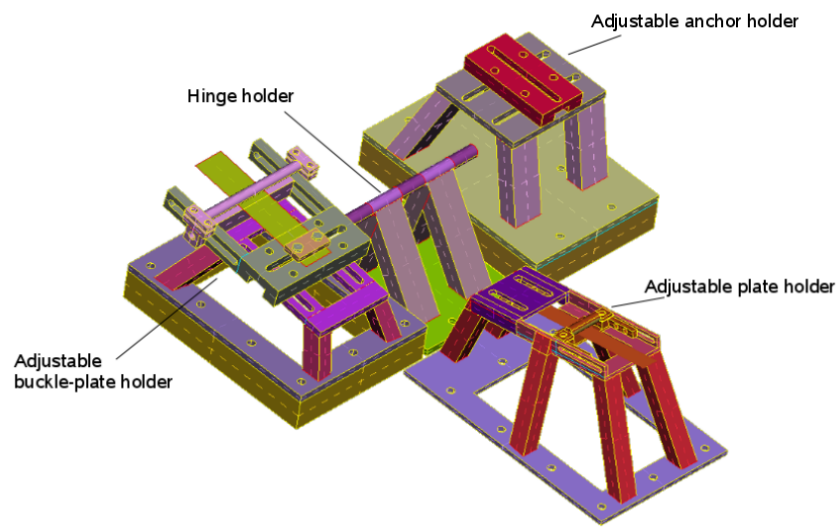


Figure 3.32: Buckle, anchor, plate and hinge holders

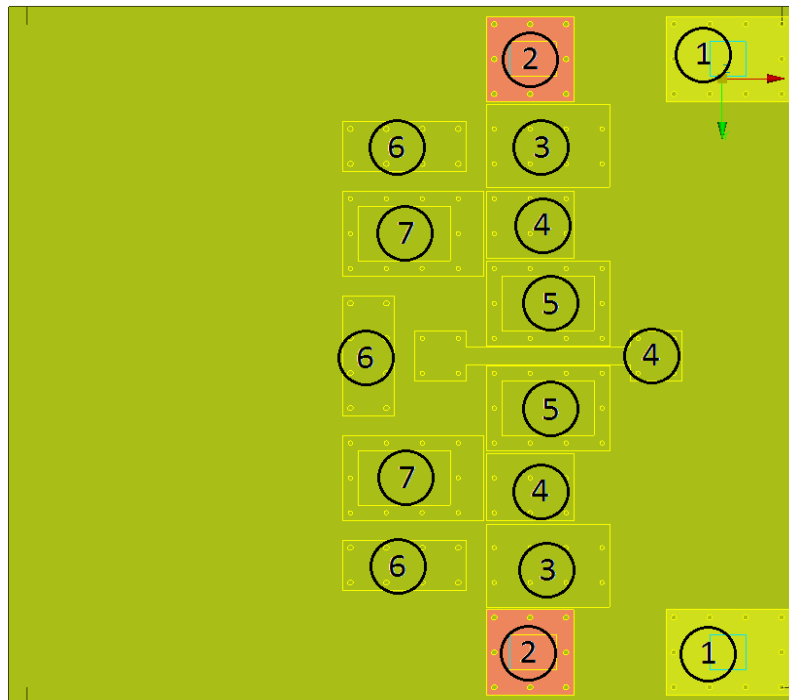


Figure 3.33: An overview of the hole plate showing how the holes have been utilised for all components to fit and be fixed to the hole plate. 1: Retractor towers, 2: Retractor tower supporting legs, 3: Anchor holder, 4: Rear seat bottom hinges, 5: Buckle holder, 6: Front seat bottom, 7: Seat bottom bendplate fixtures

- The weight of the rig, when fully dimensioned, is assumed to be at an acceptable level with respect to the crash simulator which will generate the acceleration pulse
- The concepts described are possible to produce and assemble at the workshop at VCSC
- The components described as rigid can be dimensioned to be reusable and rigid in the sense that during the tests there will they will be subjected to small elastic deformations

3.5 Results from the rig FE model

In this section the results from the rig FE models will be presented. The positioning and sizing of the deforming elements in the rig models were tuned using target data from the reference models using system identification in LS-OPT as described in Section 4.2.

3.5.1 Set-up of rig FE model

The rig FE model consist of the functional parts in the designed concept together with the rear seat, dummy and seatbelt model pertinent to each case. All components and how they are constrained are listed below:

- The hole plate modelled as rigid. The hole plate is accelerated to obtain the crash boundary condition.
- The rigid seat bottom plate, divided into two parts. The frontmost part is fixed relative to the hole plate, and the tilting rear part is mounted with joints to the hole plate to allow the tilting motion.
- The spikes applying force to the bend plates, fixed to the tilting seat bottom plate.
- The EPP foams, fixed to their respective seat bottom plate.
- The bendplates underneath the seat bottom plate and at the buckle position. The bendplates are clamped in one end that will follow the motion of the hole plate.
- The rollers providing a second bend point for the bendplates are modelled as rigid and are fixed relative to the hole plate.
- The rear seat FE model, including backrest and seat cushion. Depending on which dummy is present, one of two different models of the same rear seat is used since the seat cushions are depressed according to which dummy is seated in them. The rear seat is fixed to the hole plate using the same fixture points as in the reference models.
- Seatbelt FE model including webbing, anchor, buckle and retractor model. One of two different seatbelt models is used, depending on which dummy is used. The buckle is attached to the buckle bendplate. The retractor and anchor is attached by existing screw elements (modelled by beam elements), whose end nodes are constrained to move with the hole plate.
- Crash test dummy FE model. A HIII 95th percentile male seated at the 5th position when testing the P5 case, and a HIII 5th percentile female seated at the 4th position for the P4 case.

In order to obtain a fair evaluation of the designed rig concept, the same floor and front seat set-up existing in the respective reference model was also included in the rig FE model, see Figure 3.34. Since the dummies will come into contact with these parts during the crash, they will have an effect of the obtained result. Exchanging these parts with a foot stop device is possible, but that will, as described in Section 3.3.1, change the results.

Different configurations for the deforming plates under the rig seat bottom are obtained when trying to replicate the result from the P4 and P5 reference models with system identification, even though they have the same seat bottom plate. This is due to the fact that the shape of the seat bottom plate as well as the underlying components differ between the 4th and 5th seat position.

The configuration for the P4 seat bottom bendplates can be seen in Figure 3.35. The bendplates are clamped 72 mm from the contact point of the spikes, and the center of the lower rollers is located 44 mm from the spikes. The bendplates have a width of 16 mm and are 2.5 mm thick.

For the P5 model, the lower roller is located under the spike, which means that the bendplates will not deform. This was intentionally allowed in the system identification procedure, to allow for a configuration

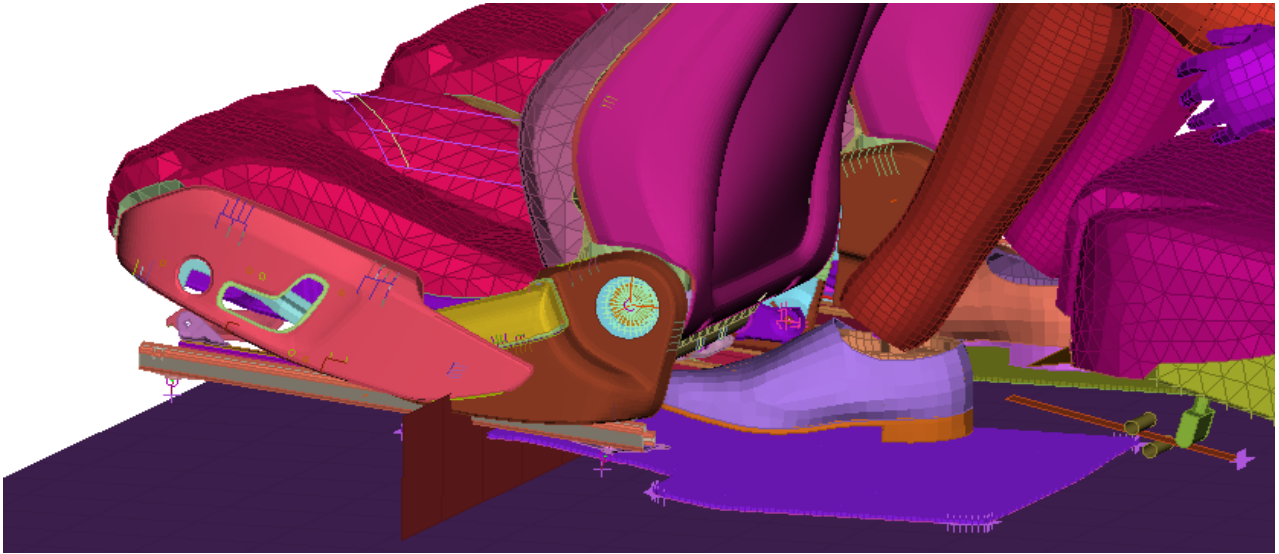


Figure 3.34: The front seats and floor parts interacting with the dummy in the P5 reference model, now included in the rig FE model. The deforming bendplates under the seat bottom of the rig can be seen in the lower right corner.

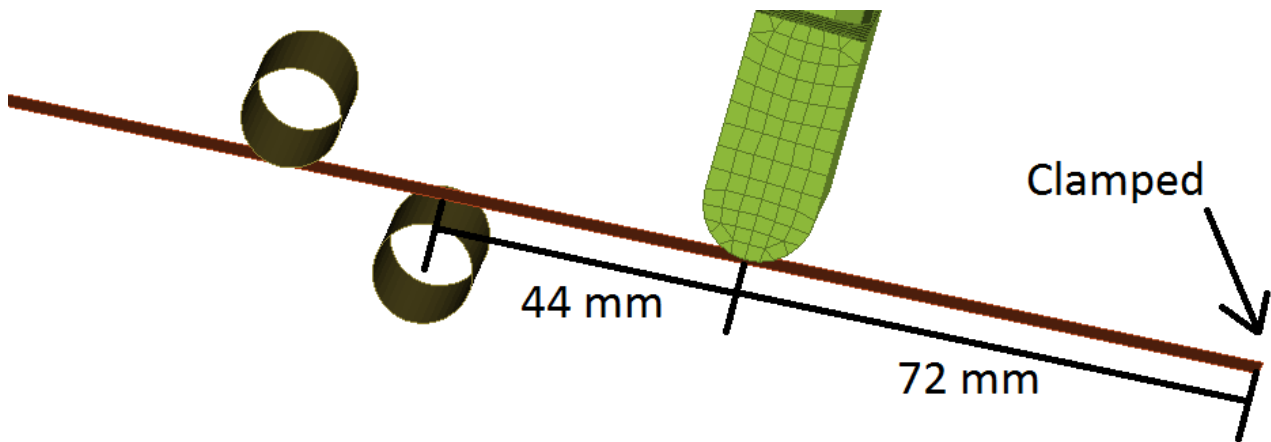


Figure 3.35: The configuration for the bendplates under the rig seat bottom in the P4 model

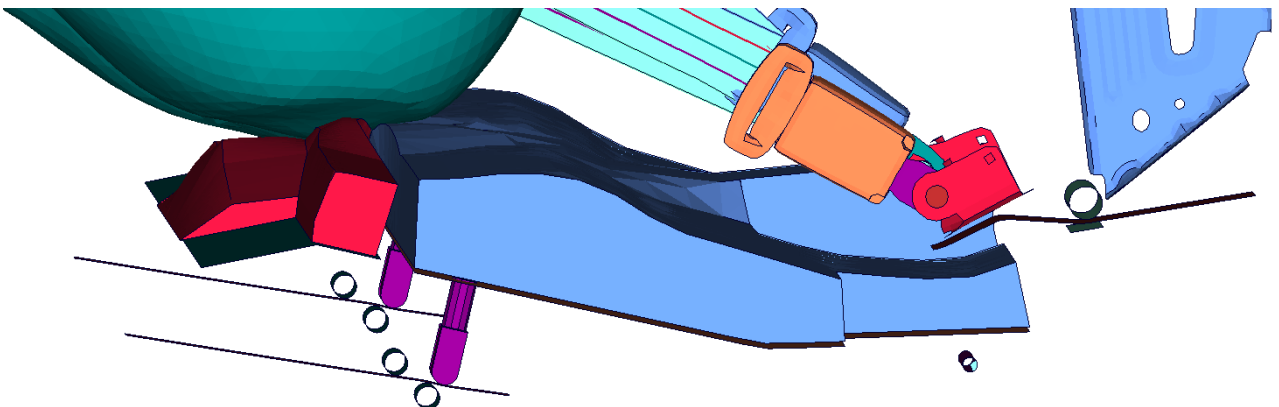


Figure 3.36: The locked bend plates under the P5 rig tilting seat bottom. The rear seat cushion is hidden from this view to show the deforming EPP foams. The deformation of the buckle fixture bendplate can be seen to the right

where the tilting motion of the rig seat bottom is locked. This means that the EPP foams in the rig seat bottom alone will represent rig seat bottom response, see Figure 3.36.

The bendplate and roller for the buckle were configured so that the fixture point of the buckle should obtain the same Z-displacement as in the P5 reference model, where the large 95th percentile male dummy and the 64 km/h initial velocity cause significant displacements to occur at the buckle fixture point during the crash. The obtained Z-displacement of the buckle fixture point in the rig can be seen in Figure 3.37.

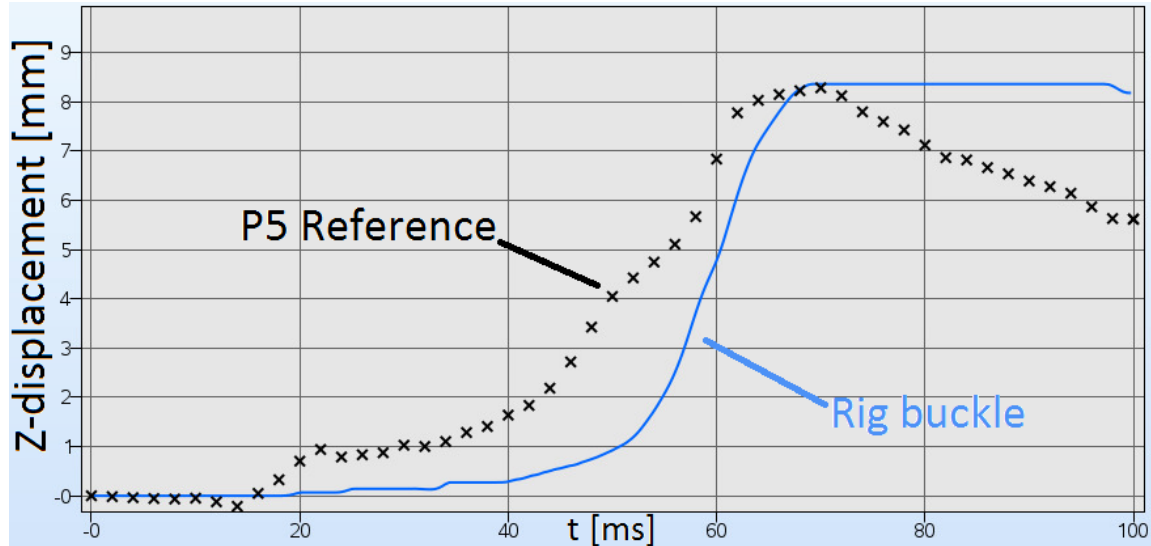


Figure 3.37: Z-deformation of the buckle fixture point for the P5 reference model and the buckle used in the P5 Rig.

In Figure 3.37 it can be seen that the same maximum Z-displacement is reached at the same time, however the Z-deformation of the rig buckle lags somewhat in time compared to the reference and the rig buckle fixture exhibits less springback. This has to do with the design of the deforming buckle fixture. With this design, it is simply not possible to achieve both the same displacement and shape. In the reference models the buckle is fixed to large supporting brackets under the seat bottom, and when loaded the reaction forces keeping the buckle in place are distributed over a larger area, causing a more elastic response. In the deforming buckle fixture concept for the rig, this load is only carried by the bendplate. Since both the compliance and the position of the buckle fixture should be possible to adjust in the generic rig, the size of the deforming fixture for the buckle is limited, in order to fit in the rig for every configuration.

In Figure 3.38, the configuration for the buckle fixture used in both rig models can be seen. The buckle is fixed at a distance of 40 mm from the clamped end of the 6 mm thick and 60 mm wide bendplate. The center of the bendplate roller is located 55 mm from the buckle fixture point. The reason that the same configuration is used in both models is that both the P4 and P5 reference models use the same fixture point for the buckle and thus, there should be no difference in compliance for this fixture point in the rig either.

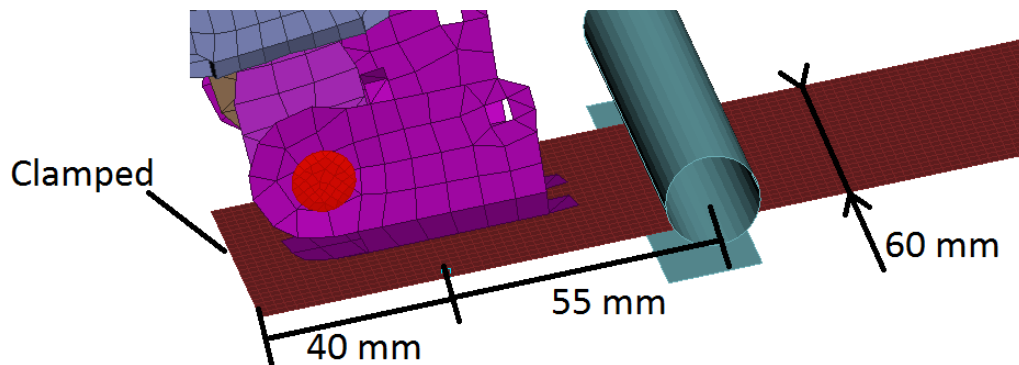


Figure 3.38: The configuration of the buckle fixture bendplate used in both rig models

3.5.2 P4 rig results

In Figures 3.39 and 3.40 the results from several dummy instruments can be seen together with the reference model results. The results obtained from the rig model in this case can be seen to closely approximate the reference model, regarding both the overall shape and amplitude of the time signals.

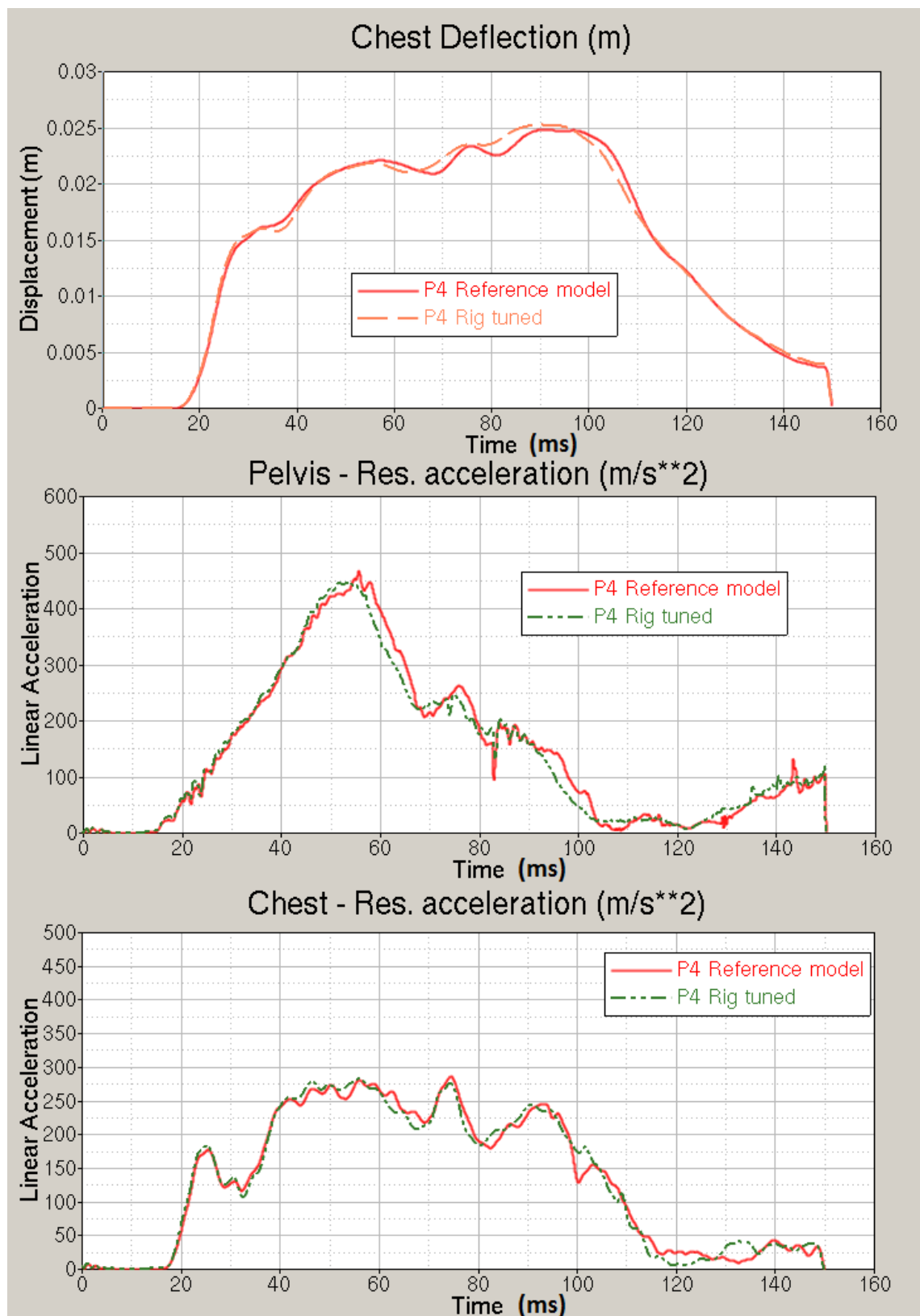


Figure 3.39: Chest deflection and the resultant acceleration of pelvis and chest for the P4 reference model and the P4 rig model

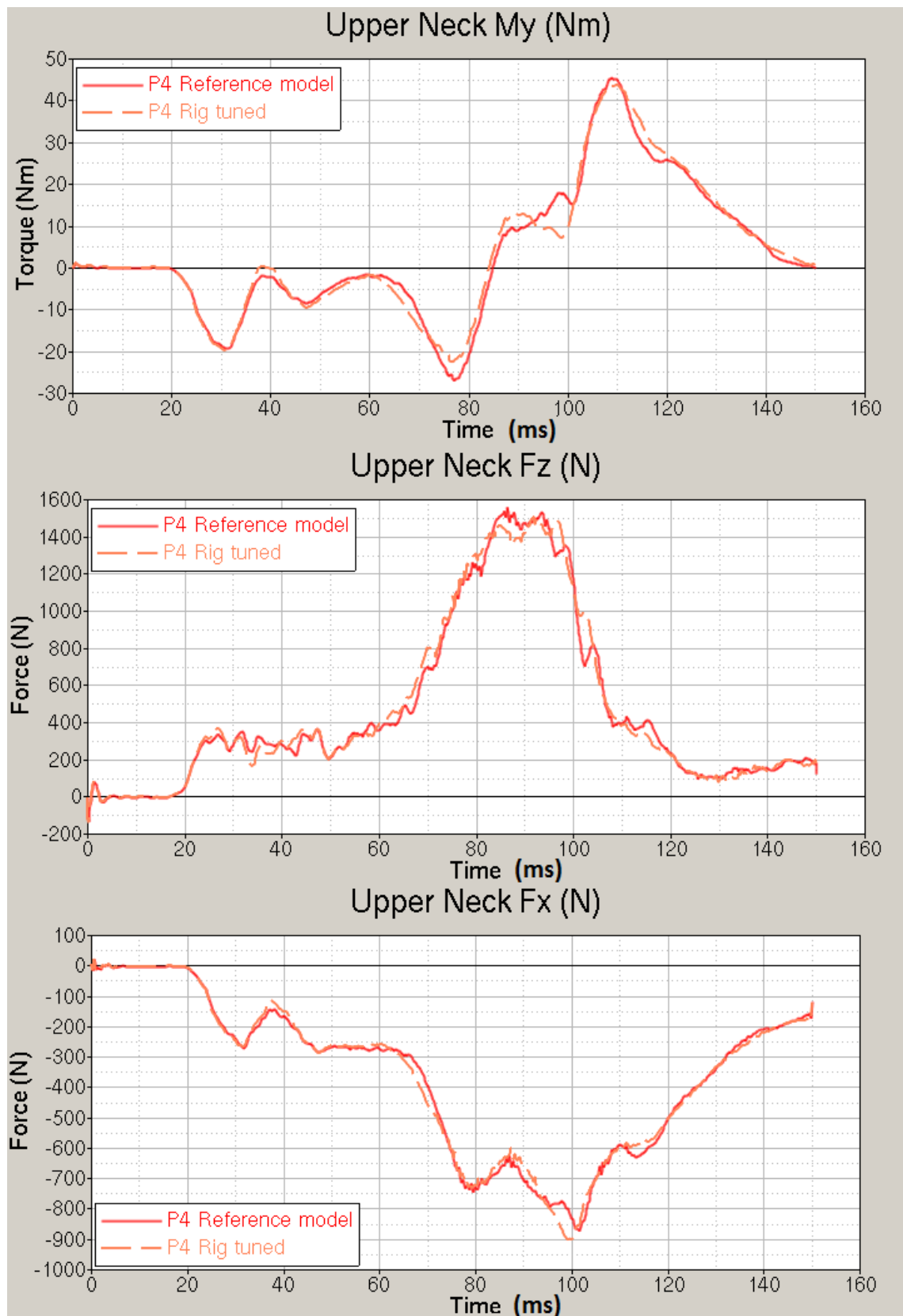


Figure 3.40: Upper neck forces for the P4 reference model and the P4 rig model

3.5.3 P5 rig results

In Figures 3.41 and 3.42, the results from several dummy instruments can be seen together with the reference model results. In Figure 3.41 it can be seen that the overall shape and amplitude of the dummy instrument time signals in the rig model matches the corresponding time signals in the reference model, although the pelvis and chest curves seem to have their peaks somewhat shifted in time relative to the reference. This phenomenon can also be seen for the chest deflection result, although less pronounced. This could be an effect of the fact that the buckle fixture is deforming with a slight delay in the rig model, causing the restraint forces on the dummy from the seatbelt to also be shifted in time. Since both the rig seat bottom and the compliance of the buckle fixture influence the results from the dummy in the rig model, it is hard to distinguish which part of the rig is responsible for which effect in the obtained result.

In Figure 3.42, the result from the upper neck My bending moment sensor in the rig model has a good fit to the reference. The upper neck Fx and Fz force sensors however have lower peak magnitudes, and also reach their peak magnitudes earlier than the reference model. It is believed that this effect is a result of the rig seat bottom and the deformation of the buckle fixture in the rig, and not related to how the retractor is mounted in the rig. In Section 3.2.1 it is shown that how the retractor is mounted does not influence the results in such a way (see Figure 3.8).

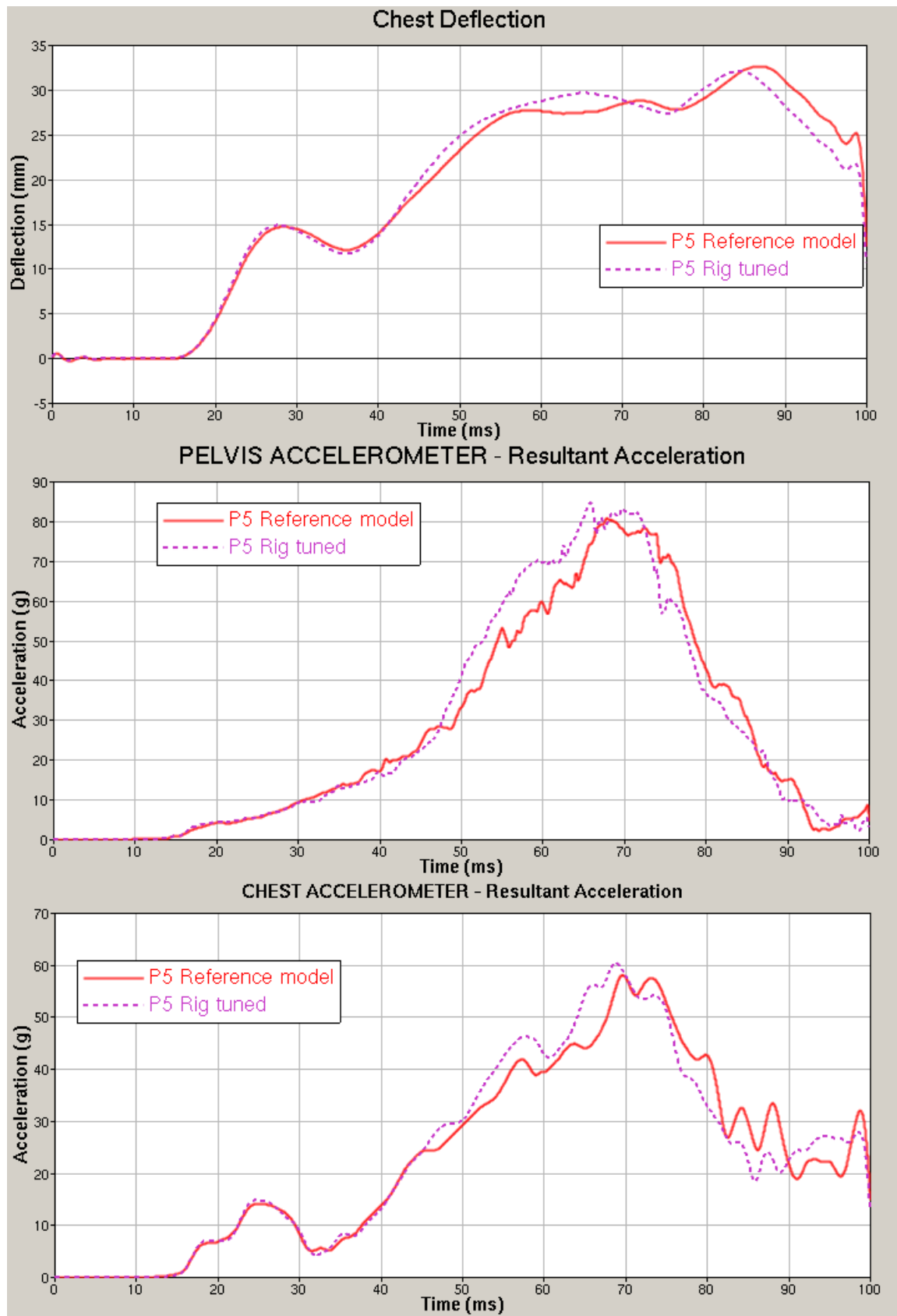


Figure 3.41: Chest deflection and the resultant acceleration of pelvis and chest for the P5 reference model and the P5 rig model

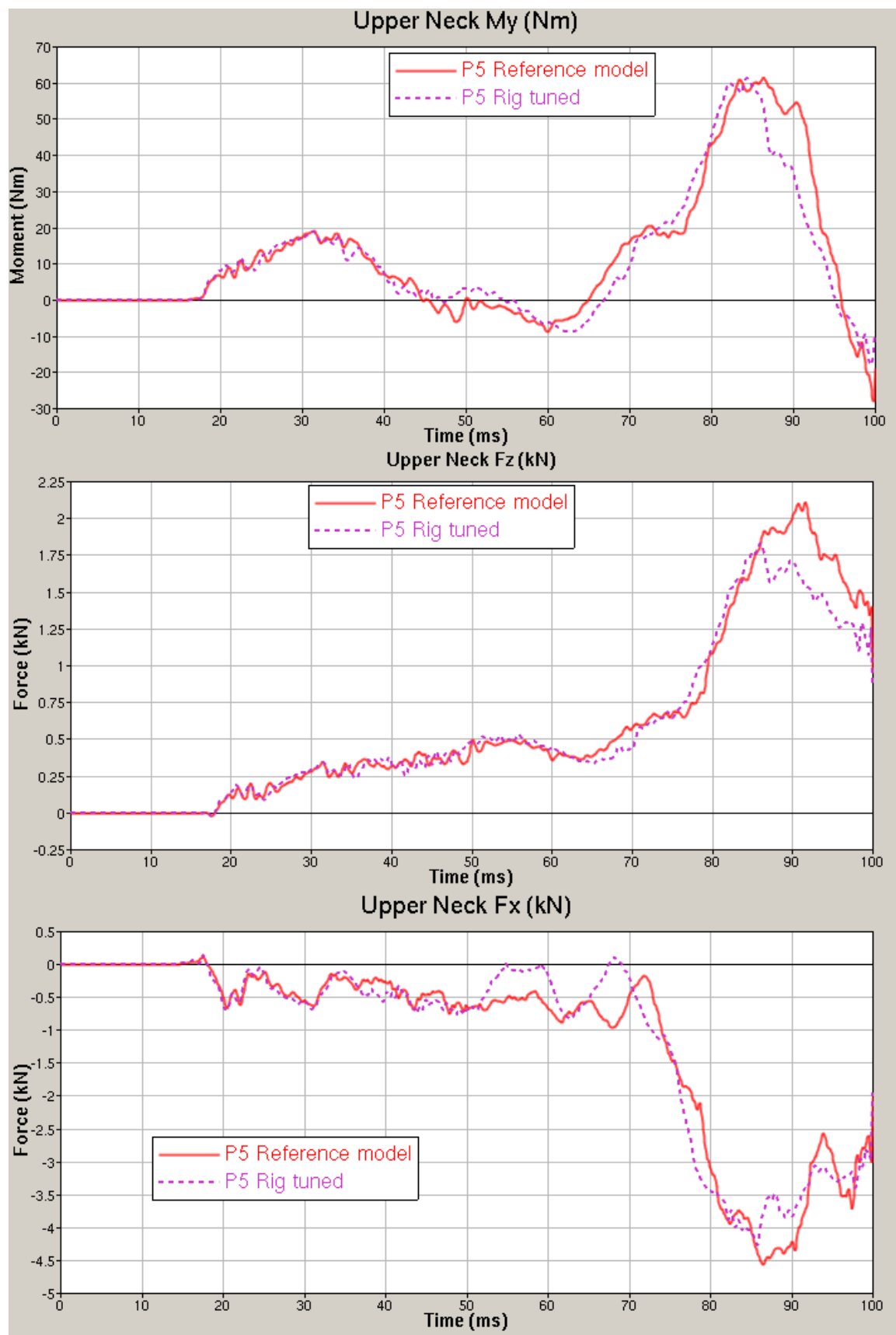


Figure 3.42: Upper neck forces for the P5 reference model and the P5 rig model

3.5.4 Rig results for offset deformable barrier crash test

Since it is desirable to use the rig for evaluating the Offset Deformable Barrier (ODB) crash test case, both the reference models and the rig models were analysed with an acceleration pulse corresponding to an ODB crash, with initial velocity of 64 km/h. The results obtained from the P4 reference model and the P4 rig can be seen in Figure 3.43.

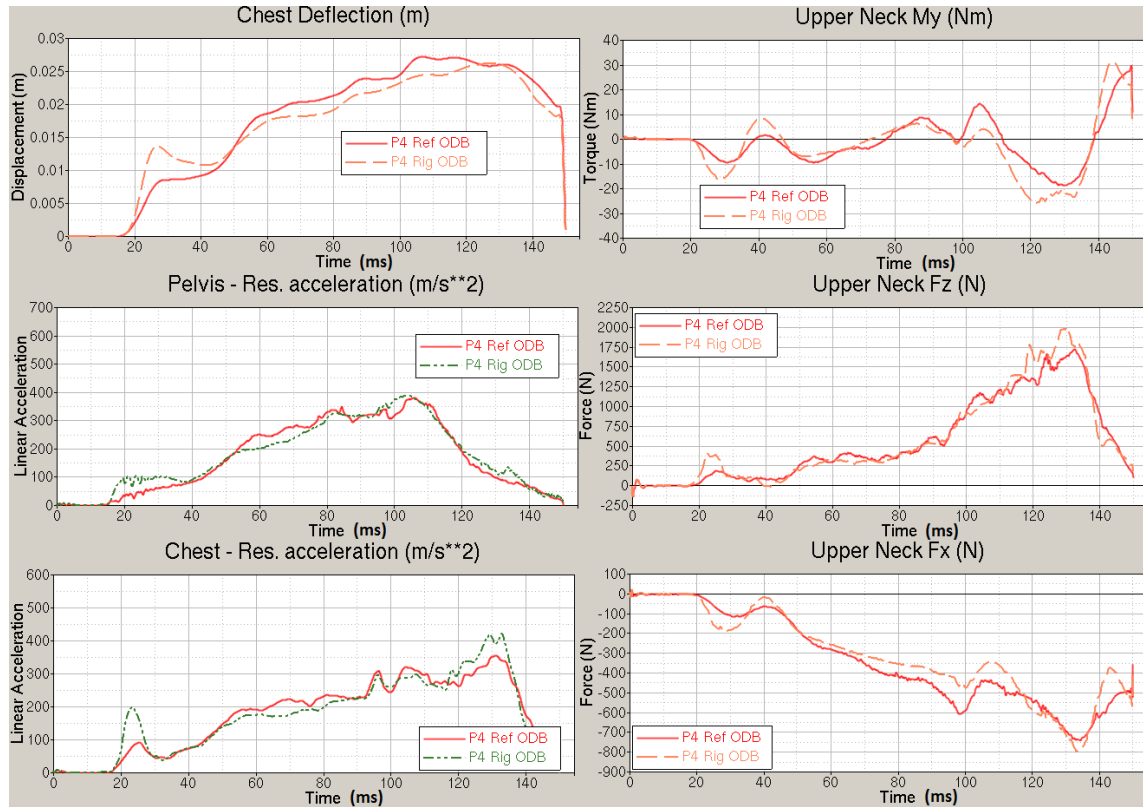


Figure 3.43: Results from the P4 reference model (P4 Ref) when crashed in an ODB case, and the corresponding results obtained from the P4 rig model for the same case.

It is clear that the P4 rig behaviour is less similar to the P4 reference in an ODB crash test case than in the full frontal rigid barrier crash test, although the rig model data follow the general trends present in the corresponding reference model data. There is also a hump in the data from the rig model that appears at 20 ms on all dummy sensors presented in the figure. The reason for this is unknown. In the P4 ODB case, the resultant acceleration is a misleading measurement, since deviations obtained in different accelerometer directions at different times even out the resultant. In Figure 3.44, the dummy pelvis acceleration measurements are plotted component wise to demonstrate this effect. The P4 rig dummy pelvis is the body part where this effect is the most prominent.

The deviating behaviour is believed to be caused by the rig seat bottom. As the rear rig seat bottom plate is rigid and constrained to move in a tilting motion, the resistance to deformation in the Z-direction is uniform along the Y-direction. The seat bottom plate in the reference model is, due to its shape, stiffer towards the outer ends in the Y-direction. This difference can explain the deviation in the dummy pelvis local y-direction accelerometer data, as seen in Figure 3.44. The dummy pelvis y-coordinate axis is parallel to the car Y-axis in the initial seated position, and little rotation occur during the crash.

In Figure 3.45, the ODB crash test results can be seen from the P5 reference and rig model respectively. Also for the P5 rig model the results deviate slightly, but they follow the general trends in the reference model.

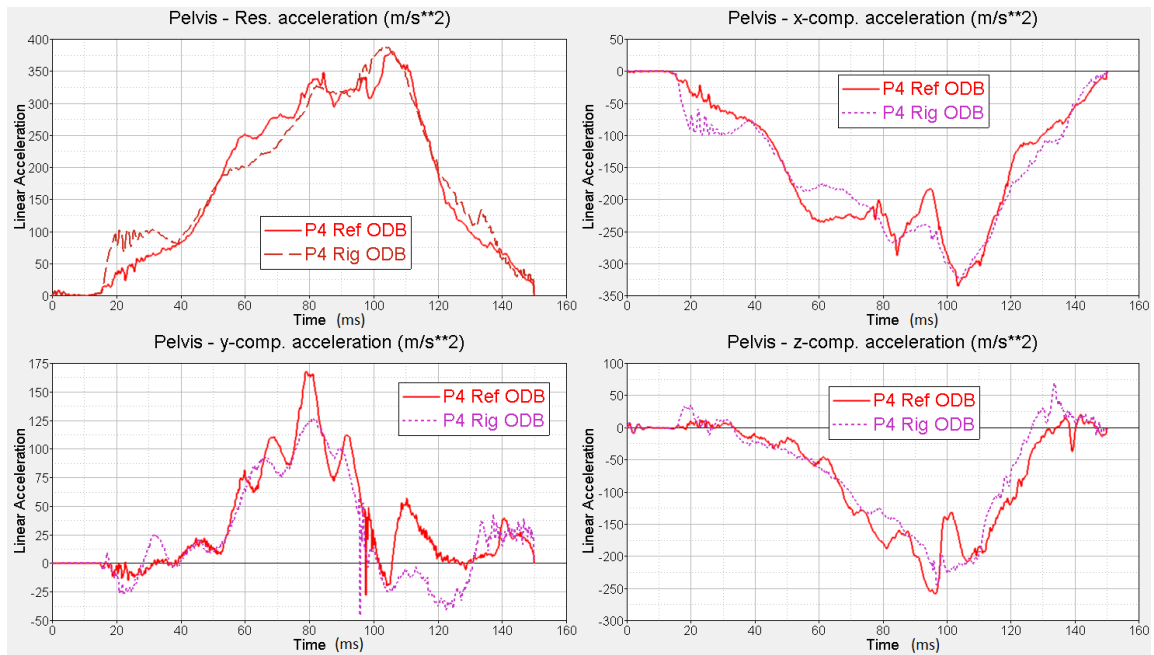


Figure 3.44: Results from the dummy pelvis accelerometer, from the P4 reference model (P4 Ref) when crashed in an ODB case, and the corresponding results obtained from the P4 rig model for the same case. Time is measured in milliseconds

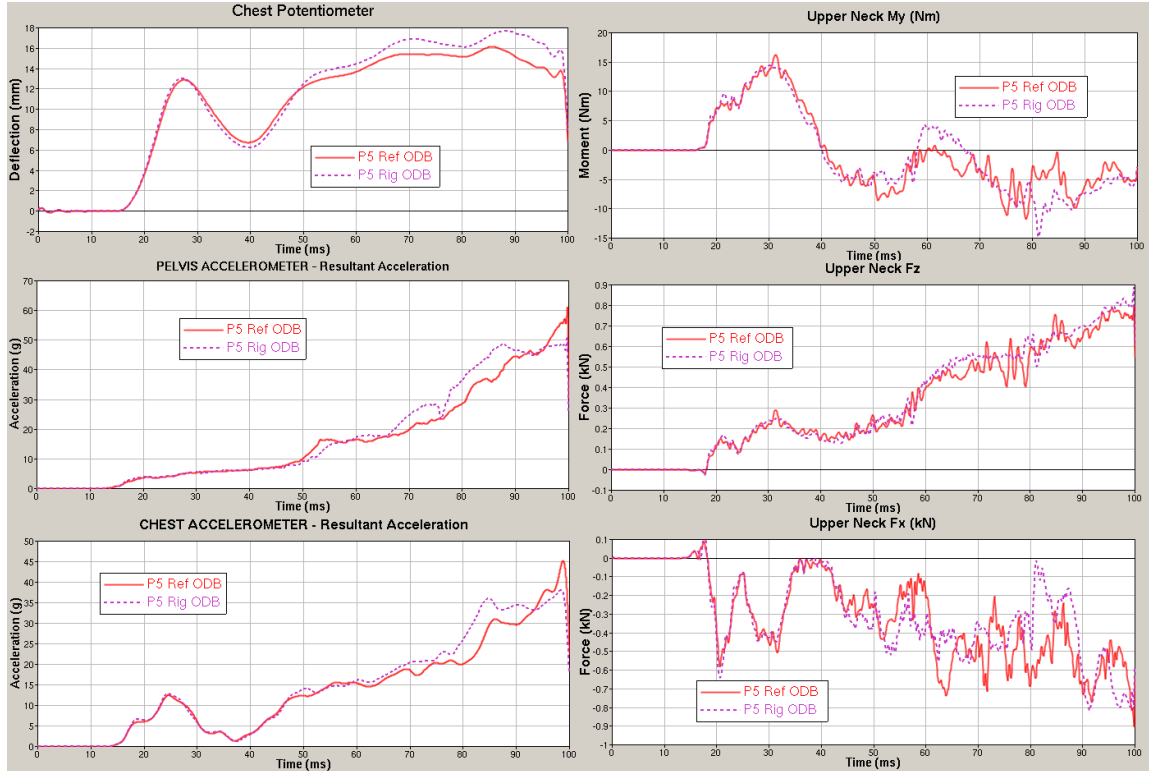


Figure 3.45: Results from the P5 reference model (P5 Ref) when crashed in an ODB case, and the corresponding results obtained from the P5 rig model for the same case.

3.6 Fulfilment of the requirements

The generic rig concept is designed with two purposes in mind; to allow for easy set-up of different cases and to capture the behaviour found in the reference models. The behaviour of the seat bottom plate in the reference models was shown to have a significant impact on the obtained results. The seat bottom plate is a part with complicated geometry fabricated with metal stamping that requires pressing tools to be constructed for every geometry. It is not easy to produce alternatively designed seat bottoms with this method since the tools are expensive and take time to develop. Furthermore, the seat bottom plate undergoes large plastic deformations in a crash, and would have to be replaced between every test. As such, a real seat bottom plate is not suitable to use in the rig, since it cannot easily be modified to investigate effects of design changes. The rig seat bottom plate utilises EPP foam material to obtain the correct shape and also part of the deformation, and the large plastic deformations are captured by the tilting seat bottom and the deforming bendplates. The EPP foam material can be cut to shape in different sections, which are glued together to obtain the final shape. With this method differently shaped seat bottoms can be built for the rig, and thus different seat cushions can be tested to evaluate different seat designs. The bendplates under the seat bottom can easily be exchanged, and their bend points moved relative to the spikes to obtain different deformation behaviour.

All three seatbelt fixture points are movable, and will thus allow for testing different seatbelt configurations. For every specific type of retractor, an adapting fixture will need to be built according to the design of the retractor before mounting it to the rig. The buckle fixture point has adjustable compliance, since deformations significant for the results was found to occur at this fixture point. The same concept can also be applied for the anchor fixture point and, with some small modifications, at the retractor position as well. The rig buckle fixture however cannot obtain the same deformation behaviour as observed in the reference model, and might need some further evaluation or a complete redesign. If the buckle fixture does not need to be as movable as in the designed concept, more freedom is available when designing another concept. The current design is the result of a trade-off between movability and adjustable compliance.

As the rig concept is based on the existing hole plate, all parts can be independently replaced if other designs are needed in the future. There is also sufficient room left on the hole plate to mount frontseats. All parts are also designed with simple geometries, and will not require special tools in order to be built; an angle grinder, a milling machine and a welder is sufficient to construct the designed parts. However, the non-deforming parts in the rig have not been fully dimensioned, only an approximate initial design has been developed. The resulting total weight of the rig is therefore unknown.

The rig should also, due to its mechanically simple design be easy to correlate with CAE models of the rig. The tilting seat bottom joint will have a certain friction, and sliding causing friction will also occur at the bendplates, when sliding relative to the rollers and the spikes. From a CAE correlation point of view, the frictional coefficients needed can easily be introduced. The bendplate contact with the circular rollers and circular point of the spikes can be modelled using analytical geometries for the circular shapes, resulting in a very accurately predicted contact. If the values of the frictional coefficients are uncertain, data can be gathered from testing and e.g. system identification can be used to estimate their values to obtain a good prediction. It is also assumed that all screw connections can be tightened sufficiently, such that no sliding at the screw fastening positions will occur. For the adjustable seatbelt fastening points, the principle of stop screws can be applied at all positions if needed, except for the retractor Y-direction on the beam. Here additional clamps can be introduced next to the retractor mounting if needed to stop unwanted sliding.

The data calculated in the rig FE-model closely follows the existing trends in the reference models, especially the P4 full frontal crash simulation. For the P5 full frontal crash test, the rig FE model also closely follow the reference model results, although with a small time shift at the peak amplitudes, believed to be caused by the delayed buckle fixture deformation in the rig model. Also for the ODB crash test, the rig models follow the trends in the reference models well, but it is believed that the results can be improved for the P4 case. If the rig seat bottom is updated to obtain stiffer behaviour towards the outer ends in the Y-direction, perhaps by using a higher density, stiffer, EPP foam or excluding the outer ends from the tilting motion by redesigning the rig seat bottom rigid plates, the rig FE model might produce more accurate results.

4 Implementation of the modelling concepts

In this chapter, CAE tools implemented during the thesis work is presented. The successful implementation of these tools means that the CAE generic rig model can be used more efficiently, but these tools can be implemented in other CAE models as well.

4.1 Ansa seatbelt module

The seatbelt webbing can be very time consuming in the pre-processing stage, since it has to be placed just as a physical webbing around the dummy. Since the seatbelt webbing is just a shell element mesh placed in space, these elements might need to be repositioned if the dummy or other parts that the webbing wraps is moved. This is to secure correct webbing placement. In Ansa there is a seatbelt module designed to aid in the pre-processing work of setting up the seatbelt model. By using this module, Ansa can set up a seatbelt entity which allows both Ansa and the user to treat the seatbelt elements dynamically. With a correctly defined seatbelt entity, Ansa can automatically update the seatbelt webbing if parts move, and the user can manually manipulate the belt which will behave much like a string.

However, usage of this seatbelt module in Ansa has not been fully implemented at the VCSC rear interior group, partly because lack of time and partly because there are some compatibility issues between the FE-model generated by this module and LS-DYNA. This section will cover the steps needed to successfully set-up the seatbelt module to automatically update the seatbelt entity, as well as the steps needed to obtain a valid LS-DYNA seatbelt FE-model.

4.1.1 LS-DYNA seatbelt

LS-DYNA has several entities defined in order to aid in the simulation of seatbelts. The pertinent entities for this section and their required configuration are briefly presented, and a full description is available in [5], from where the information in this section has been gathered. The most important entities are:

***ELEMENT_SEATBELT**

In LS-DYNA two types of elements are available for seatbelt modelling, either a single degree of freedom element connecting two nodes, or a four node shell element. For a single degree of freedom seatbelt element, a tension force will be applied between the two nodes if the current distance between the nodes is greater than the initial distance. Seatbelts modelled with single degree of freedom elements are termed 1d seatbelts, and if seatbelt shell elements are used they are termed 2d seatbelts. A 2d seatbelt must have a logically regular quadrilateral mesh (nodal numbering must follow fixed intervals in transverse and longitudinal seatbelt direction), and this mesh cannot be disjoint.

***ELEMENT_SEATBELT_RETRACTOR**

Models the behaviour of a physical retractor, such as load-limiting, webbing feed-out and pull-in, as well as keeping a small tension in the seatbelt. This entity is not mandatory in a seatbelt definition, i.e the user may implement the retractor behaviour using custom elements and entities.

***ELEMENT_SEATBELT_SLIPRING**

Used at locations where the seatbelt webbing is wrapped around a part with a sharp angle, typically at the buckle. This entity is used to pass the seatbelt around a linking point with friction using a force balance between the entering and exiting elements.

***DATABASE_CROSS_SECTION_SET, (DBCS)**

As the tensional forces in different parts of the seatbelt webbing is interesting when evaluating different safety aspects and seatbelt behaviour, the user can specify the cross-sectional force of the seatbelt to be output during the solution. This is obtained by defining a set of transverse nodes over the seatbelt, which will define the cross section, and one set of elements whose internal forces will be used to calculate the total force. A DBCS using these sets may then be defined.

LS-DYNA requires the user to specify ordered nodal sets at each slipring location and at the edge of the non-disjoint seatbelt mesh (edgeset). For each slipring, a set of nodes defining the slipring location must be

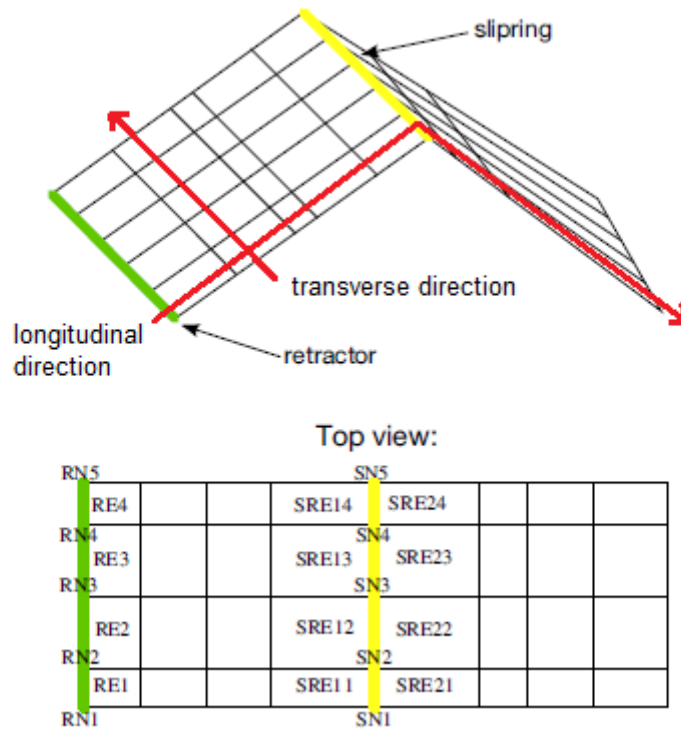


Figure 4.1: Illustration of index ordering in required sets, as well as longitudinal and transverse direction in a seatbelt webbing mesh

defined, as well as one set for the entering seatbelt elements and one set for the exiting elements, see Figure 4.1. The transverse direction of index ordering must be the same for these sets, and this order must be consistent for all sliprings in the seatbelt. This ordering must also be followed for the seatbelt edgeset and retractor set. If a retractor element definition is used, the location of the edgeset nodes should be coincident with the retractor element nodes, but if no retractor elements are used, the edgeset can be placed in any end of the seatbelt webbing mesh.

4.1.2 Setting up a dynamic Ansa seatbelt entity

The Ansa seatbelt module comes with a graphical user interface, in which the seatbelt entity is defined in a step-by-step process, which here is covered briefly. Each Ansa seatbelt consists of parts, typically a starting part at the retractor, a shoulder belt part and a lap belt part, although an arbitrary number of parts may be defined if needed. Each part has a starting nodal point and an ending nodal point. The starting and ending nodal point must be existing FE nodes. At these nodal points, the user may specify if a slipring or retractor should be placed. Additional nodal points between the starting and ending point may be defined, and during the creation of the seatbelt entity, the algorithm creating the seatbelt webbing will use these points as targets for the seatbelt to pass over, although it may not always succeed to do so. In addition, for 2d seatbelts, an entry and exit vector must be defined to orient the webbing mesh. It is important that consecutive parts of the seatbelt ends and starts in the same nodal point, otherwise the seatbelt mesh created will become disjoint.

When all parts of the seatbelt have been defined, the next step is to define the parts that the seatbelt should wrap, typically some part of the seat, the dummy torso and pelvis. These parts are stored in a list called Parts to wrap. The webbing fitting algorithm uses the shapes of these parts to determine how the seatbelt webbing should be placed. The final step is to create the seatbelt, which will result in that Ansa creates each seatbelt part consecutively, pausing after each part and allowing the user to manually manipulate the positioning of the webbing. In this process, all necessary LS-DYNA entities as described in Section 4.1.1 is created, except for the DBCS's which the user must manually define on the created webbing mesh. In order to achieve that the webbing placement updates automatically if parts are moved, the user has to turn on the so-called Auto-recreate feature for the created seatbelt entity.

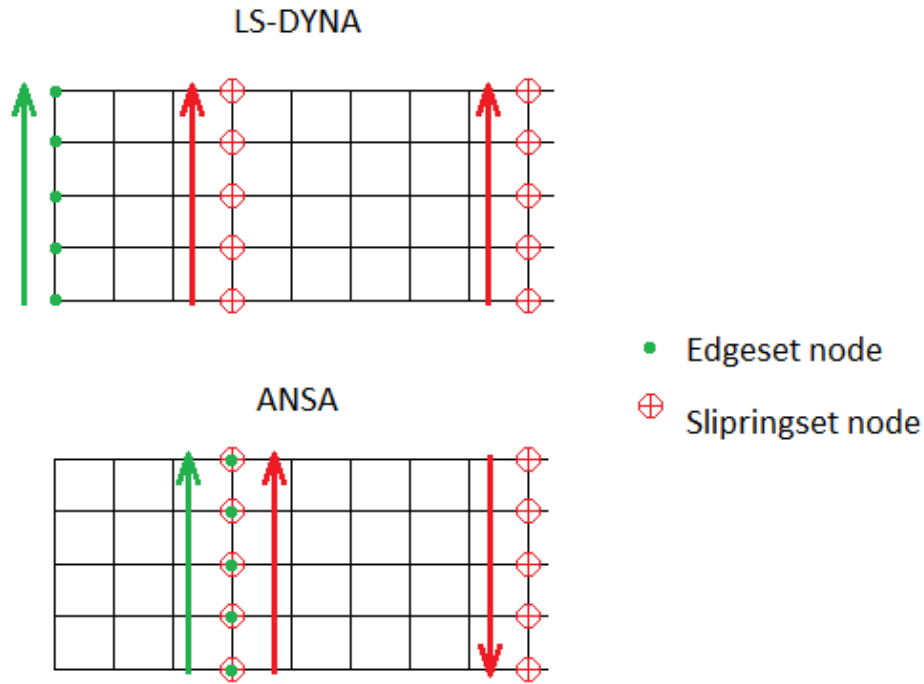


Figure 4.2: The arrows represent index ordering of required sets transverse the 2d seatbelt. Top: LS-DYNA expected uniform ordering. Bottom: Ansa generated ordering

Auto-recreate

The Auto-recreate feature for the seatbelt entity will position the seatbelt parts correctly by simply recreating all the seatbelt parts onto the moved configuration, if any of the parts defined in the Parts to wrap list are moved. When the seatbelt mesh is recreated, the seatbelt elements and nodes will be created anew, with new numbering, and thus any defined DBCS's will no longer be valid, since the sets used refer to the numbers in the old seatbelt mesh. In order for the Auto-recreate feature to react, a part in the Parts to wrap list must be moved using Ansa kinematic definitions; it is not enough to simply change the nodal coordinates of the part. However, this is not a significant issue that requires a lot of extra work, since most dummy models already have a kinematic definition that is recognised by Ansa. However, the seatbelt buckle, anchor and retractor or the rear seat does not have this predefined. If the user wishes to update the positioning of these parts and thereby also wants the seatbelt positioning to automatically update, kinematic joints and actuators that can obtain the desired movement of the parts must be defined in Ansa.

4.1.3 Compatibility issues

In version 15.2.3 of Ansa, used in this thesis, the seatbelt FE model that is created by the Ansa seatbelt module will not be recognised as correct by LS-DYNA, and therefore will not run. The issue arises with the ordered nodal sets at the sliprings and the edgeset of the seatbelt mesh, see Figure 4.2. The edgeset might not be correctly placed, and the order of indexing of sets belonging to a slipring sets might become reversed relative to the edgeset indexing. However, these issues can be circumvented, either by manually redefining the sets or by utilizing Ansa Generic Entity Builders (GEB) together with Ansa's scripting capabilities to further speed up the creation of seatbelt models, and minimise the need for manual input.

Ansa GEB

The Ansa GEB is an aid for the user to define rules based on spatial coordinates. The GEB will search for specified Ansa entities in a predefined volume around the GEB in the model space. Once the requested entity has been found, a number of predefined rules can be applied, or the GEB can provide a user defined script

with information about the found entity. In order to automatically place the edgeset of the seatbelt at one of the ends, a GEB can be placed near the endpoint of this seatbelt part and search for seatbelt elements. Once the element closest to the endpoint has been located, a script can be provided with sufficient information to re-locate the edgeset.

Ansa Scripts

Ansa scripts are written in the Python coding language. Scripts that rely on Ansa GEBs to relocate the edgeset of the seatbelt, as well as setup the DBCS's on the newly created seatbelt mesh have been created. A script that reverses the indexing of the slipping sets has also been created. The scripts are presented in Appendix C.

4.1.4 Example model

An Ansa model that contains an automatically updating seatbelt entity has been created, and was used to create the seatbelt configurations used in Section 5.1. A description of how the model was set-up, as well as a tutorial on how to use it is available in Appendix D.

4.2 Automatic parameter configuration using LS-OPT coupled with Ansa and LS-DYNA

Designing for crashworthiness can be very difficult. Large, non-linear, time dependent forces cause materials to yield, break and come into contact, which makes the analysis non-linear and effects of design changes hard to predict. Furthermore, design objectives, such as maximum structural strength and lowest possible mass, is often in conflict and no clear choice of the best design choice exists. However, if mathematical objective functions that depend on design choices made can be constructed, these objective functions can be subjected to optimisation.

LS-OPT is an optimisation software with built in capabilities to handle single and multiple objective optimisation. It can be coupled with several different preprocessors, which can be used to obtain design changes in an FE-model, and solvers to obtain the resulting objective function value. In this section, the steps needed to couple LS-OPT with Ansa and LS-DYNA are covered, and also an example model where LS-OPT has been used to configure parameters for the deforming elements in the generic rig FE-model is presented.

4.2.1 Ansa and optimisation

Ansa has built in capabilities to be coupled with optimisation software, and a predefined optimisation scheme, defined as an Ansa optimisation task, see Figure 4.3. In evaluating this task Ansa will perform three default steps:

Read design parameters

An ASCII file containing values for parameters will be read. It is by writing values to this file optimisation software can command Ansa to make requested design changes.

Make design changes to FE-model The parameters read will be applied in the Ansa model. If wanted, the parameters can first be treated in mathematical expressions. Several different Ansa entities can be parametrised, such as material properties, nodal coordinates as well as Ansa's morphing tools.

Output FE-file

The changed model is written to a requested FE-solver format.

Anywhere in this task, the user may specify other Ansa commands to be carried out, such as re-meshing parts whose elements may have become distorted, reconfigure constraints or invoke user defined scripts. Morphing in Ansa is a tool to change the geometrical shape of CAD geometries and FE-model meshes. Several morphing methods exist, as covered in [4], and morphing is an efficient tool to obtain complex design changes driven by parameters.

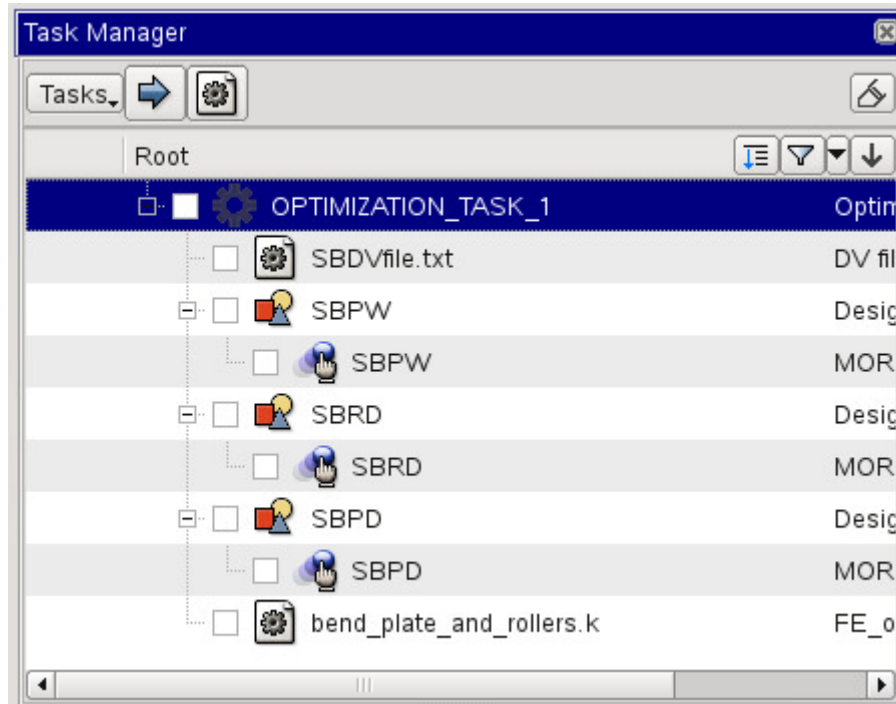


Figure 4.3: An Ansa optimisation task

4.2.2 LS-DYNA input files and optimisation

If only simple design changes need to be performed, such as changing numerical values, or scaling and translating of components, the parameters can be defined directly in the LS-DYNA input FE-files by using the LS-DYNA keywords `*PARAMETER` and `*DEFINE.TRANSFORMATION`. Parameters available for LS-OPT are defined in LS-DYNA input files as `<<Parameter_name>>` and LS-OPT will substitute each parameter with a value before submitting the input file to the solver for solution. The initial values and limits for the parameters will have to be defined by the user in the LS-OPT environment.

4.2.3 Setting up an LS-OPT optimisation task

The first step in an optimisation task is to decide which objective functions should be considered and which parameters should be manipulated to influence these objective functions. Care has to be taken by the analyst in this step to ensure that the parameters do affect the objective function, and also that changes in parameters do not cancel each other in the eyes of the objective function, e.g the objective function $O(p_1, p_2) = p_1/p_2$ can obtain the same constant value for an infinite number of combinations of parameters p_1 and p_2 .

The next step is to parametrise the FE-model, either by using Ansa and an optimisation task, or directly in the FE input files. LS-DYNA output requests needed for the objective functions to be evaluated must also be made.

The set-up of the Ansa and LS-DYNA coupled LS-OPT task is covered in detail in [6], however since LS-DYNA is run at a computing cluster at VCC, LS-OPT cannot start LS-DYNA directly as described in [6]. Instead, a script that will submit the LS-DYNA computing job to the cluster queue must be called instead of the LS-DYNA executable. This script and its usage is presented in Appendix E. As in version 5.0 of LS-OPT, Ansa must also be configured to accept commands in the Betascript scripting language, since this is what LS-OPT uses to command Ansa to run the Ansa optimisation task. This is most easily obtained by configuring LS-OPT to copy an empty `ANSA_TRANSL`¹ file to each working directory of Ansa during the optimisation task. After the preprocessing stage, the modified FE-files, must be copied to the LS-DYNA run directory, such that it can be located when LS-DYNA reads the FE-problem.

¹Ansa by default loads the `ANSA_TRANSL` file into memory when starting up. `ANSA_TRANSL` files should contain the user defined Betascripts that Ansa should automatically load into memory on start-up. Even if the file is empty, Ansa will be configured to accept Betascript commands.

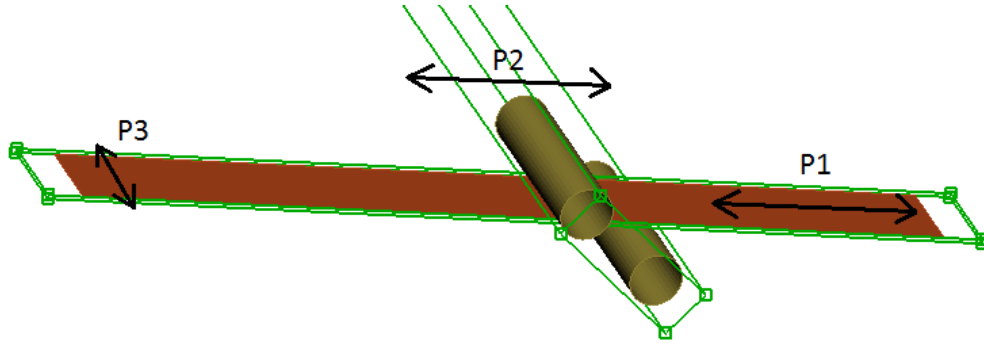


Figure 4.4: The parameter controlled Morph boxes in Ansa. P1 controls the fixing point of the plates in the rig, P2 controls the position of the roller support along the plate and P3 controls the width of the bendplate

4.2.4 Example optimisation task

Since the CAE model of the rig has several deforming elements whose thickness, width and fixture points are adjustable, this can be used to modify the behaviour of the rig. In this optimisation task, the deforming elements under the rig seat bottom should be adjusted such that the rig model seat bottom will behave as the seat bottom plate in the reference model. To obtain this, a system identification procedure will be performed in LS-OPT.

Objective function

To perform a system identification, measurement data representing the true system is needed. As described in Section 3.2, the behaviour of the seat bottom plate have significant impact on the calculated dummy pelvis z-acceleration time signal (where z refers to the local dummy pelvis coordinate system z-axis). If the rig seat bottom can be set-up to obtain the same calculated dummy pelvis z-acceleration time signal, this would mean that the rig seat bottom has a behaviour close to the original seat bottom behaviour in the reference model, at least from the dummy measurements point of view. As the objective function, a curve matching function that measures the root mean square error between the reference model pelvis z-acceleration time signal curve and the calculated dummy pelvis z-acceleration time signal curve in the rig model is used. If the error is zero, the two curves are identical, hence this objective function shall be minimised by adjusting parameters in the rig model.

Setting up parameters

The changes that can be made in the rig to affect the seat bottom behaviour, and thus the pelvis z-accelerometer based objective function, is changing the location of the bend plate fixture points, the location of the bending rollers along the plate, as well as changing the thickness and width of the bendplates. In this optimisation task the locations of the bendplate fixture point and the roller location along the bendplates, as well as the width of the bendplates is adjusted. An Ansa file containing the FE mesh of these entities is created, and parameter controlled Morph boxes are defined to obtain the geometrical changes of these parts, see Figure 4.4. An Ansa optimisation task is defined that will enable LS-OPT to request changes to these parameters. Care has been taken that the modified FE-entities will be correctly constrained in the rig model for the obtainable configurations.

Optimising

Using the recommended optimisation settings for system identification as given in [7], the optimisation task is set-up and started. A flowchart of the optimisation procedure can be seen in Figure 4.5. In the optimization loop depicted in Figure 4.5, LS-OPT determines values for the parameters and requests Ansa to modify the LS-DYNA FE-model accordingly. In the next step, the modified FE-problems are solved. In between these steps two files are copied to the LS-DYNA run folders. These are the LS-DYNA .key file describing the whole rig crash test FE-problem and the modified bendplates with rollers created by Ansa, which are included by reference in the .key file. The results from the solved FE-problems are used to construct and evaluate the

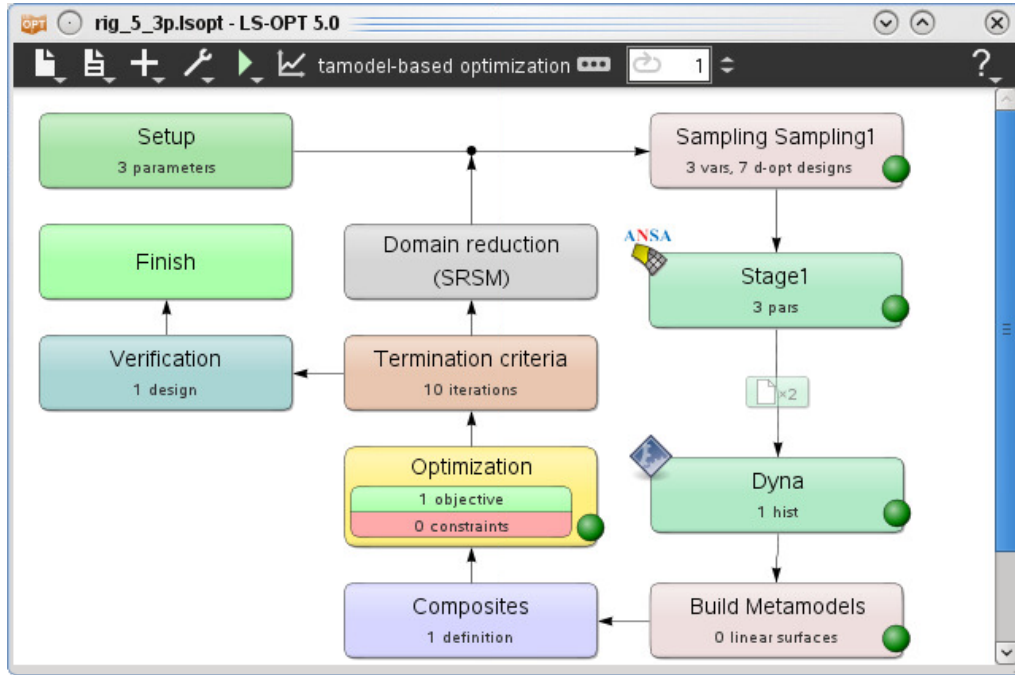


Figure 4.5: An LS-OPT flowchart.

objective function. If no termination criteria is met, new parameter configurations are chosen for a new iteration. For detailed information about all the steps performed in the optimisation procedure, see [7].

Results

The system identification procedure terminated after two iterations. In Figure 4.6, the pelvis z-acceleration curve is plotted from three different models. The target reference model, the nominal rig model and the rig model after optimisation. It can be seen that the system identification has resulted in that the dummy pelvis

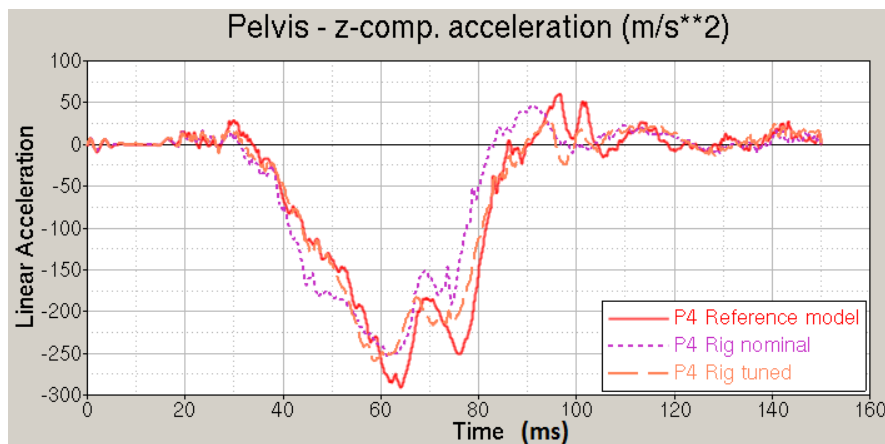


Figure 4.6: The system identification target curve from the P4 reference model along with the result from the nominal rig model and the rig model when the optimisation procedure has terminated (tuned)

z-acceleration time signal is now closer to the result from the reference model used as target. However the result is not perfect, but this was not expected, since the rig seat bottom is very different from the actual car seat bottom, although designed to obtain a similar deformation behaviour during a crash.

That the seat bottom structure has a large impact on the dummy pelvis acceleration, and thus other sensors in the dummy can be confirmed by Figure 4.7. As the pelvis z-acceleration curve comes closer to the reference curve, so does other curves in the rig model.

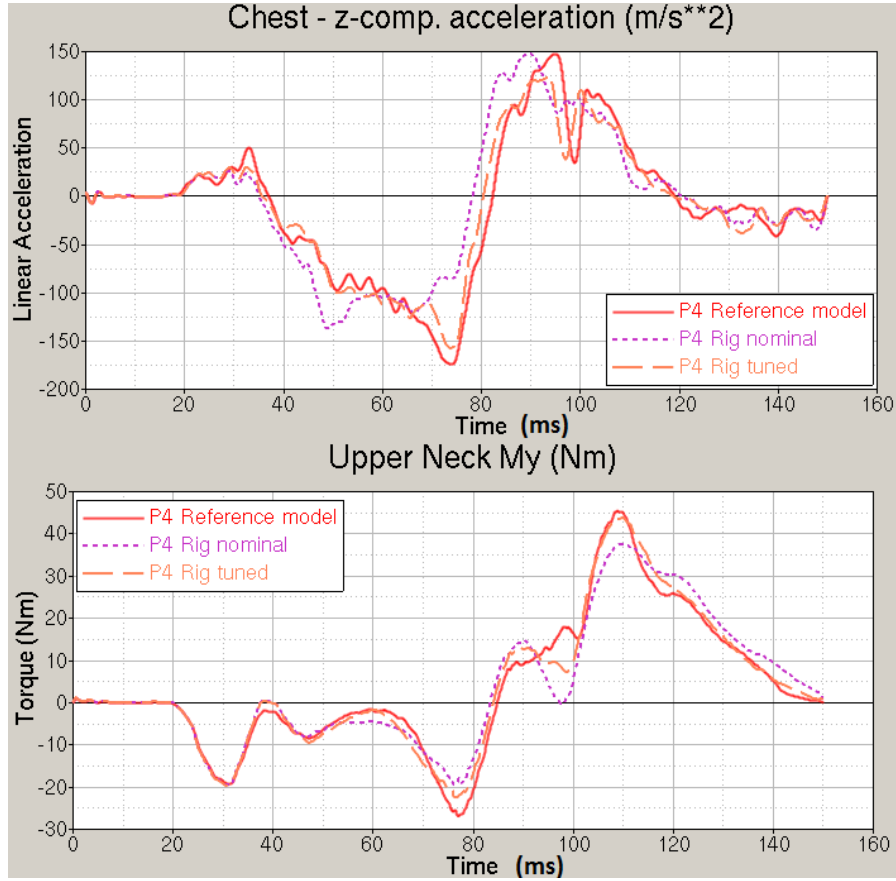


Figure 4.7: The measurement signals from dummy chest z-acceleration and upper neck y-bending moment from the reference model, the rig at nominal settings and the rig after system identification (tuned)

A total of 15 objective function evaluations was performed, seven in each iteration and one for verification. Since it can be of interest to see how the configuration of the bendplates can influence the pelvis z-acceleration time signal, the results from all 15 evaluations are plotted in Figure 4.8, although it is difficult to make out 15 separate curves. This is because many results become similar as the optimisation procedure converges. This indicates that there is little parameter sensitivity for the obtained result in a setting close to the optimum.

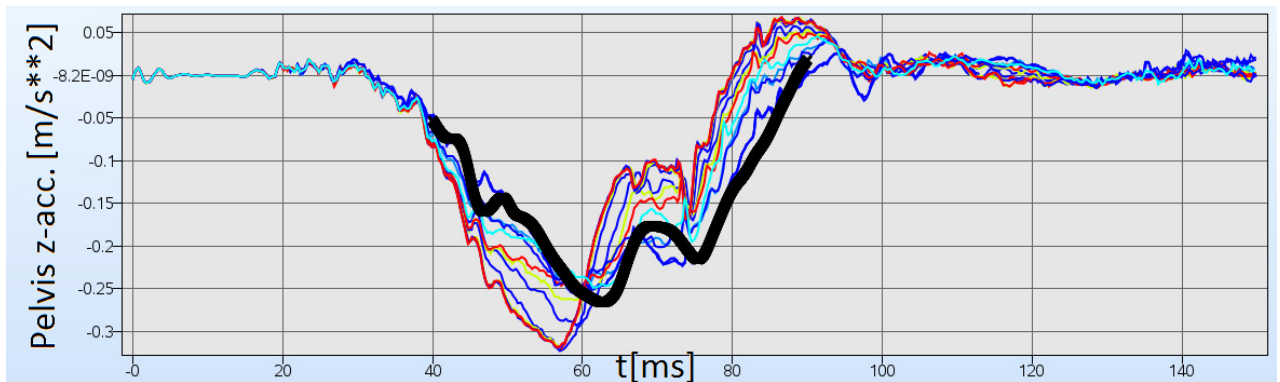


Figure 4.8: The calculated dummy pelvis z-acceleration from the rig model using 15 different parameter configurations in the optimisation, together with the curve used as target (black).

5 Parameter study

As part of this thesis the influence of some parameters on the simulation results have been studied upon request from the thesis supervisors. Preliminary results in these areas can serve as pointers when planning future work efforts. In Section 5.1, the influence of the seatbelt anchoring positions on the dummy instrument data relative to a reference in a simplified crash test model will be presented. The dummy instruments studied here are those relevant for the C-NCAP safety rating evaluation, in the full width frontal impact test. Another parameter that has been studied is the coefficient of friction for the dummy model, regarding contact with the seatbelt. Results from varying this parameter between two extremes are presented in Section 5.2. As found in Section 3.2.1, the stiffness of the seat bottom plate has a large influence on the data obtained from the dummy. Traditionally, current rear seat test rigs are built after the actual car geometry, but with significantly stiffer car body, so that the test rig may be reused without the need to replace the car body. Since the seat bottom plate is part of the car body, the influence of the relative stiffness of this part has been studied by varying the material thickness in the part. Results from this study are presented in section 5.3.

5.1 Seatbelt mounting positions

The three attachment points for the belt were varied in four ways. The retractor was moved ± 50 mm and ± 75 mm in the Y-direction relative to the reference position and ± 50 mm in the Z-direction for each Y-position, including the reference Y-position. The buckle and the anchor were moved separately ± 50 mm in the X-direction and ± 50 mm in the Z-direction for each X-position including the reference X-position. In the result figures dX, dY and dZ represents steps in the car global X Y and Z-directions respectively. Furthermore, the anchor and the buckle were moved simultaneously and their positions was defined as the angle, φ , between a vertical line through the H-point (a reference point in the dummy used for positioning) of the dummy and a line passing through the H-point and the anchor, see Figure 5.1. φ was varied between 15° and 75° in steps of 10° . Based on C-NCAP rating for the rear seat dummy the different set-ups were graded where 2 is the maximum rating. To show how the grade changed between different positions, figures were created where dots were added at the anchoring positions. Each colour corresponds to a certain rating range, see Figure 5.2 to Figure 5.4. The capital R in each figure points out the reference position.

For the anchor-buckle move, a red circle frame surrounds the dots corresponding to $\varphi = 65^\circ$ and $\varphi = 75^\circ$, see Figure 5.4. This indicates that submarining occurred here for this specific model, something not taken into account during the grading.

It should be noted that this study was performed on a simplified model for the purpose of showing possible trends rather than absolute values. For the retractor it can be seen that positive dY and dZ increase the score within the range studied and that negative dY and dZ decrease the grades.

For the buckle and the anchor respectively, it is hard to see clear trends due to the limited amount of trial points but it is indicated that moving the buckle has a higher influence on the result than moving the anchor, and that positive dX and dZ appears to have a positive impact. In Figure 5.4 it is shown that the grades, but also the risk of submarining, increase with increasing angle, φ . For all of the simulations, no head impact was observed, hence only chest deflection affected the grading. Thus, the same trends can be observed in Figure 5.5 to Figure 5.8 for chest deflection as for the C-NCAP grading.

The maximum upper neck forces, F_x and F_z can be seen in Figure 5.9 to Figure 5.12. For the retractor there seems to be a positive correlation between dY and F_x but a negative correlation for F_z . The anchor, on the other hand, does not have a significant influence on the neck forces, see also Figure 5.10. Similarly as for the C-NCAP grading, the buckle position has a larger influence and positive dX gave higher F_x while F_z decreased. For the anchor and buckle together it is hard to draw any conclusions for F_z from Figure 5.12 but F_x seems to increase for larger angles. The red marking indicates that submarining occurred here for this model.

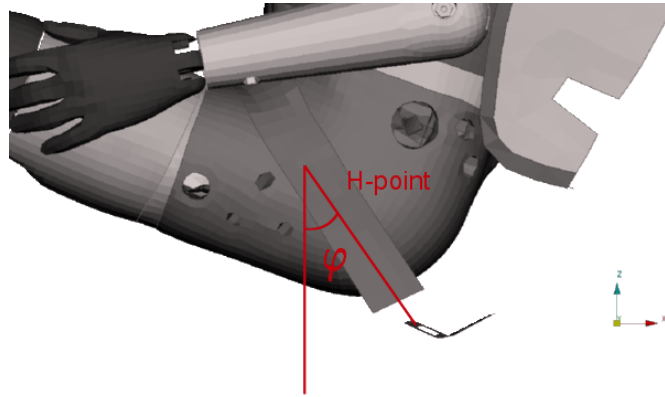


Figure 5.1: φ as the angle between a vertical line through the H-point of the dummy and a line through the H-point and the anchor

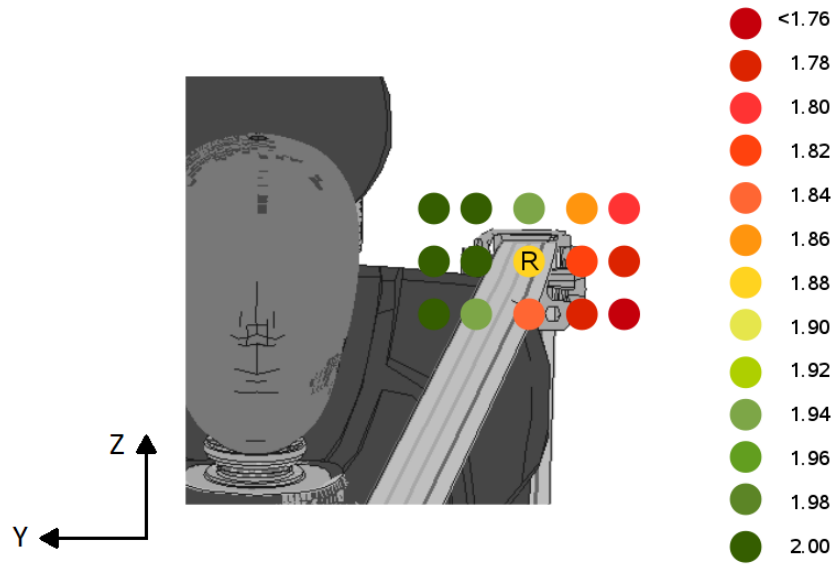


Figure 5.2: Rating based on C-NCAP criteria when the retractor position is varied

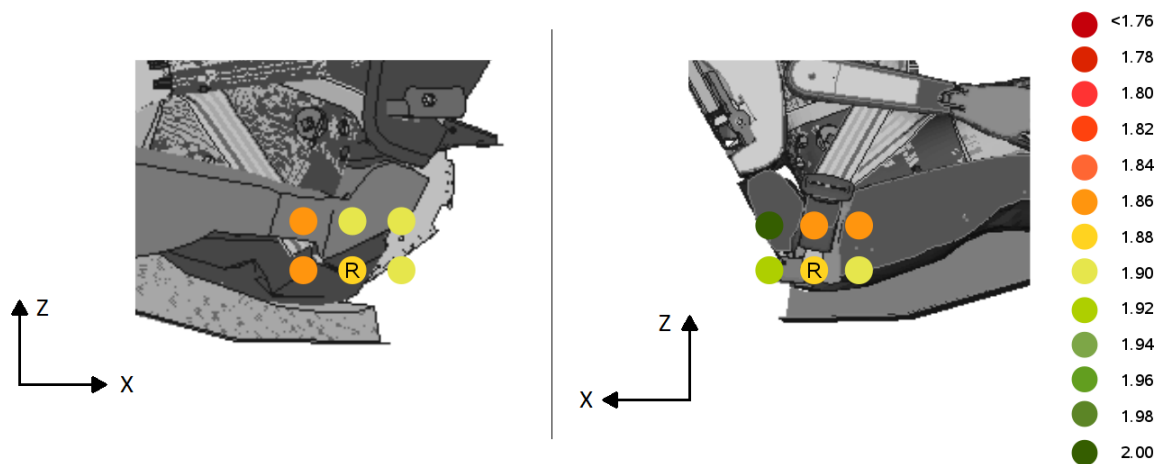


Figure 5.3: Rating based on C-NCAP criteria when the anchor (left) and buckle (right) position is varied

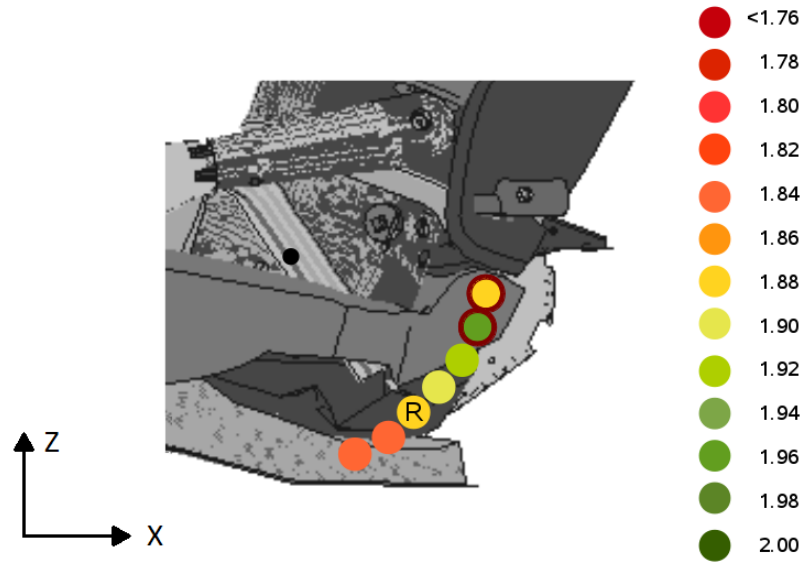


Figure 5.4: Rating based on C-NCAP criteria when the anchor and buckle are placed at different angles, φ . A red circle frame indicates that submarining occurred for this specific model

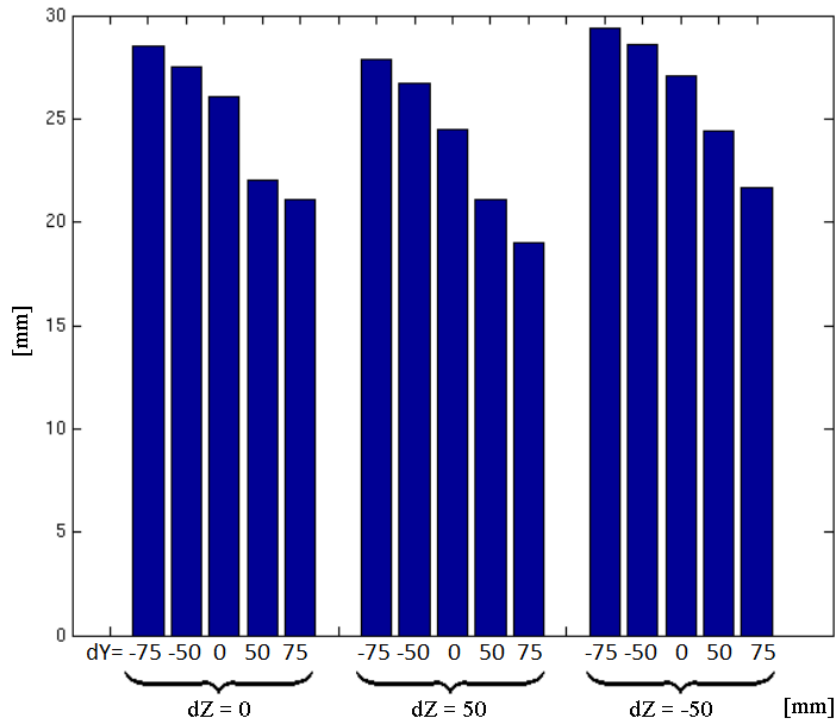


Figure 5.5: Maximum chest deflection when moving the retractor dY and dZ relative to the original position

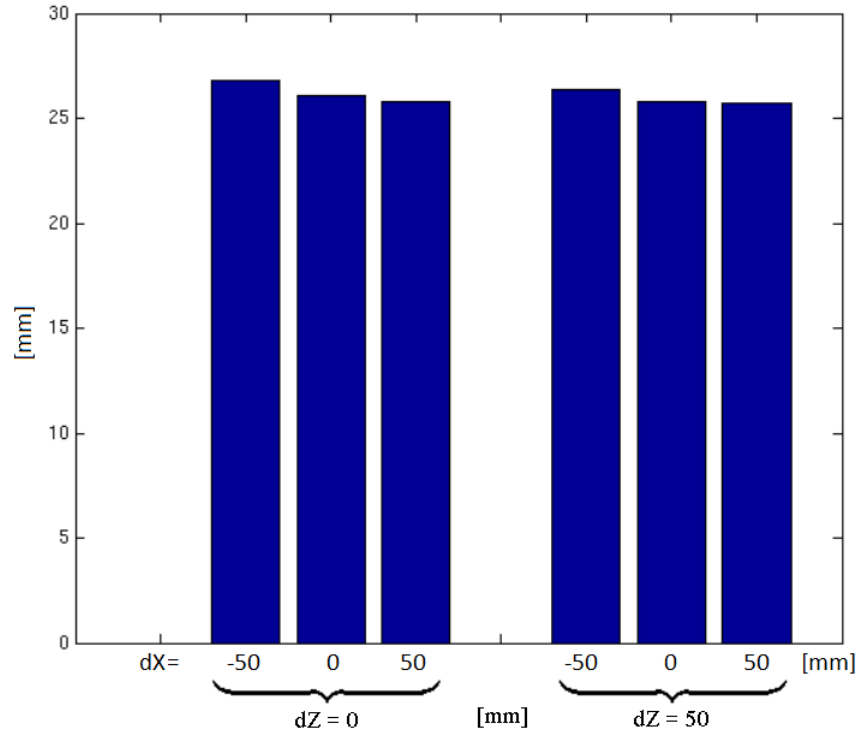


Figure 5.6: Maximum chest deflection when moving the anchor dX and dZ relative to the original position

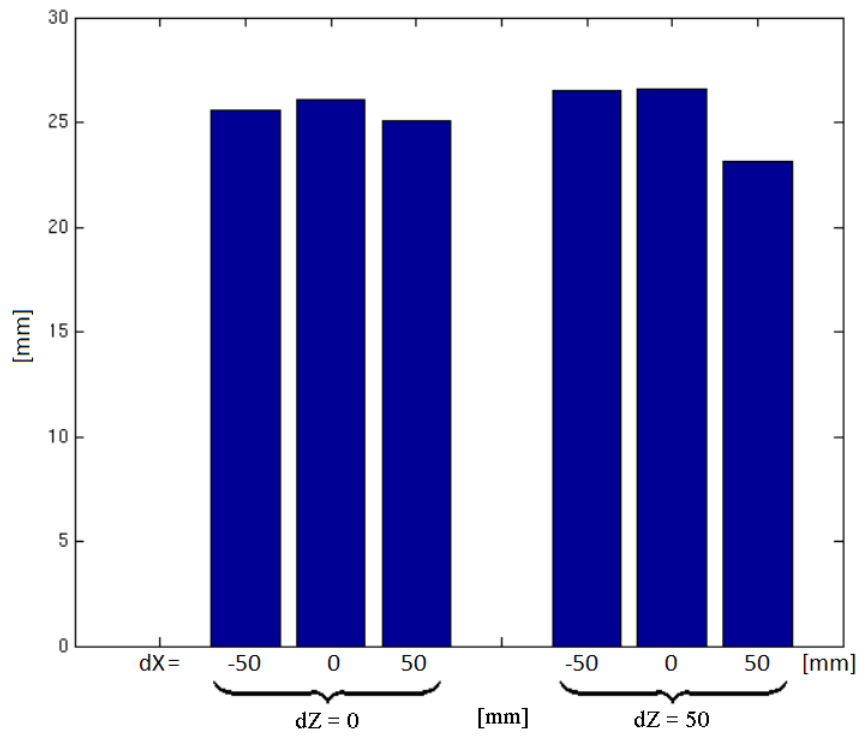


Figure 5.7: Maximum chest deflection when moving the buckle dX and dZ relative to the original position

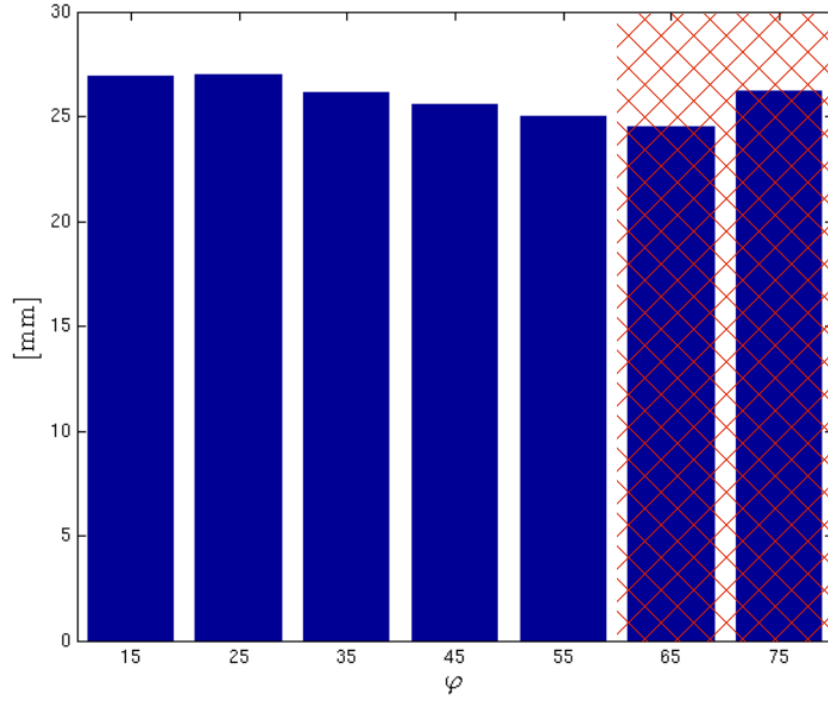


Figure 5.8: Maximum chest deflection when placing the anchor and the buckle at different angles, φ . The red marking indicates that submarining occurred for this specific model

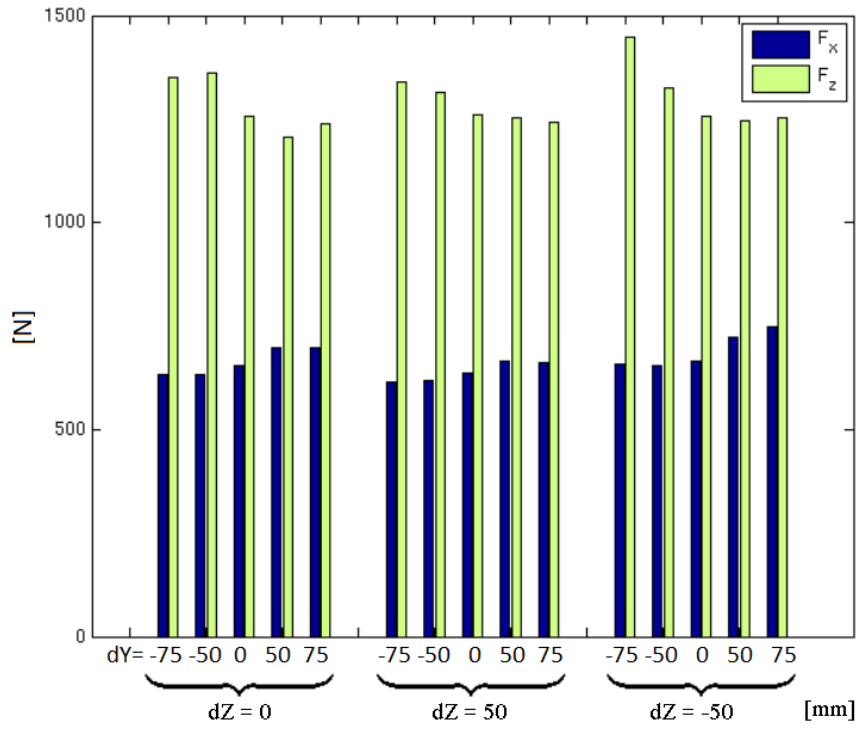


Figure 5.9: Maximum upper neck force F_x and F_z when moving the retractor dY and dZ relative to the original position

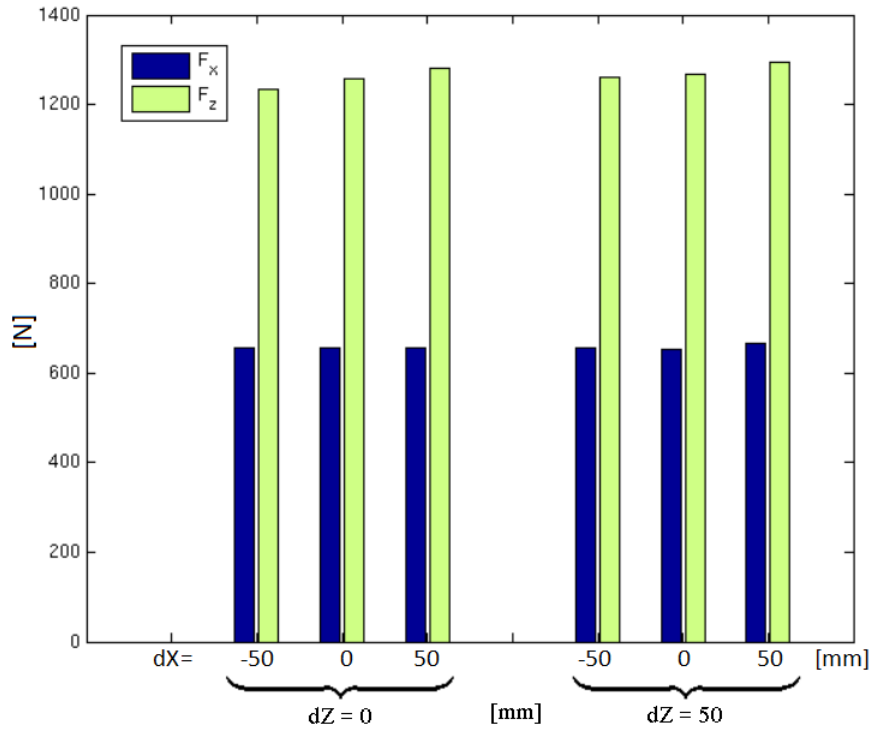


Figure 5.10: Maximum upper neck force F_x and F_z when moving the anchor dX and dZ relative to the original position

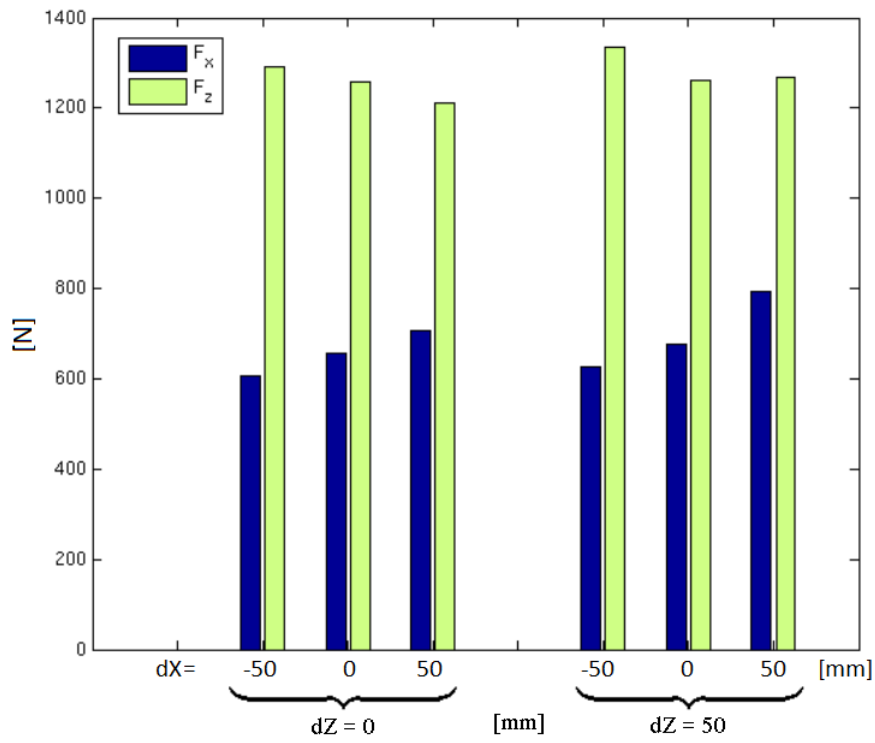


Figure 5.11: Maximum upper neck force F_x and F_z when moving the buckle dX and dZ relative to the original position

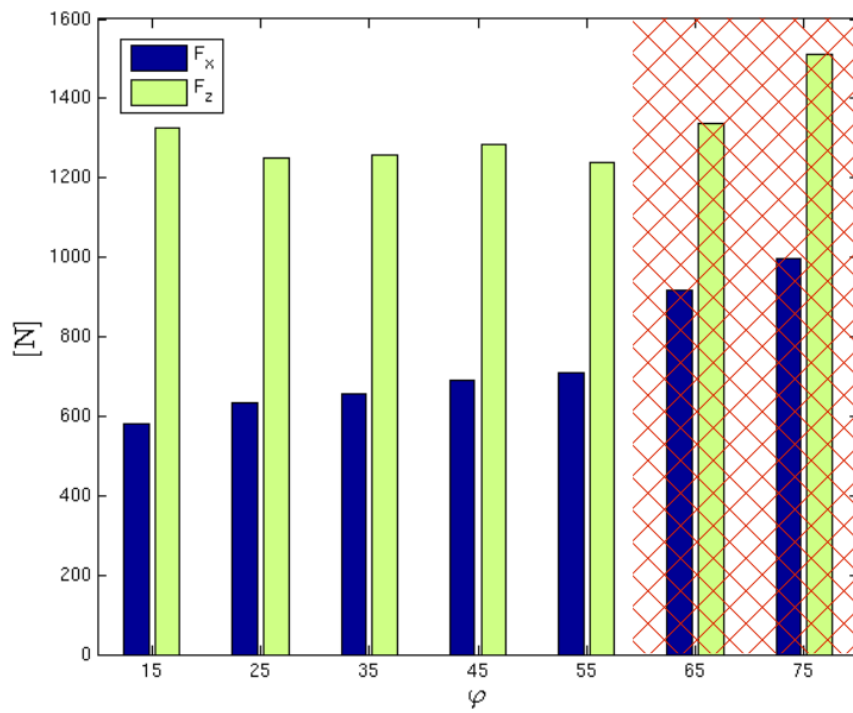


Figure 5.12: Maximum upper neck force F_x and F_z when placing the anchor and the buckle at different angles, φ . The red marking indicates that submarining occurred for this specific model

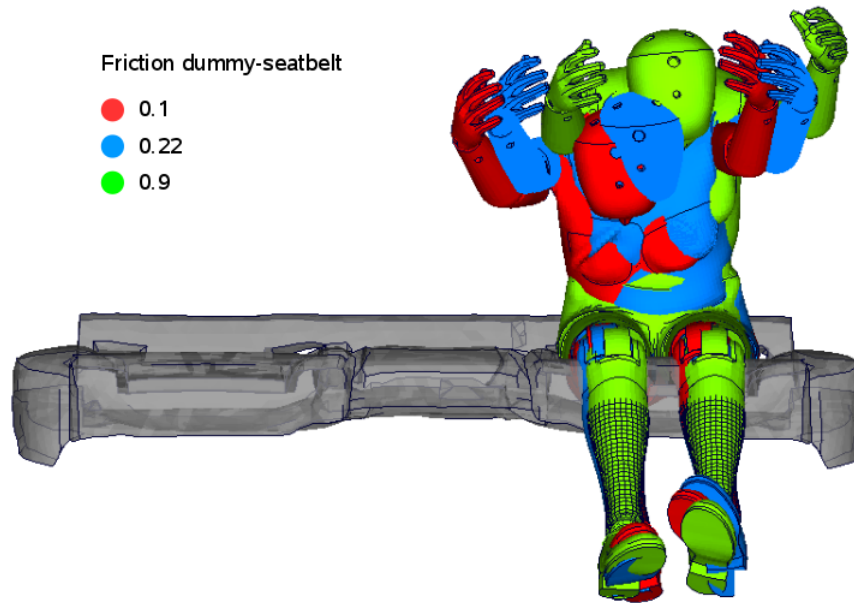


Figure 5.13: Simulations performed with three different friction coefficient between the dummy and the seatbelt.

5.2 Dummy friction

To study the influence of the friction between the dummy and the seatbelt the friction coefficient for sliding contact between these was varied from 0.22 to 0.62 in step of 0.1 and with two extreme values, 0.1 and 0.9. Figure 5.13 shows the dummy position at a certain time when the friction coefficient is set to 0.1, 0.22 (reference) and 0.9 respectively. It can be seen that, for lower friction, the upper body of the dummy is allowed to slip more down to the right hand side than for higher friction. The difference is most significant in the y-direction, something that can be seen in Figure 5.14 and Figure 5.15.

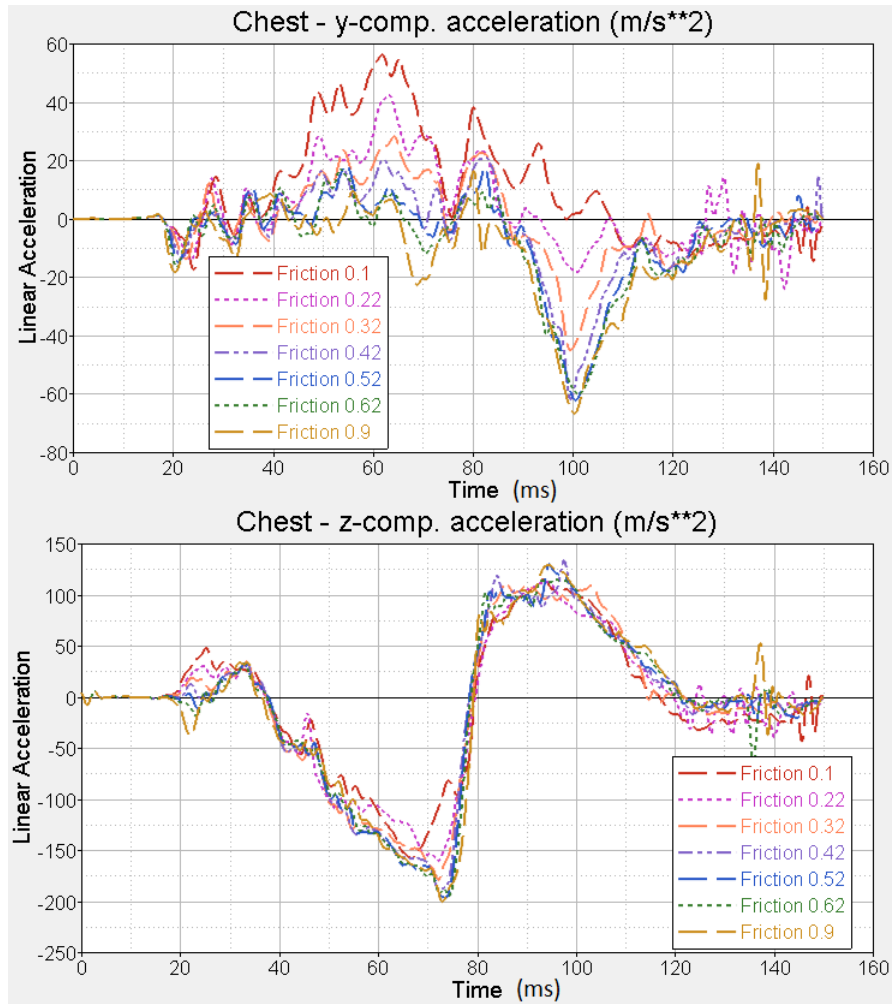


Figure 5.14: Chest acceleration in the y and z-direction respectively, for the simplified P4 model. The friction coefficient between the dummy and the seatbelt is varied between 0.1 and 0.9 (0.22 is the reference)

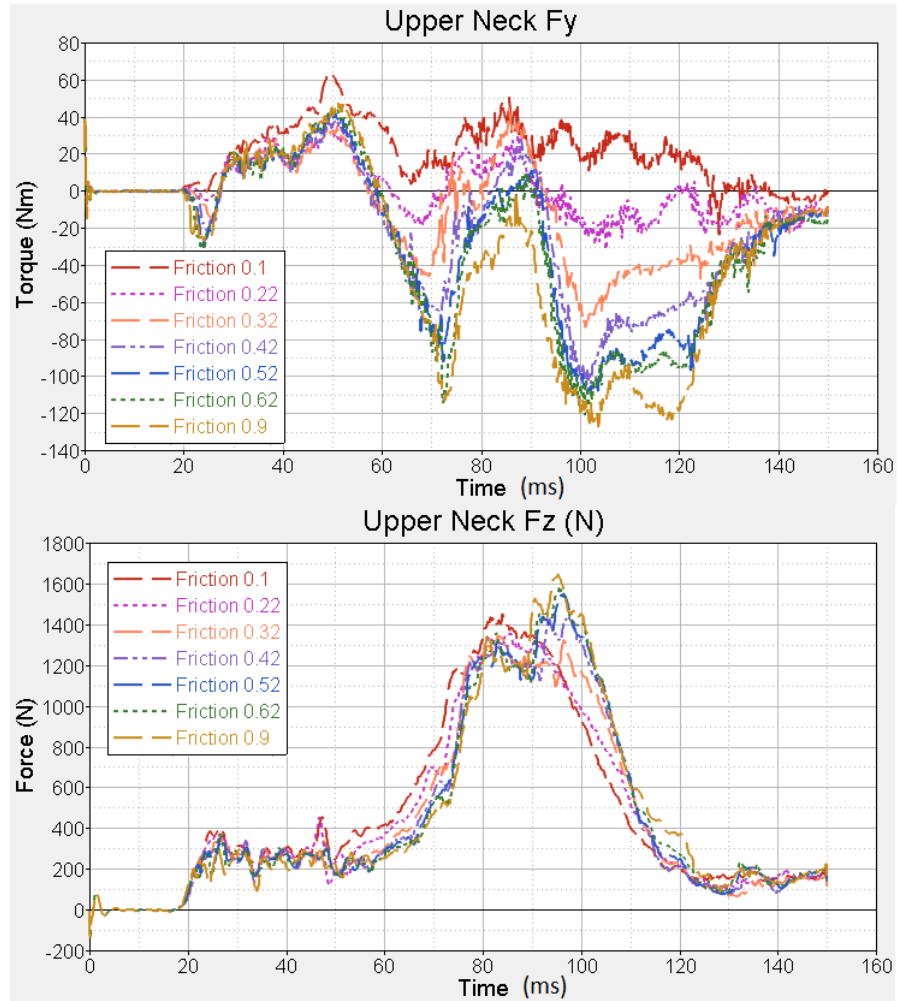


Figure 5.15: Upper neck force, F_y and F_z , for the simplified P4 model. The friction coefficient between the dummy and the seatbelt is varied between 0.1 and 0.9 (0.22 is the reference)

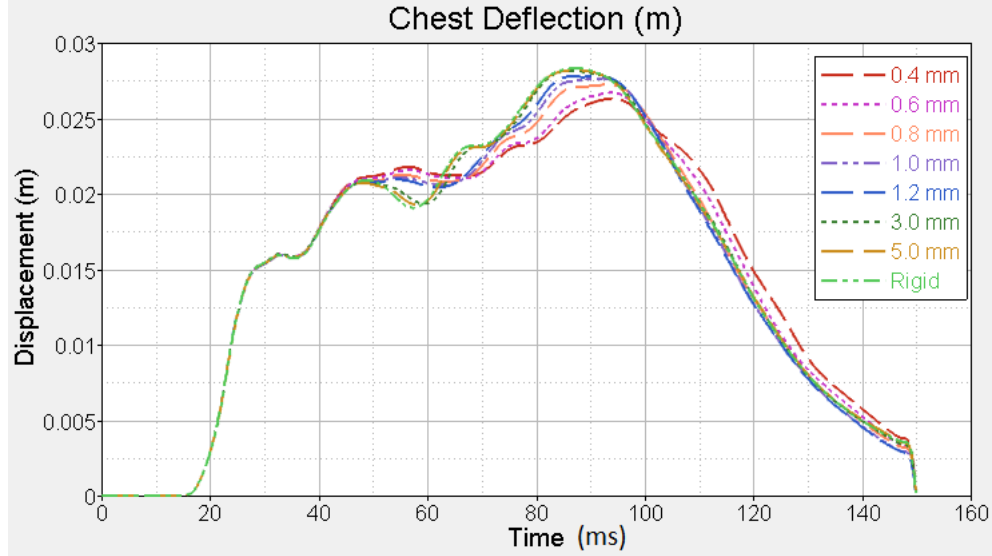


Figure 5.16: Chest deflection for the simplified P4 model using seat bottom plates with different thickness. 0.6 mm is the reference thickness

5.3 Stiffness of seat bottom plate

The thickness of the seat bottom plate was varied, in the simplified P4 and P5 models, between 0.4 mm and 5 mm. Figure 5.16 shows the chest deflection for the simplified P4 model and it is seen that when the thickness – and by that also the stiffness – increases, the results approaches the results obtained for the rigid seat bottom plate. This can also be seen more clearly in Figure 5.17 where the maximum chest deflection is plotted against the plate thickness. Between 0.4 and 1.0 mm there seems to be close to a linear correlation between the thickness and the maximum chest deflection. For higher values of the thickness, the increase of chest deflection is decreasing and approaches the value obtained with the rigid seat bottom plate. For the P4 model, there is a similar trend for the pelvis acceleration in the z-direction but the rate towards the rigid behaviour seems to be lower than for the chest deflection, see Figure 5.19. Furthermore, in Figure 5.18 it is shown that changing the seat bottom thickness changes the shape of the curve and shifts it to the right. This makes it hard to compare maximum pelvis acceleration in the same way as for the chest deflection. This behaviour is even more significant when studying the pelvis acceleration for the P5 model. The shape of the curves for the thinnest bottom plates differs a lot compared to the thicker plates, see Figure 5.20. This has to do with the fact that the point where the pelvis acts upon the seat bottom plate changes when changing the stiffness of the plate, see Figure 5.21.

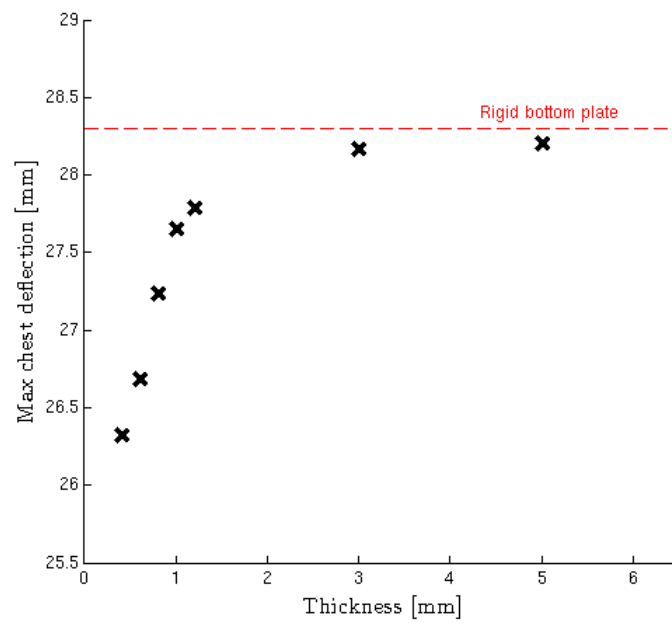


Figure 5.17: Maximum chest deflection when the thickness of the seat bottom plate is varied from 0.4 mm to 5.0 mm, for the P4 model. The dashed line shows the value for a rigid seat bottom plate. 0.6 mm is the reference thickness

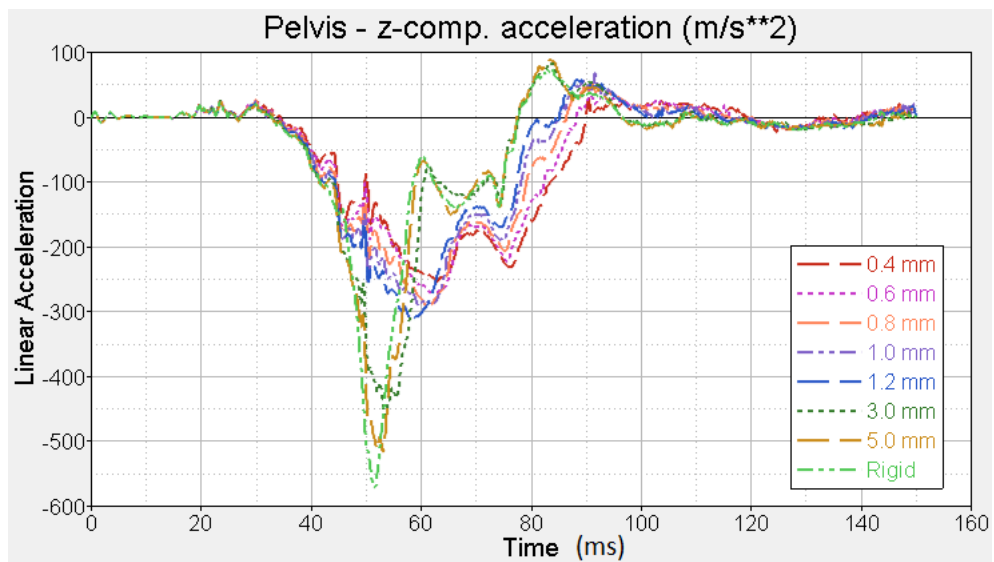


Figure 5.18: Pelvis acceleration in the z-direction for the simplified P4 model using seat bottom plates with different thickness. 0.6 mm is the reference thickness

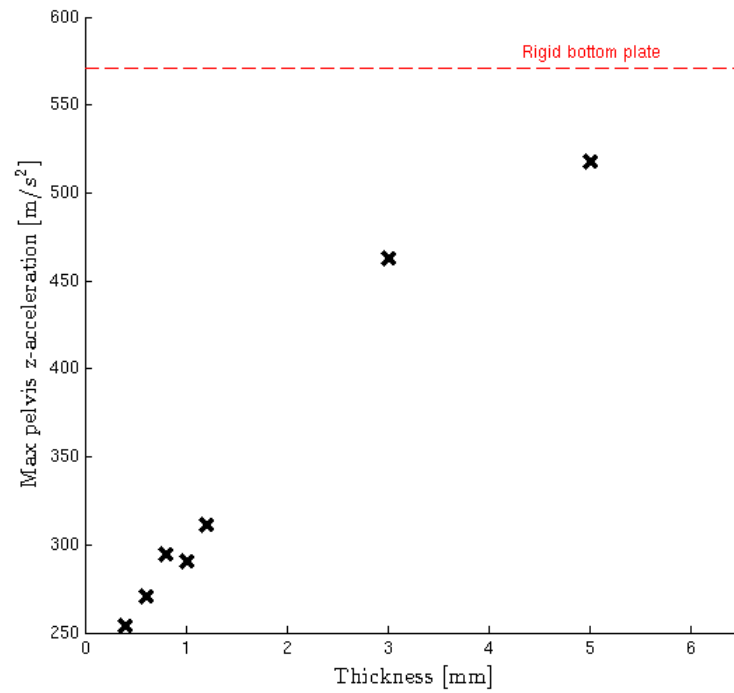


Figure 5.19: Maximum pelvis acceleration in the z-direction when the thickness of the seat bottom plate is varied from 0.4 mm to 5.0 mm, for the P4 model. The dashed line shows the value for a rigid seat bottom plate. 0.6 mm is the reference thickness

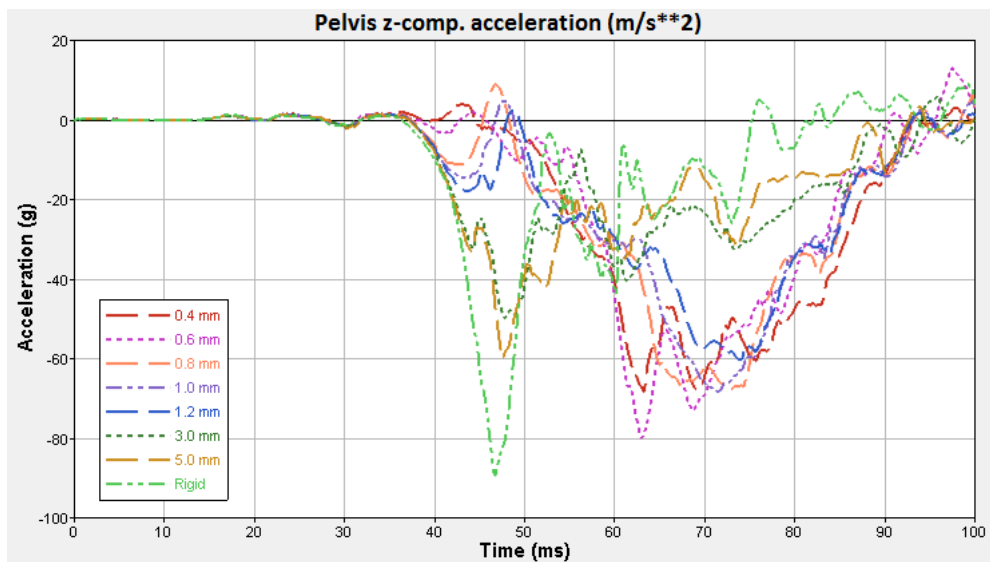


Figure 5.20: Pelvis acceleration in the z-direction for the simplified P5 model using seat bottom plates with different thickness. 0.6 mm is the reference thickness

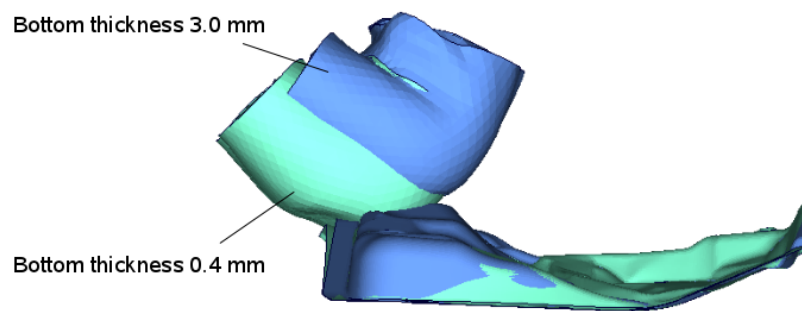


Figure 5.21: Pelvis interaction with the seat bottom plate for two different thicknesses of the plate

6 Concluding discussion

In this chapter a concluding discussion regarding the fulfilment of the thesis goals is presented, followed by recommendations for future work.

6.1 Fulfilment of goals

In this section the fulfilment of each separate thesis goal is discussed.

6.1.1 Describe components and phenomena affecting the rear seat safety

In Section 3.2 the influence of the seat bottom plate, as well as the influence of compliant versus rigid seatbelt fixture points have been described. In Section 5.3, the effects of different stiffness properties of the seat bottom plate is further investigated, with regard to dummy measurement data. It has been shown that the seat bottom plate plays an important role in the obtained results. The compliance of the seatbelt fixture points have also been shown to influence the result, and the buckle fixture point is deemed as most significant for the effects, whereas the retractor fixture compliance on the other hand does not significantly influence the results. The influence of different seatbelt anchoring positions relative to a reference position has been studied and presented in Section 5.1, although in a simplified model.

The rear seat backrest has been shown to mainly serve as an initial positioner for the dummy in a frontal crash test situation. However, it has not been studied what effects different initial positions, in terms of seat cushion angles or relative dummy positioning, would have in terms of safety, which might be an important concern when evaluating real world crash safety. As the shoulder belt runs over the backrest, it may come into contact with the backrest and cause additional frictional forces in the belt, and this effect has not been investigated.

The rear seat lower cushion has been treated as given, and no investigation of how it, as a part in a larger system, influences the rear seat safety has been conducted. This was left out of consideration since the seat cushion is very soft compared to the seat bottom plate and the fact that the seat cushion and seat bottom plate are designed together, i.e. different seat bottom design will require a different seat cushion design. In a crash situation, the design of the seat bottom plate is deemed as more significant as it has been shown that it has a strong influence on the obtained dummy measurements.

It has also been shown that how the rear seat lower cushion is attached to the seat bottom plate has little significance for the obtained results. This is interesting from a generic test rig point of view, since this enables more design options when constructing a generic rig.

The front seats play a role in the rear seat frontal crash test as, at least, the dummy legs will come into contact with them. How this happens will affect the results registered in the dummy body. If a sled test should be performed without front seats, the placement and design of the device holding back the dummy legs should be designed with this in mind.

With the aforementioned investigation and presented results, a thorough description of the phenomena and components involved in the rear seat frontal crash safety has been performed. However, the results are based on just two reference models, from the same car platform. It is not clear whether significantly different behaviour would be obtained from other car platforms or other frontal crash test cases. If the design of another car platform is roughly similar to that of the one studied in this thesis the occurring phenomena should be the same, although both the amplitudes and shapes of the obtained dummy measurement time curves will most likely differ, as indicated by the changes in results obtained when changing parameters in the studied models.

6.1.2 Develop a conceptual design for a generic rear seat test rig

The generic rig concept is designed to enable testing of several different set-ups. The main features regard the positioning of the seatbelt anchoring points and the seat bottom.

The anchoring points for a three point seatbelt can be adjusted in order to test several different set-ups. Given a specific retractor and pre-tensioning equipment, an adapter specific to the geometries of these parts need to be designed and they can be mounted and tested in the rig. A concept for a deformable buckle mounting has been developed, which can be used at the anchor fixture position as well if needed. With the possibility to

exchange the deforming bendplate, and adjust the distance for the bendplate rollers, different compliance of this seatbelt fixture point can be easily obtained.

The generic seat bottom plate design should allow for testing different design alternatives. Since the seat bottom plate in the studied car platform has a relatively complex shape, which cannot be easily obtained and altered with simple means, the concept solution is to make use of an available foam material which can be cut into pieces that can be glued together to obtain the complex shape. With this method, different designs of the seat bottom plate can be tested. The observed deformation behaviour in the seat bottom plate is captured partly by this foam material, and partly by deforming plates under the rig seat bottom. Since the bending points of these plates are adjustable and the plates themselves exchangeable, different deformation behaviours can be obtained. The simplified CAE model of the designed concept has shown that this concept can be adjusted to approximate the behaviour of the seat bottom plate in the studied reference models.

However, how well the designed seat bottom concept will approximate the deformation behaviour of a differently designed seat bottom plate is not clear. A significant factor that determines the resulting stiffness, and thus the deformation behaviour, of a seat bottom plate is the shape. However this shape is not likely to be subject to extreme changes, since the seat bottom plate must, at least, support a rear seat cushion. Furthermore, if a new design of a seat bottom plate is built and tested with good results in the generic rig, the behaviour of this new rig bottom can be used as a target when designing the actual seat bottom plate, which means that the rig can contribute with design-guidelines and requirements.

6.1.3 Develop a CAE model of the rig that can be used to evaluate different safety solutions

The developed CAE model of the designed concept allows for easy evaluation of different set-ups. The successful implementation of the Ansa auto-recreating seatbelt tool has enabled the many different seatbelt configurations tested in Section 5.1. The auto-recreating seatbelt model has only been implemented for the seatbelt used in the P4 model.

The adjustable deformable elements in the designed rig concept are present in the rig CAE model as well, and LS-OPT have been coupled with Ansa and LS-DYNA in order to tune these deforming elements to match results observed in the reference CAE models.

Some manual labour in the preprocessing stage is still required when introducing new or exchanging already existing components in the CAE model, in order to define correct constraints and contact definitions. However, the general layout of the CAE model is modular and once all components are in place, Ansa's Morphing capabilities, kinematics tool and auto-recreating seatbelt tool coupled with LS-OPT allows for many alternative designs to be evaluated.

6.2 Future work

In this section, suggested areas of future work related to each goal is presented.

6.2.1 Describe components and phenomena affecting the rear seat safety

The crash behaviour of another car platform should be thoroughly studied, in terms of finding other phenomena significant for constructing a generic rear seat test rig. Furthermore, information gathered from physical crash tests and actual crashes can be gathered and studied with this intent in mind as well.

6.2.2 Develop a conceptual design for a generic rear seat test rig

The designed concept still needs to be further investigated, before physical construction. The parts responsible for connecting the functional parts, such as seat bottom, belt fixtures and bend plates, to the hole plate needs to be properly dimensioned. The effects of any elasticity in these parts need to be investigated and accounted for when dimensioning the deformable parts in the rig.

The deforming rig buckle fixture needs further evaluation or a complete re-design in order to provide a correct deformation behaviour. When looking into this, a recommendation is to also evaluate the need for positional freedom of the buckle fixture. If little freedom is needed in certain directions, other deforming fixture designs that require more space can be introduced and evaluated.

The rig seat bottom design needs to be further evaluated and updated in order to better capture the behaviour of the reference model seat bottom plate, in the Y-direction outer ends. This to obtain higher accuracy in the calculated results from dummies seated at the 4th and 6th seat positions in ODB crash test evaluation.

6.2.3 Develop a CAE model of the rig that can be used to evaluate different safety solutions

In order to further speed up the preprocessing time when evaluating different solutions in the rig CAE model, work can be focused on automating some of the necessary steps. Given the components existing in the model and their positioning, an effort can be made to automatically position and constrain them and set up all necessary contact definitions, such that changing the test set-up in the rig model is mainly defining the set-up.

The approach used in this thesis was to pick the necessary components from the reference models, and as such, the workings (as in how constraints, cross references between parts, contacts and other related FE-entities are defined) of the developed CAE model is quite dependent on how these parts are intended to function in the original models. If models are reconstructed with the purpose to be used in a generic rig CAE model, where the positioning of some components are allowed to vary and components can be exchanged independently the automation of certain steps in the preprocessing stage can be simplified.

Ansa GEBs, scripts and the Ansa kinematics capabilities can be utilised to aid in automation of certain steps, as demonstrated with the example for the auto-recreating seatbelt model (see Appendix D).

References

- [1] Humanetics. *Hybrid III 95th Large Male Dummy*. 2015. URL: <http://www.humaneticsatd.com/crash-test-dummies/frontal-impact/hybrid-iii-95th> (visited on 05/15/2015).
- [2] Smith J.E. and Halle M.J. Injuries Caused by Seatbelts. *Trauma* **7.4** (2005), 211–215. DOI: 10.1191/1460408605ta348oa.
- [3] A. Kemper et al. Reducing Chest Injuries in Automobile collisions: Rib Fracture Timing and Implications for Thoracic Injury Criteria. *Annals of Biomedical Engineering* **39.8** (2011), 2141–2151. DOI: 10.1007/s10439-011-0311-8.
- [4] *Ansa version 15.1.x User's Guide*. BETA CAE Systems S.A, 2014. URL: <http://www.beta-cae.gr>.
- [5] *LS-Opt Users's Manual*. Version 5.0. Livermore Software Technology Corporation, 2013. URL: <http://www.lsoptsupport.com/documents/manuals>.
- [6] L. S. T. Corporation. *Coupling With Preprocessor Ansa*. 2015. URL: <http://www.lsoptsupport.com/examples/optimization/coupling-with-pre-processor-ansa/couple-ansa-with-ls-opt> (visited on 05/16/2015).
- [7] *LS-Dyna Keyword Users's Manual - Volume I*. Version R7.1 revision 54711. Livermore Software Technology Corporation, 2014. URL: <http://www.dynasupport.com/manuals>.

Appendix A NCAP crash tests

A.1 Euro NCAP

The Euro NCAP rating is based on assessment in four different areas [1]:

- Adult occupant protection
- Child occupant protection
- Pedestrian occupant protection
- Safety Assist

In each area a series of tests and evaluations are performed, each contributing with scores that are summed for each area and normalised against the maximum score available in that area. The total star rating is then calculated by summing up the normalised score from each area, with weighting applied. For the 2015 Euro NCAP rating the weighting is 40% for adult occupant protection and 20% for the remaining areas [2].

The crash test performed by Euro NCAP pertinent for this thesis is included in the adult occupant assessment, where dummy instrument data from a rear seat occupant is measured in a frontal impact crash test against a rigid barrier.

A.1.1 Euro NCAP full width frontal impact test

In the full width impact test the car is frontally crashed with a velocity of 50 km/h against a rigid barrier. In the rear seat a HIII 5th percentile female dummy is positioned at the opposite side of the driver position, which is the 4th or 6th position if the driver position is the 3rd or 1st position respectively [3]. A HIII 5th percentile female is also seated at the driver position. The maximum score from the test is 16 points, and is the average score from the driver and rear seat passenger dummy. Each dummy may obtain 16 points respectively and the scores from each dummy are then added and divided by two. The dummies bodies are divided into four regions, each which may obtain four points: "Head", "Neck", "Chest" and "Knee, Femur, and Pelvis", and the scores from each region is added for each dummy. The scoring in each region is based on two performance levels, a higher performance limit and lower performance limit, where the higher performance level awards four points and the lower performance level is zero points. If the measured criteria is in between these levels, linear interpolation will determine the score. If several criteria are involved in determining the performance level, the worst performing criterion should be used when calculating the score. In this scoring two injury criteria are used, HIC_{15} and the Viscous Criterion. Their definition can be read in Section A.1.2. The rear seat passenger performance criteria determined from dummy data is summarised below, from [1].

Head

If no hard contact of the rear passengers head can be seen on the recorded high speed film:

Higher performance limit

Resultant acceleration during 3 ms exceedence	72g
---	-----

Lower performance limit

Resultant acceleration during 3 ms exceedence	80g
---	-----

If hard contact of the passengers head can be confirmed from the high speed film:

Higher performance limit

HIC_{15}	500
Resultant acceleration during 3 ms exceedence	72g

Lower performance limit

HIC_{15}	700
Resultant acceleration during 3 ms exceedence	80g

Neck

The rear seat passenger score is the sum of scores from Shear, Tension and Extension forces in the neck with the following maximum scores: Shear 1 point, Tension 1 point and Extension 2 points.

Higher performance limit

Shear	1.2kN
Tension	1.7kN
Extension	36Nm

Lower performance limit

Shear	1.95kN
Tension	2.62kN
Extension	49Nm

Chest

The chest region is evaluated by the total chest deflection or the Viscous Criterion

Higher performance limit

Compression	18mm
Viscous Criterion	0.5m/s

Lower performance limit

Compression	42mm
Viscous Criterion	1.0m/s

Knee, Femur and Pelvis

The knee femur and pelvis region is assessed by the femur compression force.

Higher performance limit

Femur compression force	2.6kN
-------------------------	-------

Lower performance limit

Femur compression force	6.2kN
-------------------------	-------

The scores calculated from dummy data can be modified by different modifiers. If airbags are present and the contact between the dummy and the airbag is deemed unstable, 1 point will be deducted from each of the body regions the airbag is intended to protect. If the airbags deploy incorrectly 1 point will be deducted from each of the body regions the airbags are intended to protect. If the rear seat dummy's head is displaced forwardly by (X-direction) 450 mm or 550 mm relative to a reference point defined at the seated initial position, a 2 or for 4 point modifier is applied, reducing scores in the head region. This modifier can be removed if it is shown by computer simulation or additional testing that a HIII 50th percentile male does not contact the front seat, or that the HIC_{15} values is less than 700 if contact occurs. If the shoulder belt load exceeds 6 kN, two points are deducted from the chest region. If submarining occurs, as confirmed by high speed film and a 1 kN drop within 1 ms registered in any of the two iliac force sensors, 4 points will be deducted from the Knee, Femur and Pelvis region.

A.1.2 Injury criteria

In the scoring procedure applied by Euro-NCAP, two injury criteria are referred to, and these are defined below.

The head injury criterion

In crash testing the Head Injury Criterion (HIC) is often used to determine risk of head injuries for occupants. The resultant head acceleration is calculated from measurements taken from accelerometers located at the centre of gravity the dummy's head. For a crash measurement starting at time $t = 0$ and ending at $t = T$, measured in milliseconds, HIC is calculated as [4]:

$$HIC = \left[\frac{1}{t_2 - t_1} \int_{t_1}^{t_2} a(t) dt \right]^{2.5} (t_2 - t_1) \quad (A.1)$$

where $a(t)$ is the resultant acceleration measured in g's ($1g = 9.81[m/s^2]$) calculated as

$$a(t) = \sqrt{a_x(t)^2 + a_y(t)^2 + a_z(t)^2}$$

$$0 \leq t_1 \leq t_2 \leq T.$$

t_2, t_1 selected so as to maximise eq A.1. The time span $t_2 - t_1$ is fixed and smaller than or equal to 36 ms. The time span used is denoted by subscription when referring to the HIC, e.g. for a 15 ms time span HIC_{15} will be used.

The viscous criterion

The viscous criterion is used to estimate risk of injury to the chest. A potentiometer connected to a rod in the chest of the HIII can measure the chest compression during a crash, i.e where the sternum moves toward the spine. The viscous criterion is defined as [5]:

$$\text{Viscous Criterion} = \max_t [V(t) * C(t)] \quad (\text{A.2})$$

where

$V(t)$ is the instantaneous rate of chest deformation at time t

$C(t)$ is the chest compression defined as the ratio of the current deflection at time t and the initial chest thickness.

A.2 China NCAP

In China-NCAP (C-NCAP) rating procedure a five star rating may also be obtained, based on the sum of scores in different tests. No weighting is applied from different categories. The rear seat adult passenger frontal crash safety is evaluated in two crash tests; the frontal impact test against a rigid barrier with 100% overlap (similar to the Euro-NCAP test) and the frontal impact test against deformable barrier with 40% overlap. The information regarding these tests are gathered from the C-NCAP Management Regulation 2015 edition Exposure Draft, June 2014 [6]. The regulations are not yet finalised, but are expected to be applied during 2015.

A.2.1 China NCAP tests and scoring

In the 100% overlap frontal impact test the car hits a rigid barrier at 50 km/h. Two HIII 50th percentile male dummies are seated at position 1 and 3, and on the second row a HIII 5th percentile female dummy is seated at position 4, and at position 6 a child dummy is seated in a child seat. The maximum score obtainable in this test is 18 points, where a maximum of two points can be obtained from the rear seat dummy. The dummy is divided into regions of head, neck and thorax, which can be awarded a maximum of 0.8, 0.2 and 1 point respectively. Similar to the Euro-NCAP scoring procedure, a higher and lower performance limit is set for each region, and if the measured criteria is between, the score will be determined by linear interpolation. The criteria of the different rear seat female dummy regions in the 100% overlap frontal impact test are listed below:

Head

If the head is not involved in a secondary impact (where the head hits an interior part of the car during the crash, and the primary impact is the crash itself), the maximum of 0.8 points can be awarded directly. Otherwise the score is evaluated by:

Higher performance limit	
HIC_{15}	500
Lower performance limit	
HIC_{15}	700

Neck

The maximum rear seat passenger neck score is 0.2 points. If the head is not involved in a secondary impact only the neck tension force should be evaluated, otherwise the assessment criteria should be the worst performing of shear force, tension and extension bending moment

Higher performance limit	
Shear	1.2kN
Tension	1.7kN
Extension	36Nm

Lower performance limit

Shear	1.95kN
Tension	2.62kN
Extension	49Nm

Chest

The chest region is evaluated by the total chest deflection, and a maximum of 1 point is awarded

Higher performance limit

Compression	23mm
-------------	------

Lower performance limit

Compression	48mm
-------------	------

Scores for the second row dummy will be deducted by 1 point for any of the following if registered during the crash:

- Rupture of the seatbelt webbing
- Rupture/disengagement of buckle, anchor or linking point of seatbelt
- The retractor malfunctions

0.5 points will be deducted for each iliac force sensor registering submarining as a 1kN force decrease during one millisecond.

The second test involving rear seat adult crash safety is the frontal impact against a deformable barrier with 40% overlap test, see Figure 2.8. The car has an initial velocity of 64 km/h in this test. This test is also performed by Euro-NCAP, but only with child dummies seated in child restraint systems, i.e child seats, as rear seat occupants.

In this test, two HIII 50th percentile male dummies are seated at position 1 and 3, and a HIII 5th percentile female dummy is seated at position 4. In this test a maximum of 18 points are available, where a maximum of two points can be awarded for the rear seat dummy. The body of the HIII 5th percentile female in this test is divided into two assessed regions, where the first group is Head and Neck, and the second group is thorax. The Head and neck group can obtain maximum 1 point. If no secondary impact occurs to the head, 1 point is awarded directly. If a secondary impact do occur, The performance limits used for Head and Neck in the 100% overlap frontal impact test is used, and the worst performing criterion is used to determine the score. The thorax group can obtain a maximum of 1 point and is evaluated by the chest compression performance limits used for the Chest group in the 100% overlap frontal impact test. The same score deduction process regarding the seatbelt and submarining as in the 100% overlap frontal impact test is applied.

References

- [1] *Assessment Protocol - Adult Occupant Protection*. Version 7.0.2. Euro NCAP, 2015. URL: <http://www.euroncap.com/sv/foer-tekniker/protocols/adult-occupant-protection>.
- [2] *Assessment Protocol - Overall Rating*. Version 6.0. Euro NCAP, 2012. URL: <http://www.euroncap.com/sv/foer-tekniker/protocols/general/>.
- [3] *Full Width Frontal Impact Testing Protocol*. Version 1.0.1. Euro NCAP, 2015. URL: <http://www.euroncap.com/sv/foer-tekniker/protocols/adult-occupant-protection/>.
- [4] B. G. McHenry. Head Injury Criterion and the ATB. *ATB Users's Group* **2004** (2004).
- [5] K. H. Digges. "Injury Measurements and Criteria". *RTO Meeting Proceedings*. Vol. 20. RTO HFM Specialists, 1998.
- [6] *C-NCAP Management Regulation 2015 edition, Exposure Draft June 2014*. China Automotive Technology and Research Center, 2014. URL: <http://www.c-ncap.org/>.

Appendix B Simplified model

Additional results from the simplified models with rigid and non-rigid seat bottom plate respectively.

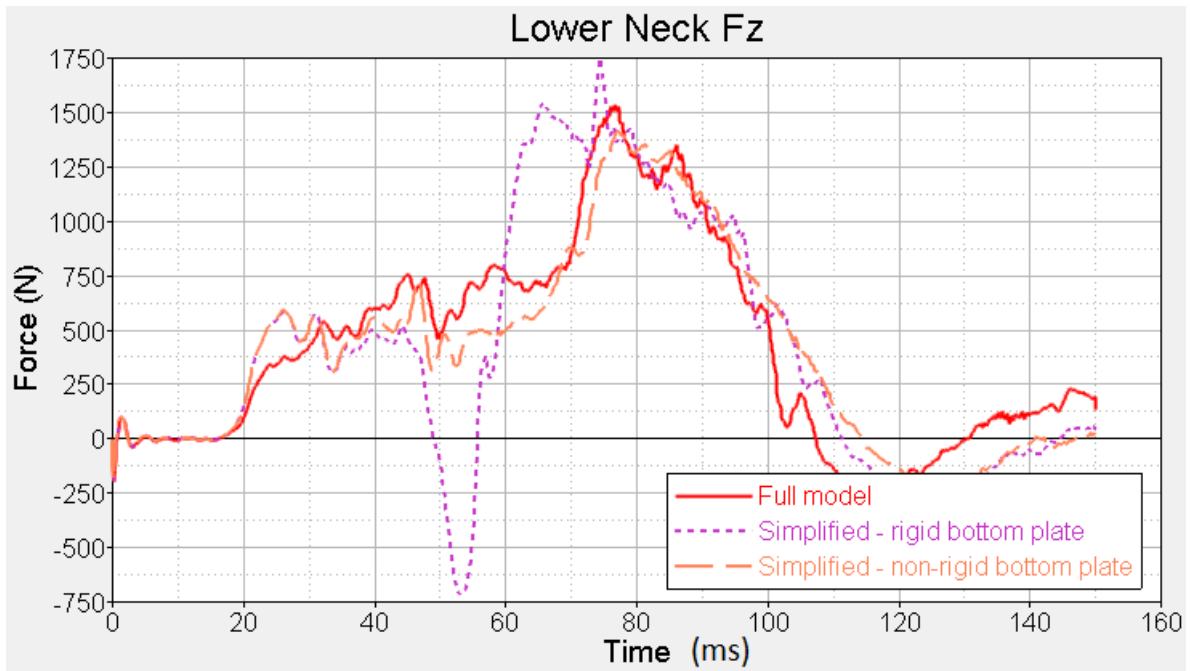


Figure B.1: Lower neck F_z for the simplified P4 model with rigid seat bottom plate compared to the full scale P4 model

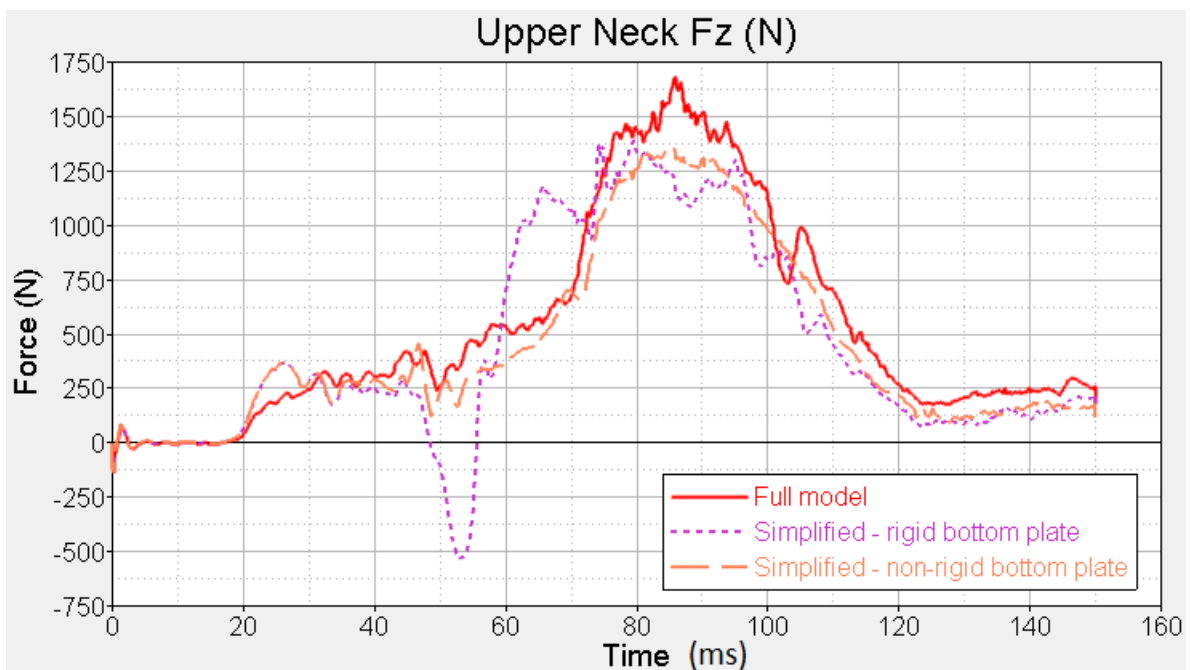


Figure B.2: Upper neck F_z for the simplified P4 model with rigid seat bottom plate compared to the full scale P4 model

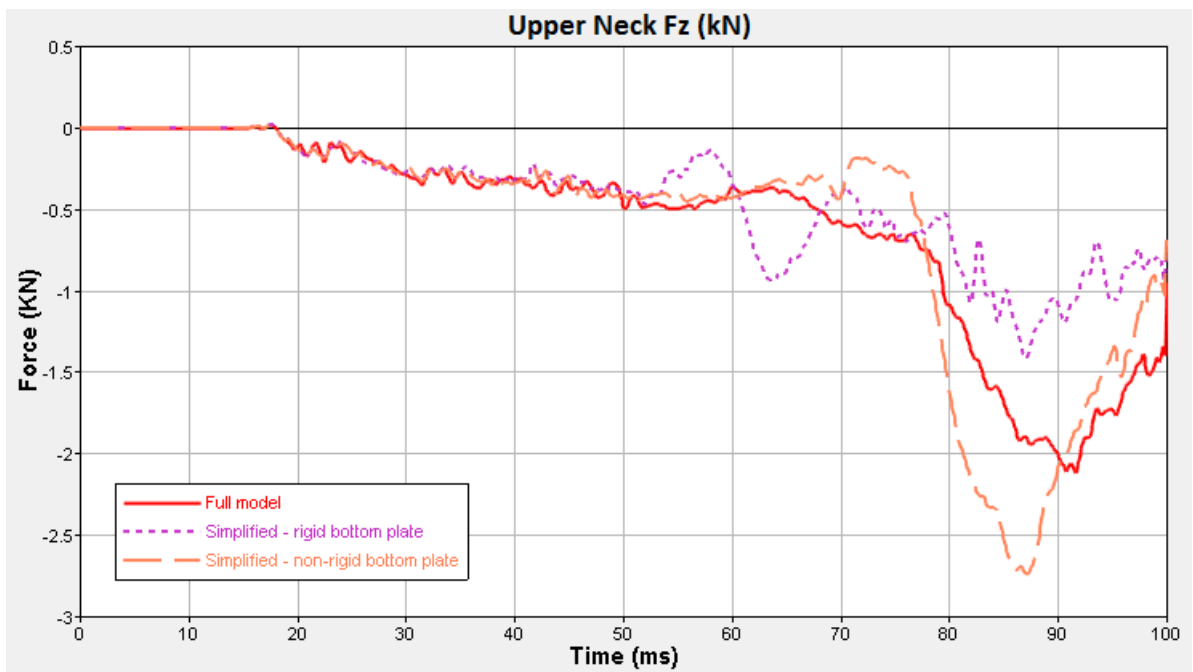
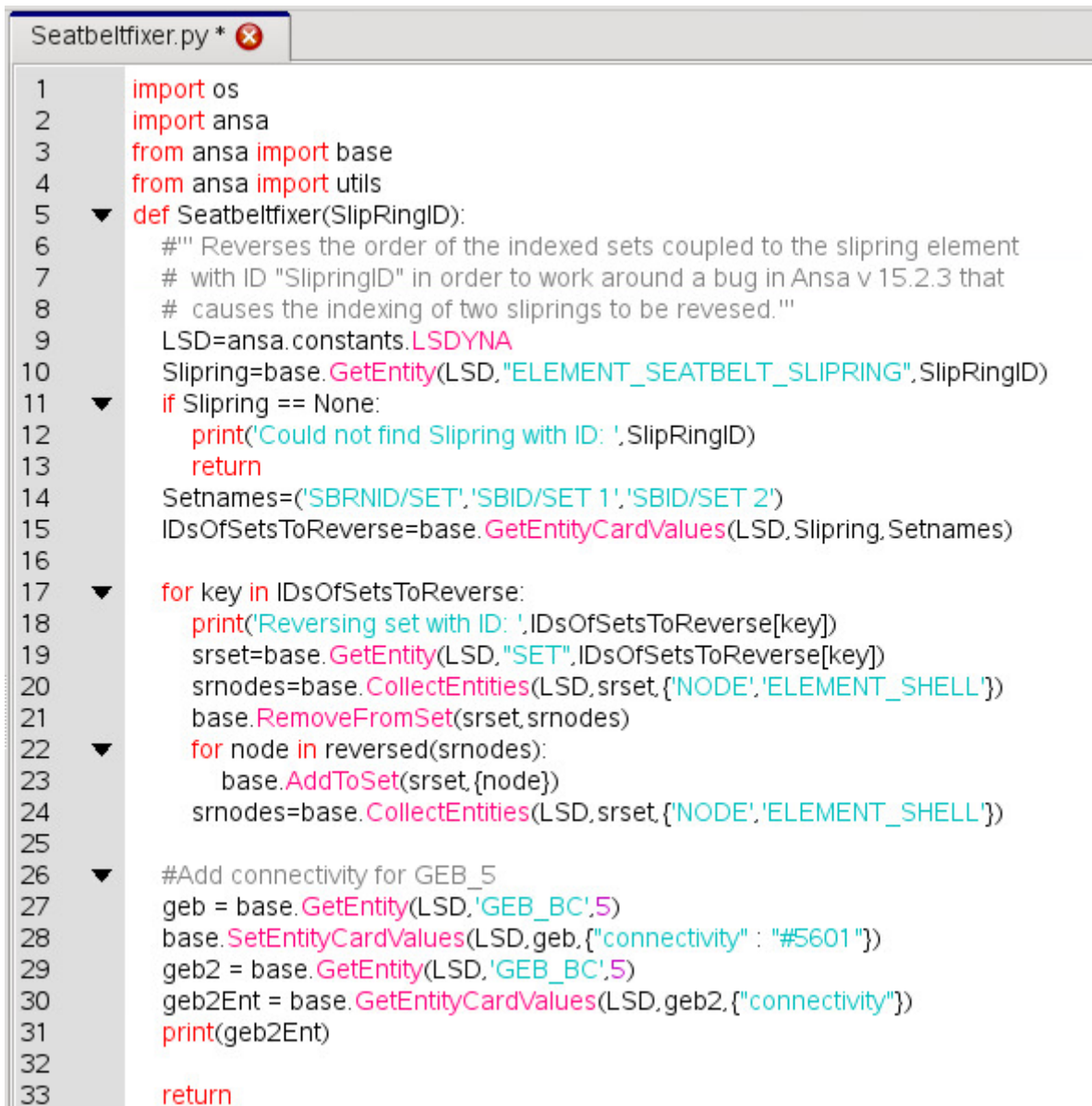


Figure B.3: Upper neck F_z for the simplified P5 model with rigid seat bottom plate compared to the full scale P5 model

Appendix C Ansa scripts

The Ansa scripts that were developed to obtain a correctly defined LS-DYNA seatbelt are presented here. The scripts are written in the Python coding language, and uses functions available in the Ansa Application Programming Interface (API), made available by importing the Ansa API code package in the script.

C.1 Reverse order of sliping sets



```
1 import os
2 import ansa
3 from ansa import base
4 from ansa import utils
5 def Seatbeltfixer(SlipRingID):
6     """ Reverses the order of the indexed sets coupled to the sliping element
7     # with ID "SlipingID" in order to work around a bug in Ansa v 15.2.3 that
8     # causes the indexing of two slipings to be reversed."""
9     LSD=ansa.constants.LSDYNA
10    Sliping=base.GetEntity(LSD,"ELEMENT_SLIPRING",SlipRingID)
11    if Sliping == None:
12        print('Could not find Sliping with ID: ',SlipRingID)
13        return
14    Setnames=('SBRNID/SET','SBID/SET 1','SBID/SET 2')
15    IDsofSetsToReverse=base.GetEntityCardValues(LSD,Sliping,Setnames)
16
17    for key in IDsofSetsToReverse:
18        print('Reversing set with ID: ',IDsofSetsToReverse[key])
19        srset=base.GetEntity(LSD,"SET",IDsofSetsToReverse[key])
20        srnodes=base.CollectEntities(LSD,srset,{'NODE','ELEMENT_SHELL'})
21        base.RemoveFromSet(srset,srnodes)
22        for node in reversed(srnodes):
23            base.AddToSet(srset,{node})
24        srnodes=base.CollectEntities(LSD,srset,{'NODE','ELEMENT_SHELL'})
25
26    #Add connectivity for GEB_5
27    geb = base.GetEntity(LSD,'GEB_BC',5)
28    base.SetEntityCardValues(LSD,geb,{"connectivity": "#5601"})
29    geb2 = base.GetEntity(LSD,'GEB_BC',5)
30    geb2Ent = base.GetEntityCardValues(LSD,geb2,{"connectivity"})
31    print(geb2Ent)
32
33    return
```

Figure C.1: Printout of the script that reverses indexing order of the sets associated with a sliping

In Figure C.1, a script that will reverse the indexing order of all the sets included in a sliping definition, given the ID of the sliping is displayed. The last part of the code under 'Add connectivity for GEB.5' fixes a small error in the Ansa model causing a GEB to lose connectivity with a particular part id, when the model is reopened. The reason for this error is unknown, but it consistently reappears.

C.2 Move edgeset script

```
edgeset_fix.py *  
1  import os  
2  import ansa  
3  from ansa import base  
4  from ansa import utils  
5  def EdgeSet(GEB,node,fromSearch,argsin):  
6      LSD=ansa.constants.LSDYNA  
7  
8      nodeEntity=fromSearch[0]  
9  
10     ents = base.ReferenceEntities(nodeEntity)  
11     for search in ents:  
12         if base.GetEntityType(LSD,search) == 'CONSTRAINED_NODAL_RIGID_BODY':  
13             constr = search  
14  
15     listOfNodeFields = ("NID1","NID2","NID3","NID4","NID5","NID6")  
16     nodesInConstr = base.GetEntityCardValues(LSD,constr,listOfNodeFields)  
17  
18     nodesToAdd = list()  
19     for i in listOfNodeFields:  
20         nodesToAdd.append(nodesInConstr[i])  
21     nodesToAdd.sort()  
22     nodesToAdd = nodesToAdd[0:5]  
23  
24     pidNo = int(argsin)  
25     pid = base.GetEntity(LSD,"SECTION_SHELL",pidNo)  
26     edgeSet = base.GetEntityCardValues(LSD,pid,{"EDGSET"})  
27     edgeSetEnt = base.GetEntity(LSD,"SET",edgeSet["EDGSET"])  
28     nodesToRemEnt = base.CollectEntities(LSD,edgeSetEnt,"NODE")  
29  
30     base.RemoveFromSet(edgeSetEnt,nodesToRemEnt)  
31     nodesToAddEnt = list()  
32     for i in nodesToAdd:  
33         nodesToAddEnt.append(base.GetEntity(LSD,"NODE",i))  
34     base.AddToSet(edgeSetEnt,nodesToAddEnt)  
35  
36     return 1
```

Figure C.2: Printout of the script that receives information from a GEB locating a particular entity in the end of the seatbelt and uses this information to move the edgeset to the end of the seatbelt

The script for moving the edgeset to the end of the seatbelt webbing is shown in Figure C.2. This script is called by a GEB locating a node in the end of the seatbelt. In this end, a 1d seatbelt element is connected to the edge of the 2d seatbelt element webbing mesh with a nodal constraint. By placing the GEB such that it always locates the node of the 1d element that is constrained to the 2d webbing mesh, the nodal constraint connecting the two can be found. In this constraint, the nodes on the edge of the 2d seatbelt mesh are referenced along with the node in the 1d seatbelt element. The order in which Ansa creates the seatbelt elements and nodes assures that the first five nodes in this constraint are the nodes that should be put in the edgeset. Once the ID's of these nodes are collected, the edgeset can be updated to contain these nodes instead.

C.3 Update sets of DBCS


```
secforc_update.py * 
1  import os
2  import ansa
3  from ansa import base
4  from ansa import utils
5  ▼ def CreateSet(GEB,node,fromSearch,argsin):
6      LSD=ansa.constants.LSDYNA
7
8      shellEntity=fromSearch[0]
9      listOfNodeFields=('N1','N2','N3','N4','EID')
10     listOfNodes=base.GetEntityCardValues(LSD,shellEntity,listOfNodeFields)
11     n1 = listOfNodes['N1']
12     n2 = listOfNodes['N2']
13     n3 = listOfNodes['N3']
14     n4 = listOfNodes['N4']
15     elem = listOfNodes['EID']
16
17     ▼ if abs(n1-n2) == 1:
18         deltaNode = abs(n1-n4)
19     ▼ else:
20         deltaNode = abs(n1-n2)
21
22     deltaElem = deltaNode - 1
23
24     secforcId = int(argsin)
25     secforc = base.GetEntity(LSD,"DATABASE_CROSS_SECTION_SET", secforcId)
26     listOfSetFields = ('NSID','SSID')
27     sets = base.GetEntityCardValues(LSD,secforc, listOfSetFields)
28     setNode = base.GetEntity(LSD,"SET", sets['NSID'])
29     setElem = base.GetEntity(LSD,"SET", sets['SSID'])
30     nodeToRem = base.CollectEntities(LSD, setNode, "NODE")
31     elemToRem = base.CollectEntities(LSD, setElem, "ELEMENT_SHELL")
32     base.RemoveFromSet(setNode,nodeToRem)
33     base.RemoveFromSet(setElem,elemToRem)
34
35     ▼ for i in range(0, 5):
36         nodeToAdd = base.GetEntity(LSD, "NODE", n1+i*deltaNode)
37         base.AddToSet(setNode, nodeToAdd)
38     ▼ for i in range(0, 4):
39         elemToAdd = base.GetEntity(LSD, "ELEMENT_SHELL", elem + i*deltaElem)
40         base.AddToSet(setElem, elemToAdd)
41     return 1
```

Figure C.3: Printout of script that updates the contents of sets used to create a DBCS

The script that updates the DBCS sets is displayed in Figure C.3. The script utilises information obtained from a GEB configured to locate a 2d seatbelt element and utilises the fact that the webbing mesh must be logically regular to update the nodes and elements in the sets needed to define the DBCS.

Appendix D Auto-recreating seatbelt model

In this Appendix, a small tutorial on how to use the Ansa auto-recreating, LS-DYNA compatible, seatbelt model is presented, followed by a description of how the model was set-up, and what it contains. This Appendix is mainly intended for the analysts at VCSC, who is not yet familiar with the set-up process of the auto-recreate feature, and as such it is assumed that the reader is somewhat familiar with the working process in Ansa as well as LS-DYNA input files.

D.1 Tutorial: Seatbelt example model

This tutorial will walk the user through the process of obtaining a modified seatbelt configuration, using an already defined auto-recreating seatbelt model in Ansa version 15.2.3.

1: Open the model

In Ansa version 15.2.3 or later, open `Move_rig_belt_pos.4.ansa`, located at:
`/vcc/cae/backup/safe3/proj/v54x/rear_interior/work/master_thesis_ida_karl/Move_rig_belt/Pos.4/`

NOTE: In this file, all the parts that the belt will need to wrap in the .key file we will eventually use it in are included. In this case its just the dummy torso and pelvis, which will not be moved. The belt will also run over the backrest, but only the part of the backrest that the belt will run over is included, other elements are deleted. This is done because if the buckle is moved into a position that means that the belt would have to go through the seat we will run into trouble with the Auto-recreate feature, since the seatbelt needs to consider the shape of the backrest at one location and ignore it in another. Furthermore, the lower seat cushion is not included either, since moving the buckle and anchor around will cause them to be positioned inside the cushion in some cases. So, either one has to create a seat cushion with holes at these positions, or one just assumes that this will be done in the future if the components are supposed to be placed there. Therefore, *there is no contact defined between the belt parts and the lower seat cushion in this model either.*

2: Load script

Load the script file `Seatbeltfixer.py`, via **Script > Add**. The file is located in subfolder to the seatbelt model, `/script/`.

NOTE: In here a function that will reverse the indexing order of sets belonging to `*ELEMENT_SEATBELT_SLIPRING` is defined. Two other scripts, used by GEB's in the model are automatically loaded, since they are referenced by the GEBs.

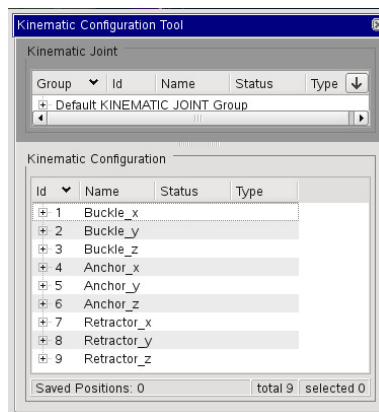


Figure D.1: Overview of the kinematic configurations used to translate the belt fixture points

3: Translate belt fixtures

In the LS-DYNA deck, open **Auxiliaries > KIN_CONFIG** and an overview of the nine kinematic configurations available will appear, see Figure D.1. To move a part, right-click the pertinent configuration and select **Articulate**

> By **actuator joint**. The 'Articulate By Actuator Joint' dialogue window appears. Enter distance, and press OK when done. Repeat process for all joints necessary.

NOTE: As soon as a joint is articulated, the auto-recreate feature will create a new webbing mesh onto the new positioning, even if the articulation is aborted with 'Cancel'. This means that any entities referring to elements or nodes in the previous webbing mesh will no longer be valid. In this model, four ***DATABASE_CROSS_SECTION_SET** (DBCS) refers to sets in the webbing mesh, and are no longer valid. Another phenomenon to keep in mind is that the ID's of elements and nodes in the webbing mesh will be created above the range of the previous mesh, *every time the webbing is recreated*, which means that this numbering can grow outside it's valid range. Therefore, the .ansa model should *not* be saved after usage, since the numbering will then reset the next time it is opened.

4: Prepare seatbelt for FE-output

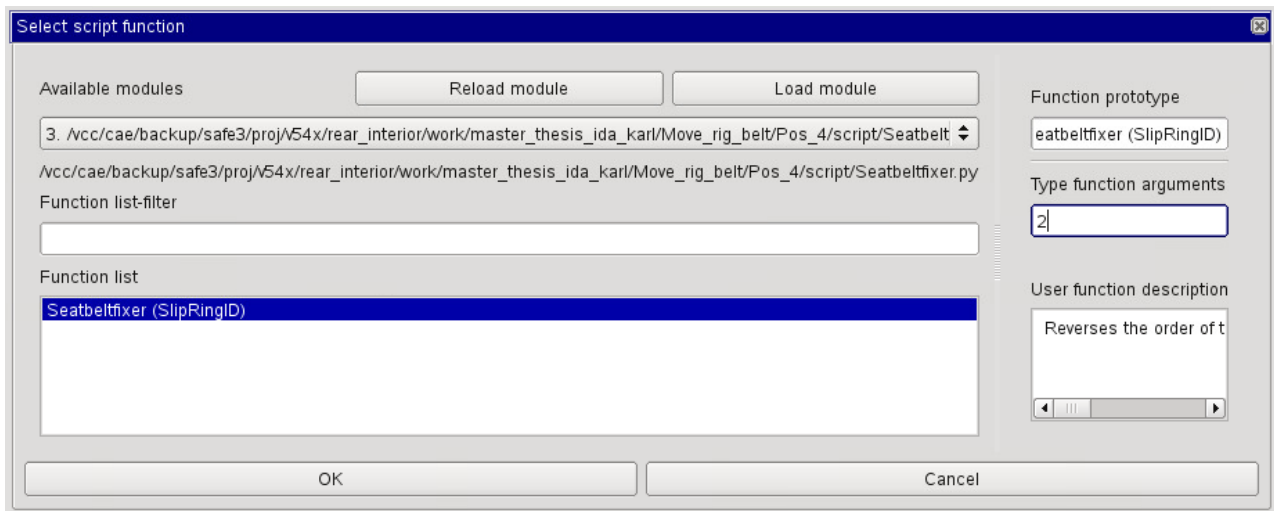


Figure D.2: The Select script function dialogue window

In order for LS-DYNA to accept the seatbelt model as correct, we shall now run the script loaded in step 2, and apply the GEB's in the model that reconfigures the DBCS's as well as moves the edgeset of the seatbelt to a correct position.

Go to **Script > Run Function** and the 'Select script function' dialogue window appears, see Figure D.2. In the drop-down menu, select **Seatbeltfixer.py** as module and select the function that appears. In the 'Type function arguments' box, enter '2', which is the ID of the slipring whose sets will be reversed. Click 'OK'

Next, in the database viewer double-click 'GEB' in the database tree, see Figure D.3. Select all GEBs, right-click and select 'Apply'. The status of all GEBs should now read 'ok'. If their visibility is on, the DBCS's should now be visible on the webbing mesh.

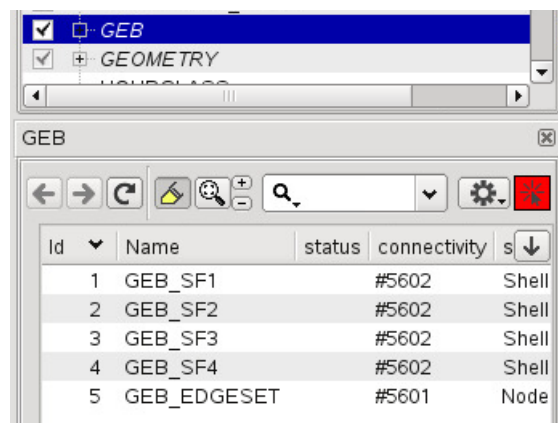


Figure D.3: The GEBs in the database viewer.

NOTE: The 'Seatbeltfixer' script function reverses the indexing order of all sets belonging to the given slipring, but it also works around a small bug encountered. The script will also set the 'connectivity' of the GEB with ID 5 to '#5601', since this setting gets lost every time the .ansa model is re-opened. The reason for this is not known.

5: Check for errors *This step can be skipped if LS-DYNA accepts the seatbelt model*

In the most cases the compatibility issues should be fixed, but it may happen that the ID of slipring 1 should have been reversed instead. It is not clear how the auto-recreate feature will set up the seatbelt for every possible configuration. Go to **Checks > Seat Belts**, and select 'All entities' from the drop-down menu. Select 'Execute'. If an error is encountered, right-click the reported error and select 'Fix' if available. Exit the Checks tool and re-open it, and perform the check on 'All entities' again. It is not enough to re-run the check without exiting the tool first. If an indexing order error for the sliprings appear again, Run the **Seabelftfixer** script again for the pertinent slipring, and then apply all GEBs again. Perform the seatbelt check to confirm that all issues are resolved. A worst case scenario that might happen is that the seatbelt module has failed to create a joint seatbelt mesh. This might happen at the buckle, and can be noticed by the fact that there will be three sliprings in the model. No fix is available for this.

NOTE: That this procedure needs to be performed has been reported to BETA CAE Systems, and they have acknowledged this as a bug in the software. An update in a future release has been promised.

6: Output FE-model

Go to 'Includes' and right-click 'assembly.k', see Figure D.4. Select **Output > Single File**. Choose an appropriate

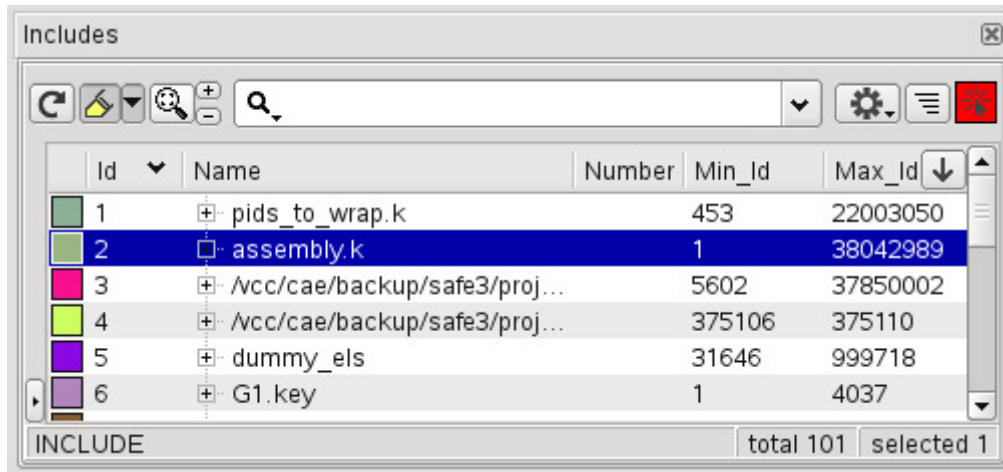


Figure D.4: assembly.k seen in the Includes viewer

name and location for the new seatbelt configuration. In the 'DYNA Output Parameters' dialogue window that appears, select 'Contents Only' from the drop-down menu in the 'Include Output' field. This will output all the FE-entities relevant to the new seatbelt configuration. If more seatbelt configurations needs to be made, go to step 3 in this tutorial.

7: Setup LS-DYNA input files

Create and name copies of the LS-DYNA .key file named **rig_rear_seat_5th_pos4.move_belt.key** and the .k file named **belt_master.5th.move.k**. These are located in the same directory as the Ansa seatbelt model. On line 120 in the new .key file replace the name and directory of **belt_master.5th.move.k** with the newly created belt master file. On line 135 in the new belt master file, replace the name and directory of **assembly.k** with those pertinent to the newly created seatbelt configuration. Now the new seatbelt configuration can be run.

NOTE: The reason for putting the seatbelt configuration in a belt master file is that the parameters and parameter expressions defining the seatbelt retractor and pre-tensioner model are defined partly in the belt master file, and partly in the assembly file. Since LS-DYNA will try to evaluate parameter expressions directly at input, these need to be defined in a top-down line-by-line correct order, otherwise the input will fail.

D.2 Set up of example model

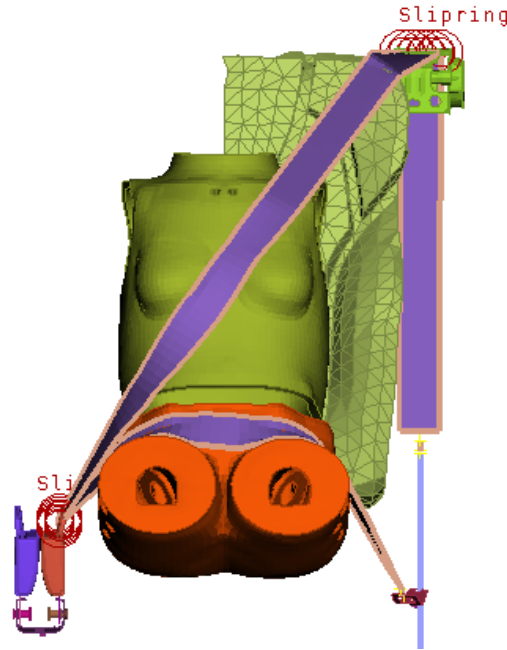


Figure D.5: The Ansa model only containing the FE-entities that the seatbelt wraps, and a seatbelt mesh

The aim of this model is to serve as a proof of concept by providing the ability to create a large number of LS-DYNA compatible seatbelt configurations. For this end, a small model only containing the relevant components of the seatbelt, and the FE entities that the seatbelt webbing wraps was created, see Figure D.5, from which the varying seatbelt configurations will be written into an LS-DYNA input file.

As the ID numbers of the created seatbelt elements and nodes must be unique when the seatbelt model is used in a larger model, all elements and nodes was numbered to ID's just below where the to-be-constructed seatbelt elements and nodes prescribed ID range should begin, and Ansa was configured to number all newly constructed entities above the current existing range. With this setting, any generated seatbelt elements will be numbered correctly upon creation.

Furthermore, since fast and easy FE-model output also is important to reduce preprocessing time, all the parts that could vary between different set-ups was collected into one input file, called `assembly.k`, which was included together with other seatbelt entities which would not vary (materials ,retractor model etc.) in a master file. In Ansa, by setting `assembly.k` to current, all FE-entites that Ansa creates will be written to this file only, which then can be output from the Ansa model easily, see Figure D.6. Care has also been taken such that the parts contained in the `assembly.k` file will be correctly constrained in the full model by using constraints referring to fixed ID's.

The fixture points of the seatbelt that should be moved are the retractor, anchor and buckle, and each of them should be able to translate in X, Y and Z direction. To obtain this the Ansa kinematics module is used. All entities (elements, nodes, constraints) belonging to each of these components were put in a respective kinematic rigid body definition. To obtain the three degree of freedom motion, three one degree of freedom slider (translational) joints for each part is configured, together with dummy rigid bodies, that the slider joints can act between, see Figure D.7.

By actuating each of these joints, an arbitrary translational positioning of the components can be obtained. An auto re-creating seatbelt entity is created. In this model, sliprings are used to wrap the webbing at the buckle and retractor position, and the 2d webbing should end just before the anchor and be constrained to the anchor via a 1d belt element that is constrained to the anchor with a nodal rigid body, effectively fastening the seatbelt to the anchor.

Since we use sliprings, we do not want the webbing to take the actual geometry of the retractor and buckle into account when created, and thus they should not be included in the Parts to wrap list for the seatbelt entity. However, since the belt will only be recreated if a part in the Parts to wrap list is moved we must

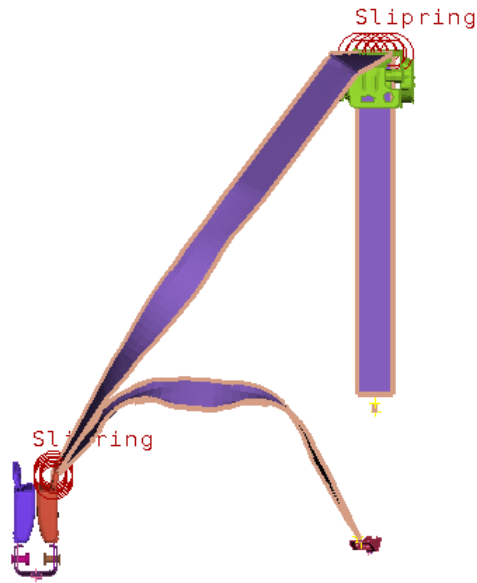


Figure D.6: The seatbelt FE entities that can change between different seatbelt configurations, defined in one LS-DYNA input file, assembly.k

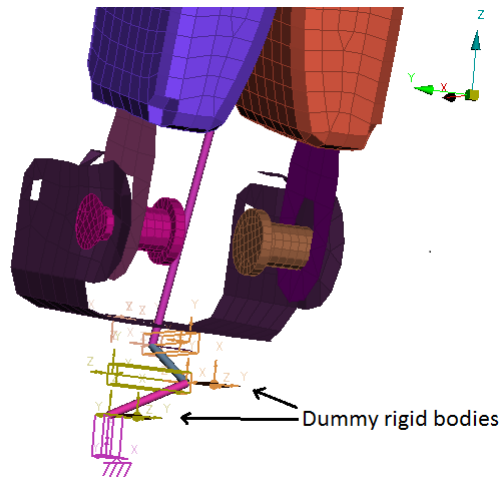


Figure D.7: The Buckle, together with the dummy rigid bodies that is included in the kinematic configuration and the kinematic slider joints acting between the bodies

include in this list, in each of the kinematic rigid body definitions, a part that the seatbelt will not be able to reach, but will move with the kinematic rigid body. This means that the part must be located before the starting point and after the ending point in the longitudinal direction of each seatbelt part. In this manner, the part is included in the Parts to wrap list, but the seatbelt wrapping algorithm need not consider it's shape, since the seatbelt webbing will not run over this part, see Figure D.8. If no part suitable to use in this manner exists, a dummy FE entity can be created and included in the pertinent rigid body definition, and then be included in the Parts to wrap list.

To be able to obtain the cross sectional forces in different parts of the seatbelt, DBCS's have been created that utilises sets of nodes and elements in the seatbelt webbing. These sets will not be valid when the seatbelt is recreated, as the numbering of nodes and elements in the webbing changes. Therefore, GEBs are created at the approximate locations where the DBCS's will be placed, and configured to search for 2d seatbelt elements, see

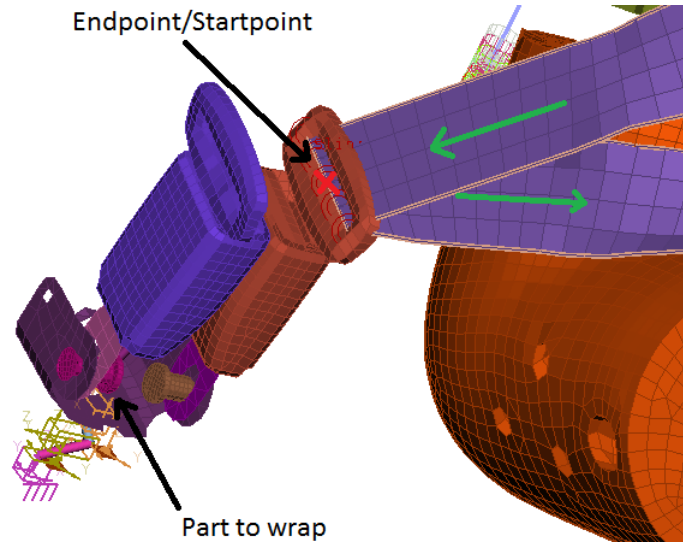


Figure D.8: The part to wrap that cannot be reached by the seatbelt, since it is located after the endpoint of the entering seatbelt part and before the starting point of the exiting seatbelt part

Figure D.9. Once an element has been found, a script that uses the fact that the element and nodal numbering in the webbing mesh is logically regular updates the sets of the DBCS's. As a last step before FE-model output, a GEB that localises the end of the seatbelt near the anchor is applied, and a script is called to move the seatbelt edgeset to the last elements in the 2d webbing, at the anchor end. If the indexing order of a slipping is reversed relative to this edgeset, a last user script can be called to reverse the order of the indexed slipping sets, given the ID of the slipping.

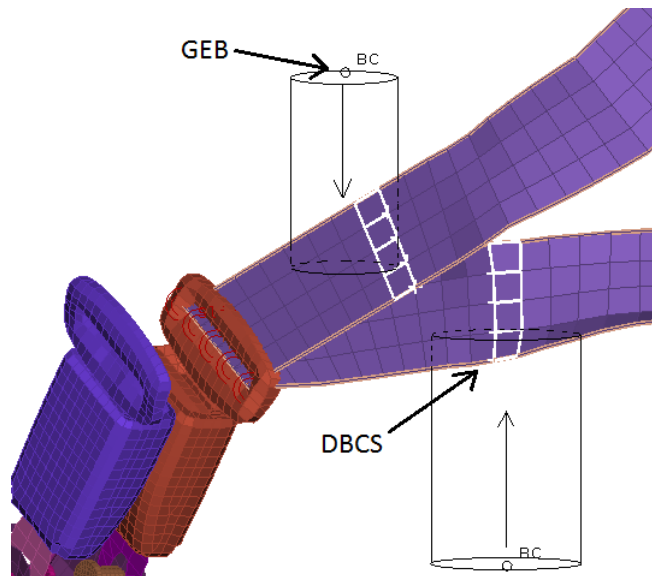


Figure D.9: The Ansa GEBs depicted with their respective search volume, created DBCS's are marked in white on the webbing mesh

Appendix E Start LS-DYNA from LS-OPT

In this section, the script that is needed to start LS-DYNA from LS-OPT, as well as the commands that needs to be defined in LS-OPT are presented.

E.1 LS-DYNA start script

The bash shell script needed to start LS-DYNA from LS-OPT is called `solver.sh` and can be seen in Figure E.1 and is self-explanatory. The permissions for the script file must be set to "rwx" for all users in the unix file system, which means that any user and program, can read-write-execute it. It can be noted that the script expects an input file named `DynaOpt.inp`. This name can be modified to another input file-name. However, once the script is called, the input file must have the name given in the script.

```
#!/bin/ksh
#####
#
NCPU=48
QUEUE=safe_normal
SOLVER=971_85274
#
/vcc/ans/app/startup/lstdyna.run -Ver $SOLVER -Ncpu $NCPU -Que $QUEUE -Opt i=DynaOpt.inp memory=800m memory2=300m
# Give the filesystem some extra time to sync.
# This may be unnecessary but we normally have much
# longer execution times anyway. You should never
# need to increase this further.
sleep 30
echo "Normal"
#
exit 0
#####
```

Figure E.1: The bash shell script used to start LS-DYNA from LS-OPT

E.2 Setting up LS-OPT solver stage

LS-OPT has a predefined LS-DYNA solver stage. However, if this predefined package is used, LS-OPT will require the user to manually list all the included files found in the main input file (files under the keyword `*INCLUDE`). This allows LS-OPT to search all the included files for parameter definitions, control that output requests have been made for data used to evaluate the objective functions and also copy all the files to every LS-DYNA run directory during the optimisation procedure. However since it is common to have very many included files in the input file, and these are automatically copied when the jobs start on the cluster, a workaround is to use a 'User-Defined' solver package, see Figure E.2.

In the figure it can be seen how the solver script is called. In this case the script is located in the LS-OPT project home directory for the current optimisation, which is two folders up in the file hierarchy from each LS-DYNA run directory in the optimisation. With this set-up the user only need to define two file operations to take place between the preprocessing and solver stage in LS-OPT. The file modified by the preprocessor, and the input file including the modified file should be copied to the solver directory before the solver stage is initialised. In the field 'Global limit' the maximum number of concurrent jobs that is sent to the cluster queue to be solved in parallel is specified. LS-OPT will want to run a number of concurrent jobs in every iteration, depending on which type of optimisation procedure and the number of parameters involved.

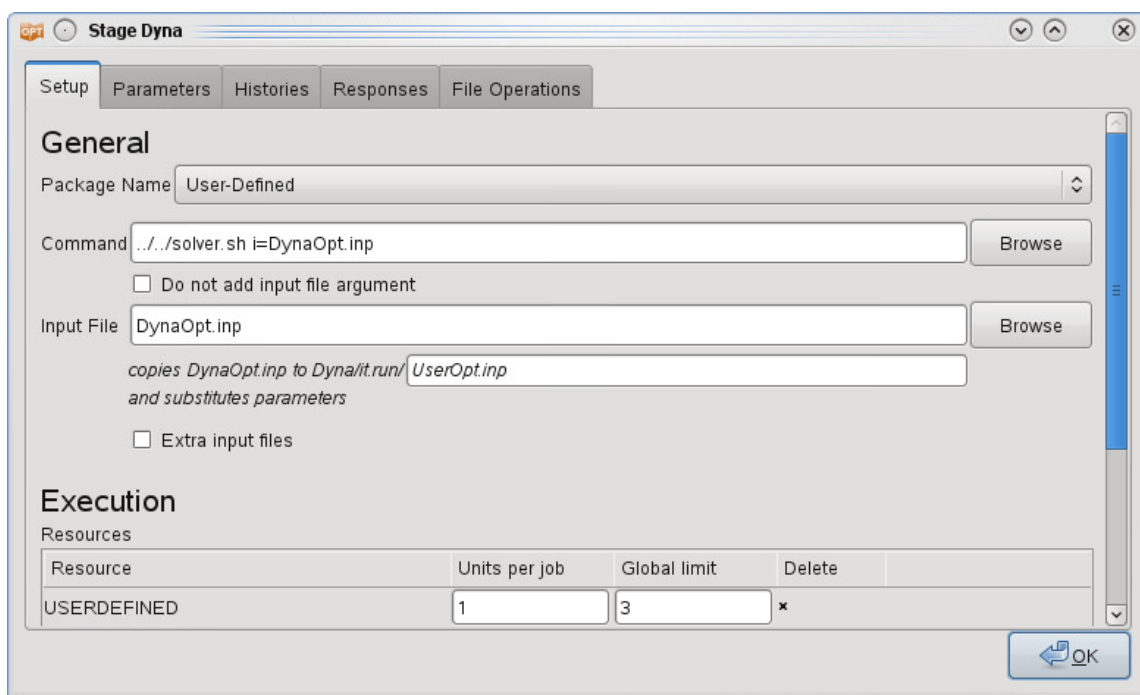


Figure E.2: The solver stage in LS-OPT where a User-Defined package calls the script to start LS-DYNA